Dual projecting neurons for the laryngeal chemoreflex apnoea

By

Rahat Ul Ain Summan Toor

(43513964)

Department of Biomedical Science

Faculty of Medicine and Health Sciences

A thesis submitted for the partial fulfilment of the requirement for the degree of Master of Research in Neuroscience

Supervisors

Dr. Qi-Jian Sun[1]

Professor: Jacqueline Phillips[1]

[1] Department of Biomedical Science, Faculty of Medicine and Health Sciences, Macquarie University, Sydney, NSW, Australia

Main text word count: 13873

Abstract character count: 232

Number of figures: 15

Conflict of interest statement

The research was conducted in the absence of any commercial or financial relationships that could be construed as a potential conflict of interest.

<u>Declaration of Originality</u>

I certify that the work in this thesis entitled "**<u>Dual projecting neurons for the laryngeal chemoreflex apnoea</u>**" has not previously been submitted for a degree nor has it been submitted as part of requirements for a degree to any other university or institution other than Macquarie University. I also certify that the thesis is an original piece of research and it has been written by me. Any help and assistance that I have received in my research work and the preparation of the thesis itself have been appropriately acknowledged. In addition, I certify that all information sources and literature used are indicated in the thesis. The research presented in this thesis was approved by Macquarie University Ethics Review Committee, reference number: 2011/039

Rahat Ul Ain Summan Toor

MQ student number: 43513964

20/05/2015

<u>Publication arising from this work</u>

A novel neuronal population in the nucleus tractus solitarius that projects simultaneously to the Bötzinger complex and caudal nucleus ambiguus

SUMMAN R. TOOR[1], JACQUELINE K. PHILLIPS[1], PAUL. M. PILOWSKY[2],

QI-JIAN SUN[1]

[1] Department of Biomedical Science, Faculty of Medicine and Health Sciences, Macquarie University, NSW 2109, Australia.
[2]Heart Research Institute and University of Sydney, NSW 2042, Australia

Acknowledgements

I would like to express my deepest gratitude to a number of people who supported me during my MRes year. First, I would like to thank my supervisor, Dr Qi-Jian Sun, for his profound knowledge in research of respiratory field, guiding me step by step into study of the current project. This work would not have been possible without his invaluable advices, direction and inspiration provided to me throughout the study.

I am also grateful to my associate-supervisor, Professor Jacqueline Phillips. Her kind positive attitude and enthusiasm enabled me to pursue this project in an open and friendly working environment. Her patient approach and rich teaching experiences have helped me a lot in data presentation, allowing me to accomplish the outcome of this project. I cannot say thank you enough for her incredible support during my write-up even over the weekends. I would like to acknowledge her invaluable time she spent on final formatting of the bibliography.

Furthermore, I would also like to thank Dr Anita Turner for her valuable advice in animal recovery experiments, and Lindsay Parker for her guidance in microscopic imaging. I would also like to thank my group member Dr Cara Hildreth and Rochelle Boyd for their kindly helps in organizing bibliography in proof reading of my thesis and also Manash Saha, Connor Underwood, Sheran Li, Jane Wilkins who helped me every time I encountered problems.

I acknowledge the Faculty of Medicine and Health Sciences and Macquarie University for providing me facility for research including my postgraduate scholarship and research funding.

I also want to pay my regards to my father for always encouraging me in my studies, and sisters Sidra Toor, Noor Toor, Sabahat Toor and brother Nouman Toor for providing a wonderful company during some stressful time along this journey. Finally, I extend my love and thanks to my husband Habib Muhammad, and my son Rayan Habib for their love and invaluable support throughout this study time.

Abstract

The activation of the SLN produces a strong inhibitory response to stop central breathing (apnoea). The neuronal mechanism underlying this apnoeic response, however, remains unknown. A characteristic non-respiratory burst activity in the expiratory laryngeal motoneurons plays a critical role in producing the apnoeic response. The potential burst-relaying neurons were predicted in the nucleus tractus solitarius (NTS), with simultaneous projections to the Botzinger complex (BotC) to stop central breathing and to the laryngeal motoneurons in the caudal nucleus ambiguus (NA) to close vocal cords. The aim of this project, was to provide anatomical evidence to support the existence of such dual-projecting neurons in the NTS. Experiments were performed on 25 anaesthetised Sprague Dawley rats. Four to five days after microinjection of the fluorescent conjugates of cholera toxin B into BotC and unconjugated CTB into the caudal NA, the rats were perfused transcardially with 4% paraformaldehyde. Unconjugated CTB visualized using Goat anti CTB tagged to Alexa-fluor 488 using immunohistochemistry protocol and sections were visualized on Ziess fluorescence microscope. Retrograde labelled neurons in the NTS projecting to BotC and NA were found in the caudal NTS. A small number of double labelled neurons with simultaneous projections to BotC and NA were found ~360um rostral to ~360um caudal to the obex mainly in interstitial and ventrolateral NTS. The study provided anatomical evidences for dual projecting neurons involved in production of apnoeic response and vocal cords adduction.

Key words: Double labelled neurons, Botzinger complex, Nucleus ambiguus, Apnoea, Nucleus tractus solitarius.

Abbreviations

BotC	Botzinger complex
PreBotC	Pre-Botzinger Complex
rVRG	Rostral ventral respiratory group
cVRG	Caudal ventral respiratory group
RTN	Retrotrapezoid nucleus
pFRG	Parafacial nucleus
NTS	Nucleus tractus solitarius
NA	Nucleus Ambiguus
SolI	Interstitial NTS
SolDL	Dorsolateral NTS
SolV	Ventral NTS
SolVl /vlNTS	Ventrolateral NTS
SolM	Medial NTS
SolIM	Intermediate NTS
CC	Central canal
AP	Area Prostrema
Sub-AP	Sub area prostrema
AmbC	Nucleus Ambiguus compact formation
Ambsc	Nucleus Ambiguus semi compact formation
AmbL	Nucleus Ambiguus loose formation
ILM	Inspiratory laryngeal Motneurons
ELM	Expiratory laryngeal mototneurons
RVLM	Rostral ventrolateral Medulla
CVLM	Caudal ventrolateral Medulla
CTB	Cholera toxin B
FG	Fluorogold
RAR	Rapidly adapting stretch receptors
SAR	Slowly adapting stretch receptors
P-Cells	Pump- Cells
Iβ-Cells	Inspiratory beta cells
SLN	Superior laryngeal nerve
RLN	Recurrent laryngeal Nerve
TBPS	Tris phosphate-buffered saline
LAR	Laryngeal adductor response
AVPN	Upper airways vagal pre-ganglionic neurons
CVPNs	Cardiac vagal pre-ganglionic neurons

Table of contents

Chapter 1: Introduction

The laryngeal chemoreflex (LCR), which is elicited by placing a drop of fluid into the larynx, produces a strong central nervous system mediated inhibitory response to stop breathing (apnoea) (Curran et al., 2005b; Heman-Ackah et al., 2009). Apart from eliciting the apnoeic response, the LCR may also result in the closure of the vocal cords, swallowing and coughing (Johnson et al., 1972; Sant'Ambrogio and Mathew, 1986; Yoshida et al., 2000; Ludlow, 2005; St-Hilaire et al., 2005; Thach, 2008). These responses work together to protect the upper airways by either preventing aspiration of foreign substances (Bosma, 1957; Sun et al., 2011b), or removing the invading particles from the upper airway (Shiba et al., 1999; Simera et al., 2015). Dysfunction of the basic mechanism for the production of LCR is thought to underlie a number of life-threatening conditions (Pickens et al., 1989; Wetmore, 1993). In particular, the respiratory inhibition associated LCR is more prominent in newborns (Thach, 2001) compared to adults with the same stimulus that produces apnoea in newborns producing only swallowing and coughing in adults. Studies suggest that the LCR may begin a cascade of events that starts with apnoea and leads to sudden infant death syndrome in a small number of infants who possess critical vulnerability (Downing and Lee, 1975; Page et al., 1996; Xia et al., 2013).

The neuronal mechanisms responsible for respiratory rhythm generation involve respiratory central pattern generators (rCPGs). The rCPGs are located in the brainstem and produce rhythmic synaptic drive for respiratory motoneurons (Bellingham et al., 1989) driving the three phases of the respiratory cycle: inspiration, postinspiration and expiration. To date the work done examining the LCR within the context of the overall control of respiration has been very limited. In previous studies, it has been found in piglets that, when there is elevation of brain temperature within or near the nucleus tractus solitarius (NTS), LCR apnoea is prolonged (Curran et al., 2005b). Dialysis of gabazine (a GABA$_A$ receptor antagonist) into the NTS reversed the thermal prolongation of the LCR (Xia et al., 2007). Furthermore, microinjection of an adenosine antagonist into the NTS also reversed the thermal prolongation of the LCR (Xia et al., 2008). Based on these studies, we know that hyperthermia activates GABAergic mechanisms in or near the NTS that are necessary for the thermal prolongation of the LCR. Furthermore, activation of adenosine receptors, located on

GABAergic neurons in the NTS, contributes to thermal prolongation of the LCR. However, the exact neurogenic mechanism of how the reflex apnoea is generated in the brain and which neurons in the NTS serve as an interface between the upper airways and rCPGs are not known. A lack of studies describing the anatomical substrate and sensory pathways of the LCR prevent us from fully understanding the pathological implications of any pathway reconfigurations and for their clinical relevance.

The LCR generation mechanism can be studied under experimental conditions using stimulation of superior laryngeal nerve (SLN). The electrical stimulation of SLN has been successfully used to study different LCR responses such as apnoea (Curran et al., 2005a; Xia et al., 2007; Heman-Ackah et al., 2009), swallowing (Doty, 1951; Kessler and Jean, 1985; Oku et al., 1994; Feroah et al., 2002; Shiba et al., 2007; Sun et al., 2011a; Sugiyama et al., 2014), sneezing and coughing (Ambalavanar et al., 2004; Shiba et al., 2007; Sugiyama et al., 2014). Depending upon the stimulation intensity applied to SLN, the type of LCR response can differ under the same experimental conditions (Kessler and Jean, 1985; Ezure et al., 1993). The SLN provides the sensory innervation to the larynx. It is a branch of the vagus nerve containing both afferent and efferent fibres. The afferents provide sensory innervation to the muscles of larynx and its mucosal lining. Most of the sensory inputs from the different regions of the larynx reach the central nervous system via SLN afferents whose cell bodies are located in the nodose ganglion, and terminals end at various sub-divisions of the NTS, mostly in the interstitial NTS (Soll) (Furusawa et al., 1996; Van Der Velde et al., 2003).

The NTS provides a critical interface between a variety of peripheral sensory inputs and the central nervous system for a wide range of neural control mechanisms including the sensory input for LCR (Jean, 2001; Saito et al., 2002a). It is involved in transferring sensory input from pulmonary afferent input via the vagus nerve for Hering-Breuer reflex (H-B reflex). This reflex is involved in terminating inspiration in a process called 'inspiratory switch off' (IOS) which includes reconfiguration of the rCPGs (Ezure, 2004; Dutschmann and Herbert, 2006a; Kubin et al., 2006; Dutschmann and Dick, 2012). The lung inflation during inspiration activates the pulmonary stretch receptors present in the smooth muscle lining of the lungs which respond to stretch by sending sensory inputs via the vagus nerve to the pons to terminate inspiration allowing expiration to occur. Likewise, the sensory input from

2

the upper airway via SLN for various LCR responses is also mediated through the NTS and has been reported to change the activity of respiratory neurons (Marchenko and Sapru, 2000; Shiba et al., 2007; Kline, 2010; Sugiyama et al., 2014). During high frequency stimulation of the SLN, many inspiratory neurons are silenced but expiratory neurons are either inhibited or tonically activated (Pantaleo and Corda, 1985; Bongianni et al., 1988; Czyzyk-Krzeska and Lawson, 1991). The mechanisms of transfer of the sensory input from pulmonary stretch receptors in the H-B reflex to rCPGs, via an indirect route involving NTS to pons and rCPGs is well established. However, the transfer of the sensory input for the LCR to rCPGs whether by a direct or indirect connection between the NTS and rCPGs is not yet known. Determining this pathway is critical if we are to understand reflex apnoea.

The rCPGs is a collective term used for different regions within the ventral respiratory column (VRC) that work systematically to generate respiratory rhythm and its different patterns depending upon the demand of the body (Smith et al., 2007; Smith et al., 2009; Feldman et al., 2013; Richter and Smith, 2014) under different physiological conditions. As shown in Figure 1.1, the VRC extends caudally from the facial nucleus in the ventrolateral medulla, and consists of the Bötzinger complex (BötC) followed by pre-Bötzinger complex (pre-BötC), rostral ventral respiratory group (rVRG) and caudal ventral respiratory group (cVRG) (Duffin et al., 1995; Smith et al., 2009). The BötC and pre-BötC are the two key components that produce the initial respiratory rhythm and different respiratory patterns in the VRC (McCrimmon et al., 2000; Smith et al., 2007). A group of chemosensitive neurons identified in the retrotrappezoid nucleus/para-facial region (RTN/pFRG), located just rostral to the BötC underneath the facial nucleus (Smith et al., 1989; Smith et al., 2009) is also considered an important component of the rCPGs. Many of these chemosensitive RTN neurons drive the respiratory rhythm generator neurons according to the levels of expired CO_2 (Abbott et al., 2009; Guyenet et al., 2009; Pagliardini et al., 2011; Takakura et al., 2014). Although the scientific opinion is divided, the neurons in the pFRG are considered critical for generating expiratory rhythm.

The central respiratory rhythm is a periodic generation and transitioning of the different respiratory phases (inspiration, post-inspiration and expiration) which

TRANSVERSE VIEW
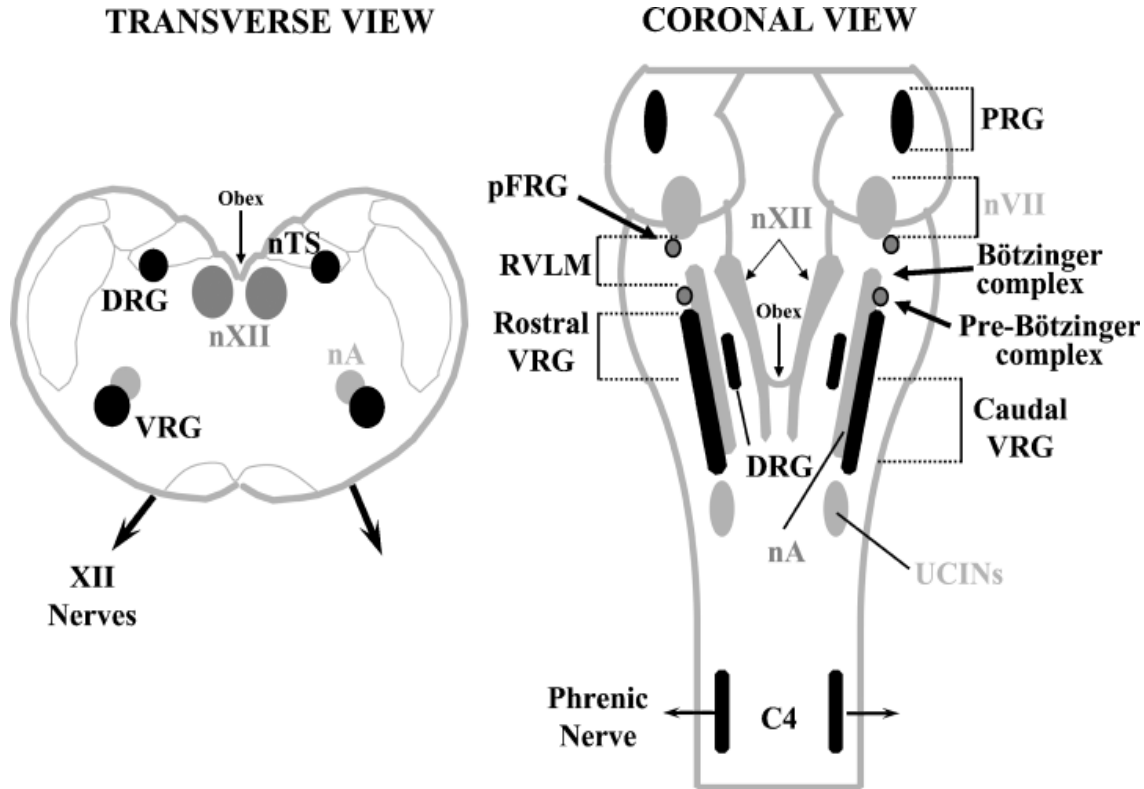
CORONAL VIEW

Figure 1.1 schematic representations of VRC and caudal nucleus ambiguus (nA) in brainstem. In the coronal view, the bilateral organization of two columns of VRC and caudal NA is shown. The obex is shown in the middle with NTS region along its sides as shown in transverse view. Abbreviations: NA, nucleus ambiguus; nVII, facial nucleus; nXII, hypoglossal nucleus; nTS, nucleus of the solitary tract; DRG, dorsal respiratory group; PRG, pontine respiratory group; RVLM, rostral ventrolateral medulla; pFRG, para-facial respiratory group; VRG, ventral respiratory group; and C4, corresponding segment of the spinal cord Source (Duffin, 2004)

involves the synchronised activity of neurons and muscles in upper airways, thoracic and abdominal cavity. The inspiration is generated by a network of pre-inspiratory and inspiratory neurons in the pre-BötC (Feldman et al., 2003; Feldman et al., 2013). Most of these pre-BötC neurons are excitatory in nature, with voltage-dependent pacemaker-like properties (Smith et al, 1991) and are critical for inspiration. They interact with expiratory neurons in the BötC to generate different respiratory patterns (McCrimmon et al., 2000). The neurons in the BötC are inhibitory in nature, with wide connections with other respiratory neurons (Ezure, 1990). In response to the sensory inputs in different physiological conditions, breathing patterns generated by the mutual activity of neurons in BötC and pre-BötC are then conveyed to pre-motor neurons in the rVRG and cVRG before transporting to different motoneurons that

control the larynx, diaphragm and other respiratory-related muscles (Feldman et al., 1985; Merrill and Lipski, 1987) for different breathing motor outputs. Both rVRG and cVRG neurons are excitatory in nature, with rVRG neurons modulated with an augmenting inspiratory pattern but cVRG neurons modulated with an augmenting expiratory pattern (Dobbins and Feldman, 1994; Ezure et al., 2003). The discharge pattern of rVRG phrenic motoneurons, is observed with electrophysiological recordings by recording the activity of phrenic nerve called as phrenic nerve discharge (PND), to monitor the respiratory activity.

During SLN evoked apnoea the sensory input has been reported to influence the activity of phrenic and laryngeal motoneurons. An intravenous injection of chloride ions (Cl^-) reverses the hyperpolarised membrane potentials of the recorded phrenic motoneurons, suggesting a direct inhibition involved in the apnoeic response (Bellingham et al., 1989). Further studies showed that the SLN evoked apnoea can be abolished by intravenous injection of bicuculline, a $GABA_A$ antagonist, suggesting that there exists a central GABAergic pathway in the apnoeic response (Abu-Shaweesh et al., 2001). With regard to the laryngeal motoneuron response to SLN evoked apnoea, all the inspiratory laryngeal motoneurons (ILM) were found to be silenced, but expiratory laryngeal motoneurons (ELM) were found to be tonically activated (Barillot et al., 1984b; Jiang and Lipski, 1990; Jean, 2001; Ludlow, 2005). The inspiratory and expiratory laryngeal motor neurons (ILM and ELM) control the dilator and constrictor muscles of the larynx during respiration respectively. The firings of ILMs during inspiration opens the vocal cords and permits air-flow into the lungs (Baekey et al., 2001; Sun et al., 2002). The activities of ELMs during expiration partially constrict the vocal cords to prevent the collapse of the lungs (Berkowitz et al., 2005; Ono et al., 2006). Both the laryngeal motoneurons are located in the caudal nucleus ambiguus (NA), just above the rVRG and cVRG (Ono et al., 2006; Sun et al., 2008) in the ventrolateral medulla.

In a recent study, conducted by our group, the effects of varying stimulation frequency of the SLN on phrenic nerve discharge and ELM tonic activity was studied. As shown in Fig. 1.2, when the SLN was stimulated at a low frequency (1-5 Hz) during extracellular recording from an ELM, there were absences of PND, and the absence

of a PND was preceded by a burst of ELM activity. As stimulation frequency of the
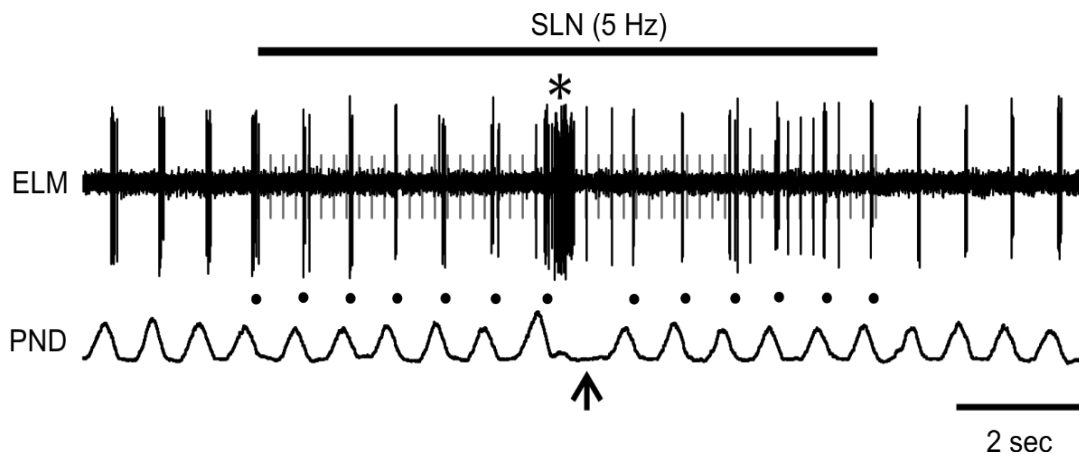

Figure 1.2 Responses from an expiratory laryngeal motor neuron (ELM) and phrenic nerve discharge (PND) to 5 Hz stimulation of the superior laryngeal nerve (SLN). The arrow indicates the absence of one PND that is preceded by a burst activity of the ELM (asterisk). The regular post-inspiratory firing of the ELM during the SLN stimulation is marked by the filled dots. (Modified from Sun et al., 2011)

SLN increased, more burst activities of the ELM were generated, and this, together with resulting absence of PND, led eventually to phrenic apnoea (Sun et al., 2011a). The intimate association between the ELM burst activity and missing PND suggested that there is a potential relationship between the two phenomena. However, the ELM are exclusively laryngeal motoneurons and project their axons to the recurrent laryngeal nerve (RLN), and do not have any connection with rCPGs that could produce the resulting phrenic apnoea. It was proposed that the same synaptic drive that produced the ELM burst might also produce the same burst activity in respiratory neurons that have inhibitory connections to the respiratory pace-making neurons in the pre-BötC or BötC. A possible role for the BötC neurons involved in the apnoeic response was further examined using microinjections of the GABA agonist, isoguvacine, to inactivate the inhibitory neurons in the BötC (Sun et al, 2011). The postinspiratory neurons in the BötC express inhibitory markers and are known to project to phrenic pre-motor neurons in the rVRG (Oku and Dick, 1992; Haji et al., 2002). Furthermore, the BötC inspiratory neurons cause inhibition of neurons in the pre-BötC during early expiration (Bongianni et al., 2010; Richter and Smith, 2014).

As shown in Fig. 1.3 an initial microinjection of isoguvacine into the ipsilateral BötC significantly weakened the apnoeic response to SLN stimulation, while, as expected, the ELM burst activity was not affected. Since these burst activities are known to

6
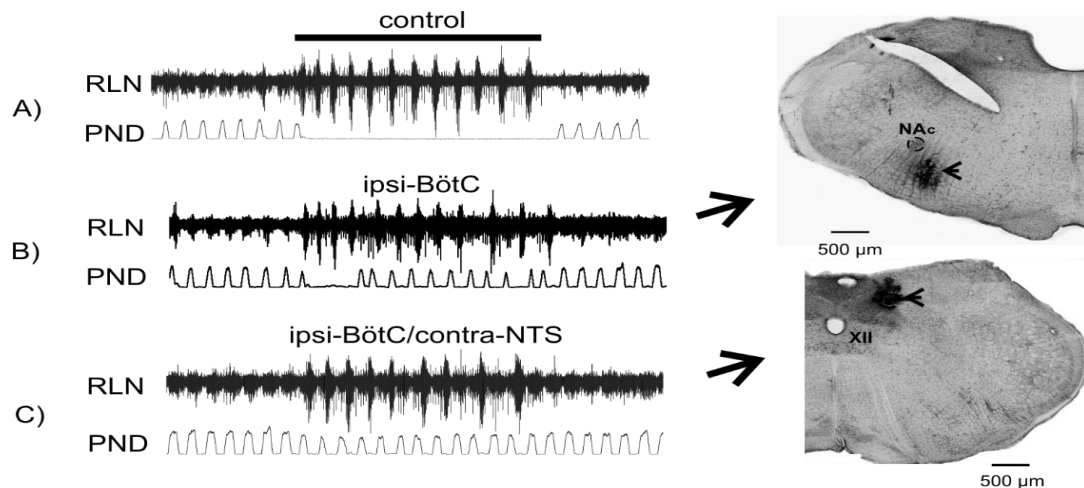
Figure 1.3 Effect of microinjection of isoguavacine (ISO) on expiratory laryngeal motor neuron burst activity and phrenic nerve discharge (PND), monitored by recording from the recurrent laryngeal nerve (RLN) during superior laryngeal nerve (SLN) stimulation. **(A)** Normal apnoeic response during the SLN stimulation. **(B)** Effect of a microinjection of ISO into the ipsilateral BötC. **(C)** Effect of a subsequent ISO microinjection into the contralateral nucleus tractus solitarius (NTS). Scale bars = 500 μm, (NAc) The nucleus ambiguus compact formation and XII: Hypoglossal nucleus. . (Modified from Sun et al., 2011).

synchronise bilaterally in the NTS (Jean, 2001), a feasibly hypothesis is that the contralateral BötC neurons might also be activated during the SLN stimulation to contribute to the apnoeic response. Since direct bilateral inhibition of the BötC would stop central respiration, an isoguvacine injection was made into the contralateral NTS to prevent the BötC neurons from activating the synchronised burst activity. As shown in Fig. 1.3C, after the microinjection of isoguvacine into the contralateral NTS, PND did not cease during SLN stimulation. Based on these electrophysiological and pharmacological findings, a bifurcating projection from the NTS to both nuclei: the BötC and caudal NA was proposed, which functions to control the ELM burst and phrenic apnoeic response (Sun et al, 2011). In particular, the former (NTS-BötC) sends burst activity to the BötC to initiate the apnoeic response, while the latter functions to send the same information to the ELM to close the vocal cords.

The projection from the NTS to BötC has been previously demonstrated using tract tracing studies (Alheid et al., 2011). There is also good evidence to show that there are projections from the NTS to the laryngeal motoneurons (LMN) located in the caudal NA (Hayakawa et al., 2000; Sugiyama et al., 2011). However, the predicted bifurcating NTS projections to both of these nuclei have, thus far, not been confirmed

with any anatomical evidence. Therefore, the aim of the present study was to identify neurons in the NTS that have dual projections to both the BötC and the caudal NA nuclei, and thereby provide anatomical proof of the existence of a bifurcating pathway. The primary hypothesis addressed therefore was that "if dual projecting neurons exist in the NTS with simultaneous projections to the BötC and the caudal NA, acting as a neuroanatomical substrate for the temporal association between apnoea and vocal cords adduction". This concept is illustrated in Figure 1.4. We tested this hypothesis by using a multiple tract tracing technique to address the following aims:

<u>Aims and objectives</u>

1. To identify neurons in the NTS with simultaneous projections to the BötC and the caudal NA. This was done by microinjecting retrograde tracer into BötC and the caudal NA. The presence of retrograde labelled neurons in the NTS with simultaneous projection to BötC and the caudal NA was examined.

2. (a) To determine the rostral to caudal distribution of traced neurons (single labelled and double labelled) within the NTS. This was achieved by analysing the NTS column between brain regions (Interaural -3.00 to (-5.64mm).
    (b) To determine the number of dual projecting neurons in comparison to the number of single labelled neurons in the NTS from the BötC and the caudal NA. This was achieved by analysing the NTS column between brain regions (Interaural -3.00 to (-5.64mm).
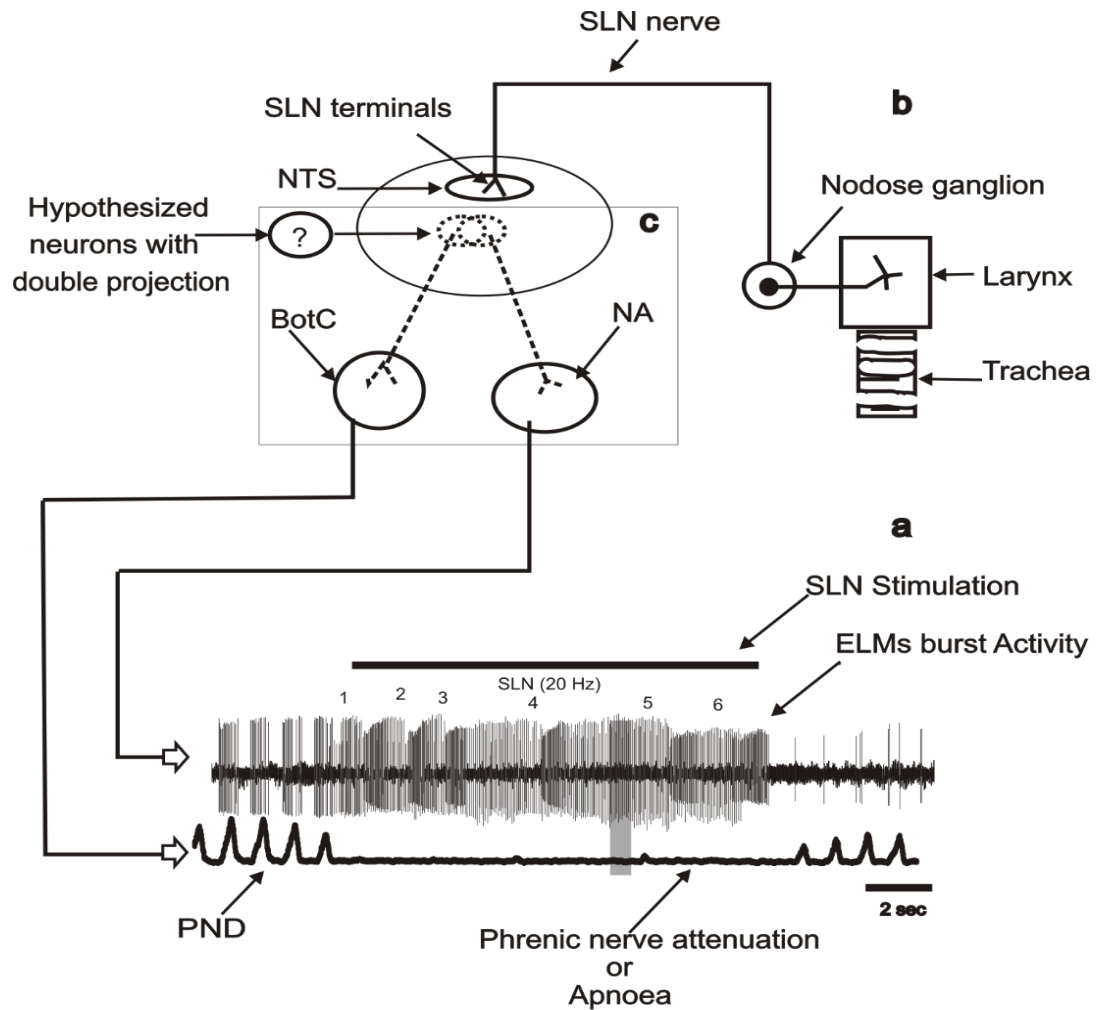
Figure 1.4 Overall concept of the project (a) Temporal association between expiratory laryngeal motor neuron (ELM) burst activity and phrenic nerve attenuation. Superior laryngeal nerve (SLN) stimulation of 20Hz inhibits phrenic nerve discharge (PND). (b) Sensory pathway of SLN nerve (c) Hypothesised neurons with dual projection to BötC and the caudal nucleus ambiguus (NA): neurons in the BötC controls PND and in the caudal NA control vocal cords (Modified from Sun et al., 2011).

Outcomes

The result of this study would provide confirmation of the existence of dual projecting neurons in the NTS responsible for apnoeic responses during SLN stimulation. This study would provide the first anatomical proof of the pathway of neurons involved in mediating SLN sensory input to rCPGs. The study of such neurons is critical in understanding the generation mechanism of LCR apnoea in both normal and pathological conditions. Therefore, we will determine the presence of dual projecting neurons in the NTS by using multiple retrograde tracts tracing technique.

Chapter 2: Methods

All the experimental procedures for this study were approved by The Macquarie University Animal Ethics Committee (ARA 2011/039) and were carried out in accordance with the Australian Code of Practice for the Care and Use of Animals for Scientific Research (National Health and Medical Research council 8th Edition, 2013). The animals used in this project were obtained from the Animal Resources Centre Perth, Western Australia, and housed at the Central Animal House Facility Macquarie University. Animals were group housed with libitum access to standard rat chow and water. Experiments were performed on male Sprague Dawley rats (body weight: 380-550g, n=25). Out of 25, n=13 were used for the optimization of the experimental protocol.

2.1 Anaesthesia

For the acute non-recovery experiments the animals were deeply anaesthetized with an intraperitoneal (i.p.) injection of urethane 1.3g/kg with an additional dose of 130 mg/kg (as required). For the recovery experiments for the injection of retrograde tracers, the animals were anaesthetized with ketamine (0.75mg/kg, i.p. Ceva, Australia) / medetomidine (0.5mg/kg, i.p. Pfizer, Australia). The depth of the anaesthesia checked regularly during surgery by examining the withdrawal response reflexes and a top-up dose of ketamine (0.075mg/kg, i.p.) was administered as required during the procedure. At the end of the procedure, the α_2 adrenergic receptor antagonist Atipamazole, (1.5mg/kg i.p. Zoetis, Australia), was administered to reverse the effect of medetomidine. For the terminal perfusion protocol, animals were deeply anaesthetized with sodium pentobarbital (72mg/kg, i.p.).

2.2 Surgical procedures

The animals were transferred from the Central Animal House Facility to the research laboratories of the Department of Biomedical Science, Macquarie University. *Retrograde tracer injections.*
Animals were anaesthetised and a subcutaneous (s.c.) injection of analgaesic carprofen (5mg/kg, Norbook Laboratories, Australia) was administered for pain relief and an antibiotic cephazoline (20-40 mg/kg, s.c. Hospira, Australia) used for prevention of infections. The body temperature of the rat was maintained at 36-37°C using a rectal

thermometer probe with homeothermic Monitor (Harvard, SDR Clinical Technology, Australia). The fur on the back of the neck and left side of the face was shaved and an eye lubricant was applied to protect the corneas. The rat was then moved into a stereotaxic frame for surgery. Ip injections of 0.9% saline (0.1ml/g BW) were given every half hour during surgery to maintain hydration status.

All surgeries were performed under aseptic conditions. A midline incision was made along the skull and connective tissues separated to expose the bone. The lambda landmark was identified on the skull and a small hole drilled 1.5 mm lateral from the midline and 3 mm caudal to the lambda suture line (Figure 2.1). A craniotomy was carefully made with the help of a fine bone rongeurs and the brain exposed by extending the hole into a skull opening extending 1- 2.5 mm lateral from the midline and from 0 - 4.5 mm caudal to the lambda suture line (zero being the lambda suture line and 4.5 close to cerebrospinal junction). Bone wax was applied to seal the edges of the bone to avoid embolism. The dorsal surface of the brain was exposed after removal of the dura mater.

2.3 Facial nucleus mapping

The caudal pole of the facial nucleus was mapped in order to determine the location of the BötC (Lipski, 1981; Pilowsky et al., 1990). Firstly, the facial nerve was exposed by making a small cut on the left side of the face. A standard bipolar electrode was
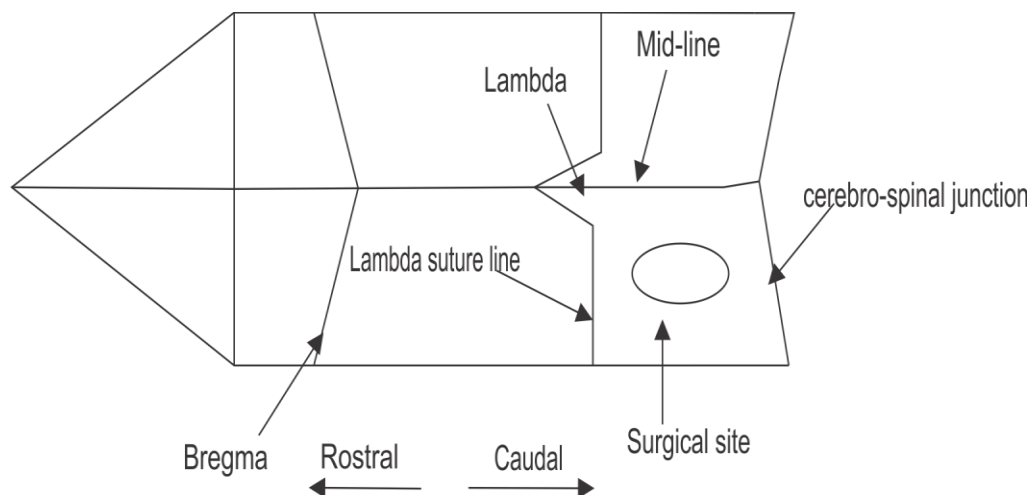

Figure 2.1 Schematic of the anatomical landmarks on the rat skull. The surgical site represents the hole that was dig in rat's brain for microinjections to the BötC and the caudal NA. The rostral to caudal distances were measured from the lambda suture line taken as zero point.

placed on one of the two branches of the facial nerve for stimulation. A grounding wire was inserted into the surrounding muscle and an electrical stimulation (1 Hz, 0.2 ms pulse width) was applied. The threshold was determined by increasing the stimulating voltage until the facial muscle and whiskers started twitching in response to the stimulation. The stimulation intensity was then set at 1.5 times the threshold. Low impedance microelectrodes for mapping the facial nucleus were pulled from borosilicate glass capillaries (GC120TF-10, Harvard, SDR Clinical Technology, and Australia) by a microelectrode puller (Sutter P2000, USA). Electrodes were filled with 3M NaCl and resistance was adjusted between 5-10 MΩ. Mapping was initiated by placing the recording electrode into the brain at 1.5 mm lateral from the midline, 2 mm from the lambda suture line, and 8-10 mm deep from the dorsal surface of the brain using an electrode manipulator (PI C-819.20, CH

Products, USA). The facial field was determined as a strong downward deflection of constant response latency of about 2 ms from the stimulation artefact once the electrode was found inside the field of nucleus. The consistent recording at the caudal pole were made as described by (McMullan, 2013). Once the caudal pole of facial nucleus was found, the electrode moved 200 um caudal to the facial nucleus to record expiratory unit activities. Once the expiratory activity found, it was regarded as a good indication for location of the BötC. All the coordinates were recorded at this point for the BötC microinjection.

2.4 Preliminary experiments

A series of pilot studies were undertaken. The first was done to optimize the coordinates of the two injection sites for BötC and NA microinjections with reference to the lambda suture line in a non-recovery experiments (n=5). A microinjection of pontamine Sky Blue (1%) (Sigma Aldrich USA) was made to the BötC and the caudal NA. After microinjection, the animals were immediately perfused with fixative as detailed below in section 2.7 and the results were used to adjust the coordinates.

The second series of pilot study was performed to optimize the combination of retrograde tracers used and recovery time frames for efficient retrograde labelling to the NTS from the injection sites (n=8). Different combinations of tracers such as Fluorogold (Fluorochrome, LLC, USA), Dextran (Invitrogen USA), fluorescent conjugates of CTB (CTB-555, CTB-488) (Invitrogen USA), and unconjugated CTB

(Invitrogen USA) were tried for the microinjections. The animals were allowed to recover for 3-5 days as detailed below in section 2.6. Tissues from some of these animals were also used to optimise the immunohistochemical protocol for the detection of unconjugated CTB, with dilutions of primary antibody being tested.

2.5 Pressure microinjection of retrograde tracer

2.5.1 BötC microinjections

Following localisation of the BötC through mapping of the facial nucleus as detailed in section 2.3, the recording electrode was replaced with a microinjection electrode (1.0 MM ×0.25 MM "4", A-M System. Inc. USA) of diameter 20 -40um, filled with retrograde tracer (1% v/v of cholera toxin B (CTB) conjugated to Cy3 (CTB-555). Injections were targeted at 2.6 - 2.8 mm caudal to the lambda suture line (equivalent to 0.3-0.5 mm caudal from the facial nucleus), 8.8 - 9.2 mm deep from the dorsal surface, and 1.6 - 1.7 mm lateral to the midline. A 20 nl pressure injection was made using 1ml Hamilton syringe. One to two minutes after the microinjection, the injection electrode was gently removed out of the brain.

2.5.2 Nucleus ambiguus microinjections

The stereotaxic coordinates for the caudal NA were obtained from the rat atlas(Paxinos et al., 2009). The microinjections were targeted at 4.0 - 4.5 mm caudal to the lambda suture line, 1.5 - 1.6 mm lateral to midline and 8.6 - 8.9 mm deep from the dorsal surface of brain. A 20 nl pressure injection of unconjugated CTB (1% v/v) was made as detailed above. All the microinjections were made on the ipsilateral side.

2.6 Animal recovery and post-operative care

The wound sites were closed with surgical thread and the animals closely monitored during their recovery period in a warmed environment. After full recovery (usually 4 - 5 hours) the animals were returned to the animal house. In the post-operative period, carprofen (2.5mg/Kg) was administered (once daily) for pain relief as required. Sub-cutaneous fluid injections were also administered as required to maintain hydration. The animals were provided with supplementary diet (88-0004 Napa Nector) along with the normal standard meal during the recovery period.

2.7 Perfusion and fixation

Three to five days after the microinjections of retrograde tracers, the animals were returned to the laboratory and deeply anesthetized with an i.p. injection of 20% (v/v) solution of sodium pentobarbital (72mg/kg). The heart was exposed and animals were transcardially perfused with 200 - 250ml 0.9% saline followed by 4% paraformaldehyde solution (400 - 500ml). A heparin injection (Hospira, Australia) (1U) was administered onto the ventricle prior to the perfusion. The brain was removed and the brainstem dissected and then postfixed overnight in the same fixative at room temperature.

2.7 Immunohistochemistry

After removing the dura, the brainstem was mounted on the platform of a vibrating microtome (Leica Biosystems, VT1200 S, Germany) supported in place with 2% w/v gelatine. Fifty µm thick coronal sections were cut and collected in tris phosphate-buffered saline (TPBS, 10 mmol/L Tris, 0.9% NaCl, 10 mmol/L phosphate buffer, pH 7.4). The sections were collected into four series separated by 200µm. One series of sections were rinsed with TBPS (3×30 min) and then mounted directly onto slides for direct visualisation of CTB-555. The sections in other three series were used for immunohistochemistry to visualise unconjugated CTB. Sections were washed with PBS Tween 20 (0.1%, 3×30 min) and then incubated for 20 min in a blocking solution of 10% normal horse serum (v/v, Jackson Immuno Research, USA) in TPBS containing 0.05% merthiolate (TPBSm, Sigma, USA). The sections were then incubated in primary antibody (goat anti CTB, 1:50,000) as previously optimised for staining quality, for 72 hours on a shaker at room temperature. The sections were then washed with TBPS (3×30min), followed by 30 min incubation in normal horse serum (2% v/v) in TBPSm. At this point the sections were incubated in secondary antibody (donkey anti goat conjugated to for fluorescein isothiocyanate (FITC, 1:500, JACKSON Immuno Research laboratories, USA) for 24 hours at x temperature. Sections were again rinsed with TBPS (3×30 min) and were mounted on clean, dry slides and cover slipped using Dako fluorescent mounting media (Vector Laboratories, USA).

2.8 Microscopy and image analysis

Sections were visualized using a ZENPRO epifluorescence microscope (Zeiss Gottingon, Germany), with Zeiss standard band pass fluorescent filters for FITC and tetramethylrhodamine (CTB-555). Digital micrographs of the injection sites were obtained using a 5X objective lens with tiled images. Digital micrographs of the NTS region spanning across interaural regions -3.00 to -5.64mm) were taken using a 10X objective and tiled.

Images were analysed for the number of single labelled and double labelled neurons in the NTS. The Interaural level of the NTS relative to the obex was determined based on neuroanatomical landmarks. Sections were then identified as rostral to obex (distances as positive numbers) and the caudal to obex (distances as negative numbers). The numbers of single labelled and double labelled neurons were then counted per section for each animal (both ipsilateral and contralateral to the site of injection). Results for each animal were then plotted using GraphPad Prism Version 6 software. The region of the NTS with the maximum number of the retrograde labelled neurons was then further analysed for the distribution of labelled neurons within various NTS sub-divisions.

Chapter 3: Results

3.1 Summary of outcomes of pilot studies

The pontamine skyblue experiments allowed refinement of the coordinates for the BötC and caudal NA injection site with respect to lambda suture line. In the atlas (Paxinos et al., 2009), the rostral-caudal coordinates for BötC range from interaural -3 to -3.48 mm, (corresponding to Bregma 12.00 mm – 12.48 mm) with a depth of approximately 8mm below the surface of the brain and 1.8 to 2 mm lateral from the midline. Using Bregma co-ordinates to determine the BötC microinjection required the exposure of a wider area on the skull, and we therefore used the lambda land mark as a point of reference to minimise the surgical exposure site. The optimized rostral to caudal coordinates for the BötC caudal to the lambda suture line ranged from 2.5 to 3.0 mm. The lateral coordinates for the BötC were optimized from 1.8mm to 1.65mm lateral to the midline. The depth for the BötC injections, determined by recording facial field, varied between 8.6 - 9.2 mm deep from the dorsal surface of the brain.

For the caudal NA, atlas co-ordinates range between: rostral to caudal Interaural -4.56 to -5.16mm, located at a depth of 8 - 8.5 mm from the dorsal surface of the brain and ~2 mm from the midline. Our final coordinates adjusted by analysing the injections sites with reference to the BötC injection site and caudal to lambda suture line were: rostral-caudal 4.0-4.5 mm, the lateral coordinates of 1.5 to 1.6mm were found right to target at the NA. The depth for the caudal NA was adjusted with reference to the depth of BötC microinjection. The microinjections to the caudal NA were always made 2 – 3 mm shallow than BötC. The coordinates for the depth of NA from 8.6-8.8mm were found suitable to target NA

As part of our studies to optimise the use of two retrograde tracers, one from the NA and one from the BötC, we trialled different combination of CTB-555 such as CTB-555 + CTB-488, CTB-555 + unconjugated CTB, CTB-555 + Fluorogold, Dextran + CTB-488 and Dextran + unconjugated CTB. Of the different combinations, the combination of CTB-555 injected into the BötC and unconjugated CTB injected into the NA provided the best results, based on reliability of retrograde labelling from each site and ability to differentiate the tracers in the NTS. CTB-555 gave the best result in terms of retrograde labelling with high signal to noise ratio. It did not need any amplification to detect robust retrograde neuronal labelling.

Fluorogold had very low native fluorescence and would have required secondary detection with an anti-fluorogold antibody to achieve adequate detection. Additionally, Fluorogold injections had a large spread around the injection site when compared to that of CTB-555 and unconjugated CTB. When used at a concentration of 4%, Fluorogold produced necrosis at the injection site. The dilution of Fluorogold to 2% reduced tissue damage but resulted in more diffused injection sites and less efficient neuronal labelling. Similar to the Fluorogold, the Dextran produced a large amount of diffusion at the site of injection and was unsuitable as a retrograde tracer.

Experiments were also undertaken to determine the best recovery time period for each tracer. Three to 4 days were essential for retrograde labelling for all CTB tracers, except CTB-488, which we could not get to work out in any of the trial experiments. For Fluorogold, even after 5-days the labelling was poor however while a recovery period of 7-15 days is recommended in the literature for Fluorogold (Alheid et al., 2011) necrosis at the injection site was evident after five days.

The tracer combination of CTB-555 into the BötC and unconjugated CTB into the NA was determined as giving the best results and final optimisation experiments were undertaken to ensure there was no cross labelling of CTB-555 when using the CTB primary antibody to detect the unconjugated CTB. Titration experiments were undertaken with different primary antibody (goat anti-CTB) concentration (1:10,000, 1:12,500, 1:25,000, 1:50,000), with a concentration of 1:50000 resulted in no cross labelling of the CTB-555. A total of n=12 animals were then studied under the defined optimized conditions. Out of these, four had successful microinjection to the BötC (Fig. 3.1A) and out of these 2 also had successful NA microinjections (Fig. 3.5A). The results of these 2 animals were selected for this study.

3.2 BötC projecting NTS neurons
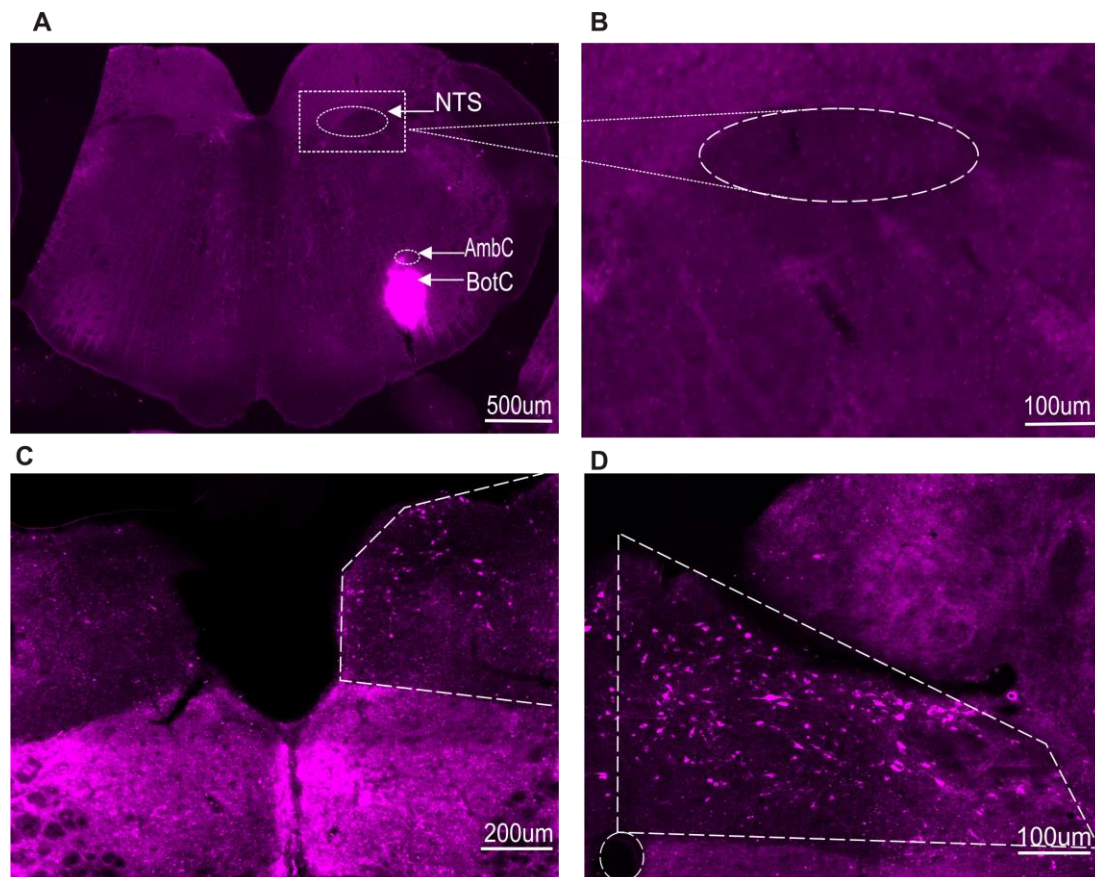
Figure 3.1. BötC microinjection and retrograde labelled neurons in the nucleus tractus solitarii (NTS). (A) BötC injection site. The injections were considered within BötC when located caudal to facial nucleus and ventral to the compact part of the nucleus ambiguus (NAc), which is visible dorsal to the BötC. **(B)** At the level of the BötC, no retrograde labelling is evident in the NTS. **(C)** The NTS region 0.84mm rostral to the obex and **(D)** 0.36mm rostral to the obex, showing an increasing number of retrograde labelled neurons. The NTS region is highlighted in each panel.

The successful microinjection of CTB-555 into the BötC was confirmed anatomically by direct visualization of the sections under the fluorescent microscope (Fig. 3.1A). Successful injections were within the coordinates of the BötC as described in the atlas for BötC and the injection site was found at level (Interaural -3.24 mm) (Fig. 3.1). The injections sites were 2.79 ± 0.3mm deep from the dorsal surface of the brain, covering an area of $\sim 250 - 252$ mm^2. The centre of the injections was 1.8 - 2.0 mm lateral from the midline. At the level of the BötC injection site, no retrograde labelled neurons were found in the NTS (Fig. 3.1B). Analysis of the NTS from rostral to caudal showed gradually increasing number of retrograde labelled neurons towards the obex (Fig. 3.1C, D).

18

3.2.1 Rostral to caudal distribution of BötC labelled neurons in the NTS

Retrograde labelled neurons in the NTS were assessed from 2.6 mm to -0.36 mm relative to the obex (total of ~ 3 mm). As illustrated in Figure 3.2, very few BötC labelled neurons were found in the ipsilateral NTS at 1.2 mm rostral to the obex, however the numbers of ipsilateral neurons increased gradually with the peak of retrograde labelled neurons occurring at 0.48 mm rostral to the obex. The number of neurons in the ipsilateral NTS then appeared to decline from 0.36 mm rostral to -0.36 mm caudal to the obex.

The numbers of neurons labelled in the contralateral NTS were also counted. Compared to the ipsilateral neurons, there was a smaller distance over which labelled neurons in the contralateral NTS were present (being over the range 0.36 mm rostral to -0.36 mm caudal to the obex). There appeared to be fewer retrograde labelled neurons on the contralateral side per section before the obex, however caudal to the obex the number of retrograde labelled neurones on the ipsilateral and contralateral sides were comparable (Fig. 3.3).
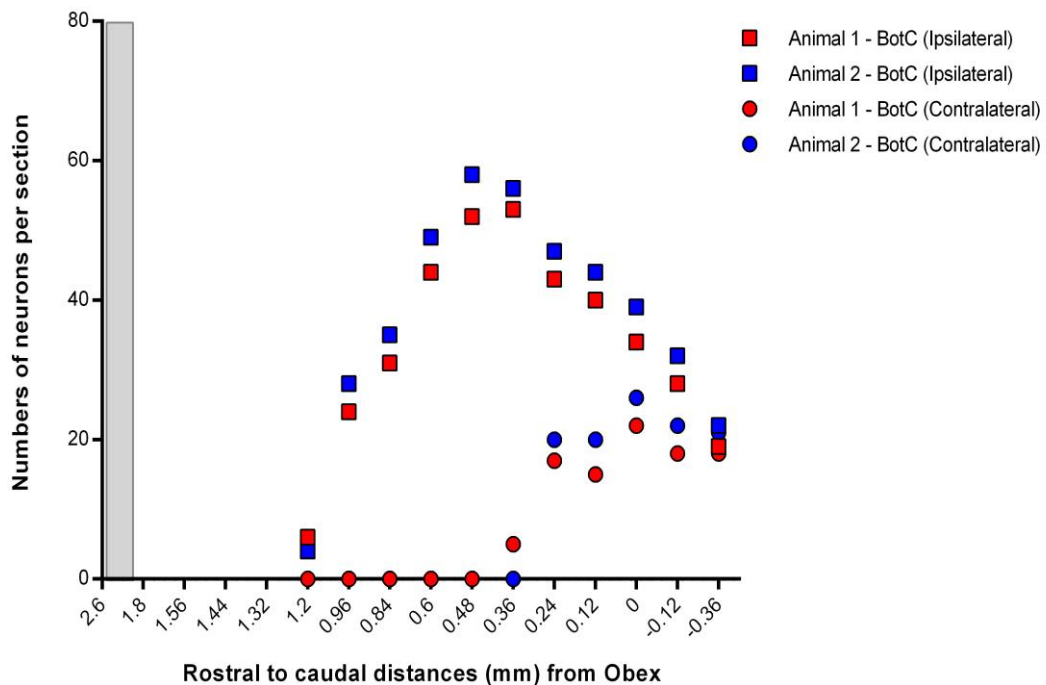

Figure 3.2. Rostral to caudal distribution of nucleus tractus solitarii (NTS) neurons with projections to the BötC. Neurons were mapped from the BötC injection site (2.6mm rostral) to -0.36mm caudal to the obex point at zero. The number

of neurons counted per section at each level is shown for Animals 1 and 2, with neurons on the ipsilateral and contralateral side of the injection are indicated. The shaded grey column at 2.6mm rostral indicates the site of the BötC injection
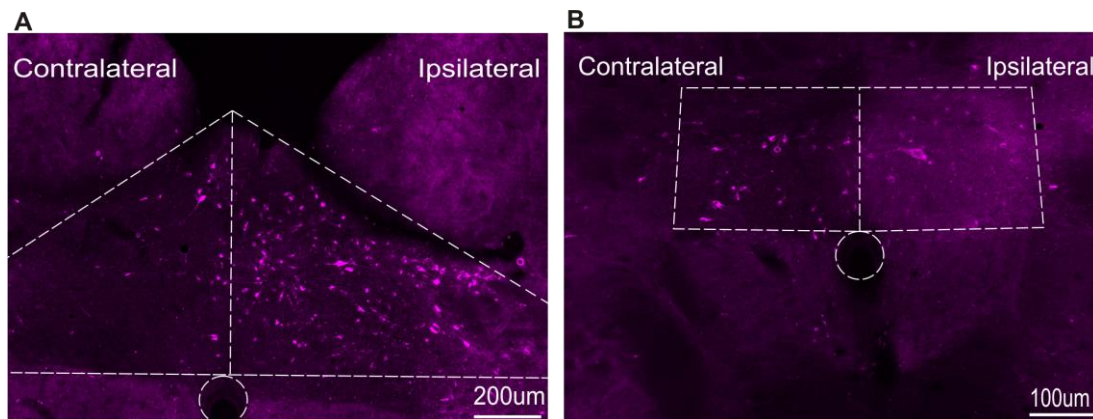
Figure 3.3. Rostral to caudal differences in the number of neurons retrogradely labelled from the BötC in the nucleus tractus solitarii (NTS). Panel **(A)** at 0.36mm rostral to obex illustrated the presence of retrograde labelled neurons from the BötC ipsilateral to the injection site with very few labelled neurons on the contralateral side. Panel **(B)** at-0.36mm caudal to the obex shows retrogradely labelled neurons from the BötC both ipsilateral and contralateral to the injection site. The NTS region is highlighted in each panel.

3.2.2 Distribution of BötC labelled neurons within NTS sub-compartments

The distribution of BötC labelled neurons within different sub-compartments of the NTS was assessed at 0. 36mm rostral to the obex, being that region with the higher number of labelled neurons (Fig. 3.4). Overall, retrograde labelled neurons were found throughout the NTS however they appeared to be grouped in specific NTS sub-compartments. Towards the medial aspect they were seen in in medial (SolM) and intermediate (SolIM) NTS. More dorsally, neurons were located in the caudal (SolDl), interstitial (SolI) and ventrolateral (SolVl) NTS. A few neurons were also seen in ventral part of the NTS (SolV). Comparing between the dorsolateral (SolDl, SolI, SolVL) and mediolateral (SolM, SolIM and SolV) regions of the NTS, the BötC labelled neurons were primarily a in column along the dorsolateral aspect, with separate grouping of neurons in mediolateral half. Very few retrograde labelled neurons were found in sub area prostrema (SubPD) and commissural NTS (SolC).
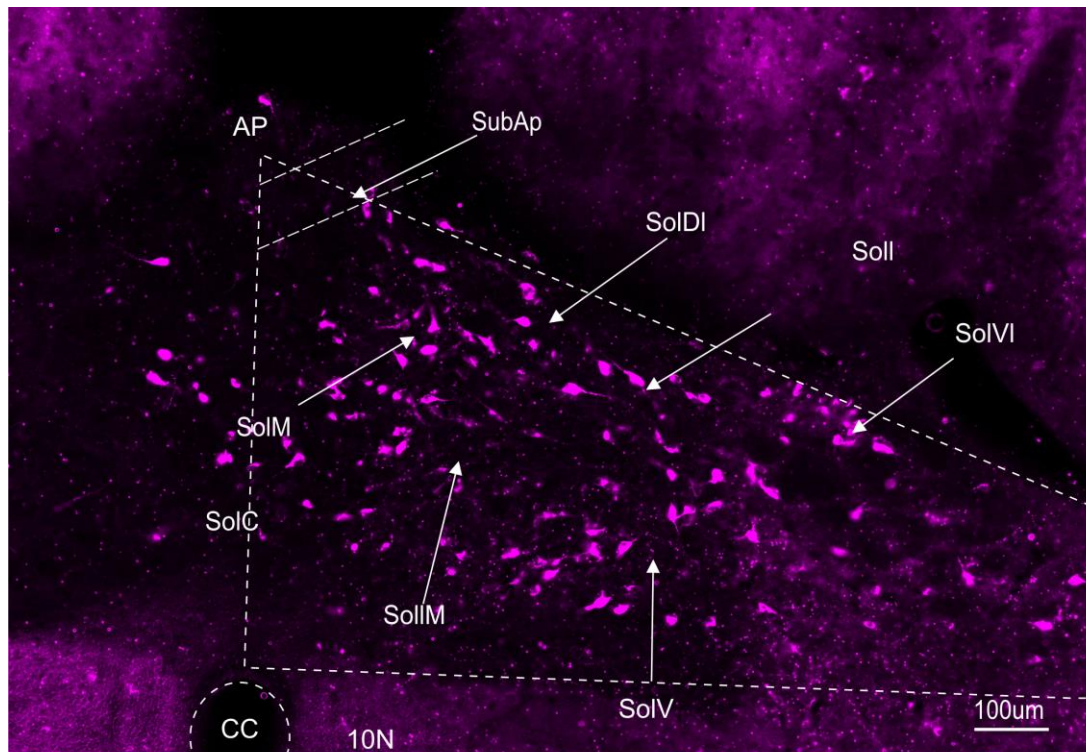
Figure 3.4. Distribution of neurons retrogradely labelled from the BötC within the different subcompartments of the nucleus tractus solitarii (NTS). Figure illustrates the NTS ipsilateral to the BötC microinjection. The dorsal regions of the NTS are the dorsolateral (SolDl), interstitial (SolI) and venrolateral (SolV) regions. The other sub-compartments include the ventral NTS (SolV) and medial regions (SolM), intermediate (SolIM), commissural NTS (SolC) AP (area prostrema) and Sub AP (sub area prostrema). The CC (central canal) and 10N (dorsal motonucleus 10) are also indicated.

3.3. NA projecting NTS neurons

The successful microinjection into the caudal NA was confirmed histologically to a location 0.24 mm rostral to the obex (Fig. 3.5A). The rostral – caudal coordinates for injection site targeted were found (Interaural – 5.16 mm) (Fig 3.5A). Injection sites for the NA were 1.8 -1.9 mm deep from the dorsal surface and covered an area of 127 - 130mm^2, with the centre of the injection 1.7 - 1.8 mm lateral from the midline. Unlike the BötC microinjection, retrograde labelled neurons were found in NTS at the injection site (Fig. 3.5B) and were detected in the NTS both rostral and caudal to the injection site, being distributed between 1.2 mm rostral to -0.36 mm caudal relative to the obex.
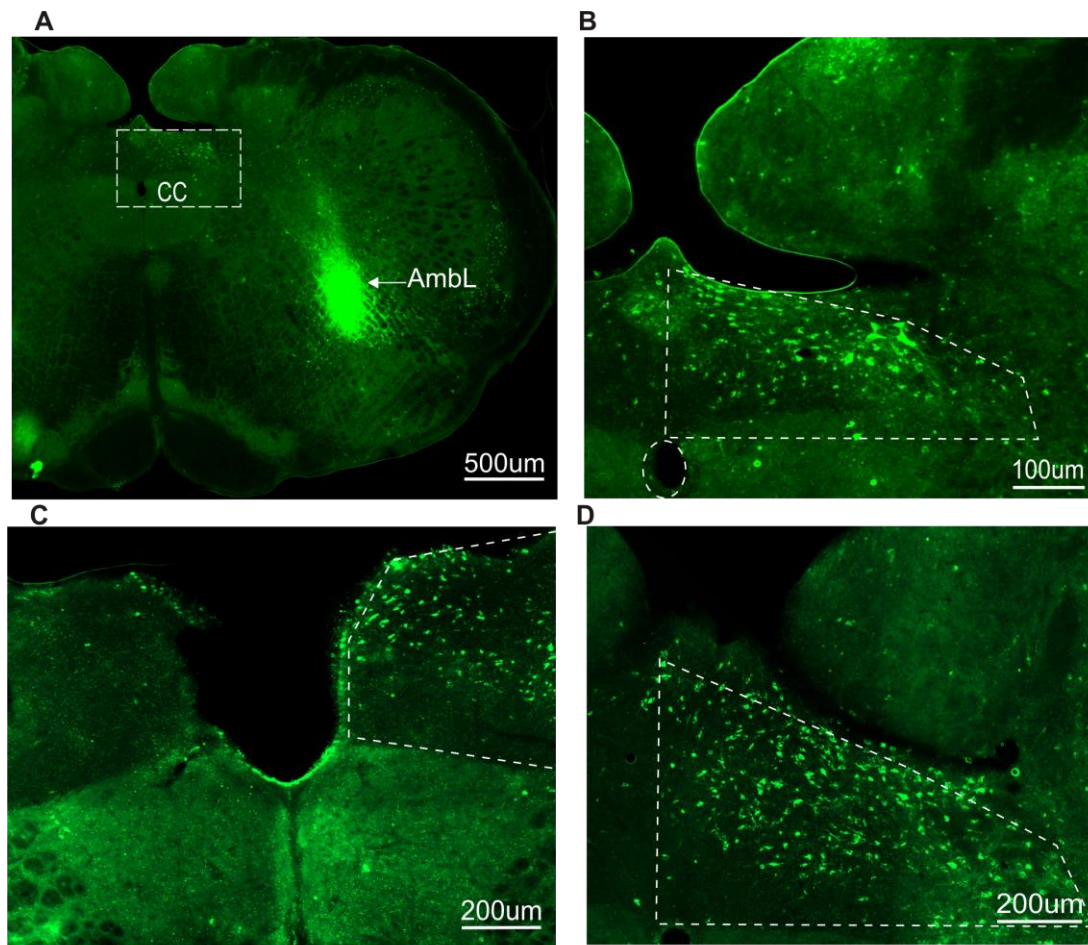
Figure 3.5. Caudal nucleus ambiguus (NA) microinjection and retrograde labelled neurons in the nucleus tractus solitarii (NTS). (A) The injection site at 0.24mm rostral to the obex at zero **(B)** Retrograde labelled neurons were evident in the NTS at the level of the injection site. **(C)** Retrograde labelled neurons from the NA within the NTS at 0.84mm rostral to the obex and **(D)** 0.36mm rostral to the obex. The NTS region is highlighted in each panel.

3.2.1 Rostral to caudal distribution of NA labelled neurons in the NTS

The numbers of retrograde labelled neurons in the NTS were assessed over the same region as for the BötC labelled neurons. As illustrated in Figure 3.6, some NA labelled neurons were found in the ipsilateral NTS at 1.2 mm rostral to the obex, and the numbers of ipsilateral neurons increased gradually with the peak occurring approximately 0.36 mm rostral to the obex. The number of NA labelled neurons then reduced at the level caudal to the obex. Like the BötC labelled neurons, the number of neurons labelled on the contralateral side of the NTS were found to be less than those seen on the ipsilateral side between 0.84 mm to 0.12 mm rostral to the obex, however numbers of retrogradely labelled neurones on the contralateral side increased further

caudal and at 0.24 mm and 0.12 mm rostral to the obex appeared to be comparable to the neurons labelled on the ipsilateral side. The number of neurons on the contralateral side then decreased caudal to the obex. Overall, the number of retrograde labelled neurons at each interaural point appeared greater than the number of BötC labelled neurons at the same level (Figure 3.7).

Figure 3.6. Rostral to caudal distribution of nucleus tractus solitarii (NTS) neurons with projections to the nucleus ambiguus (NA). Neurons were mapped from the BötC injection site (2.6mm rostral) to -0.36mm caudal to the obex point at zero. The number of neurons counted per section at each level is shown for Animals 1 and 2, with neurons on the ipsilateral and contralateral side of the injection are indicated. The grey column at 2.6mm represents the level of BötC injection site and the hashed grey column at 0.24mm represents the NA injection site.
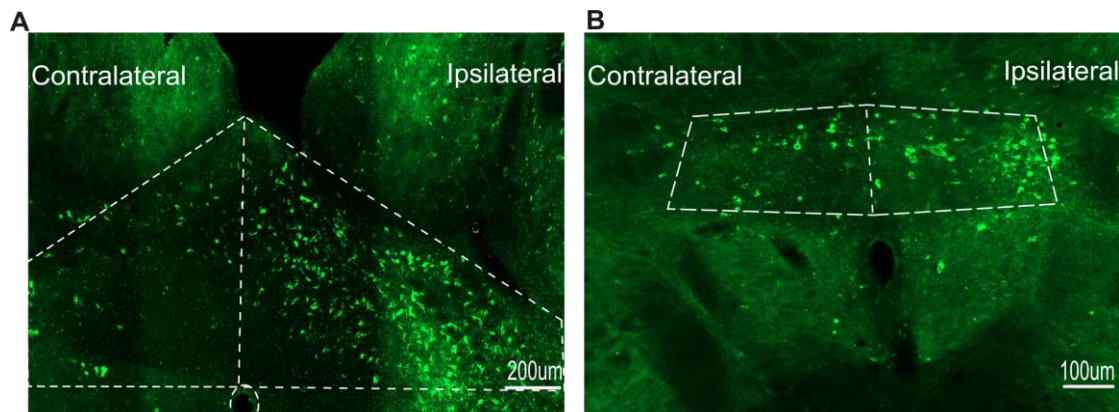
Figure 3.7. Rostral to caudal differences in the number of neurons retrogradely labelled from the nucleus ambiguus (NA) in the nucleus tractus solitarii (NTS). Panel **(A)** at 3.6mm rostral to obex illustrates the presence of retrograde labelled neurons from the NA ipsilateral to the injection site with very few labelled neurons on the contralateral side. Panel **(B)** at -3.6mm caudal to the obex shows comparable numbers of retrogradely labelled neurons from the NA ipsilateral and contralateral to the injection site. CC: central canal. The NTS region is highlighted in each panel.

3.2.2 Distribution of NA neurons within NTS sub-compartments

Neurons with projections to the NA were present in all the sub-compartments of the NTS. Retrograde labelled neurons were found in dorsal (SolDl, SolI,), lateral (SolV, SolVL) and medial (SolM, SollM) compartments at relatively equal frequency (Fig. 3.8). Compared to neurons with BötC projections at the same interaural level, the SolI sub-division of the NTS showed the most obvious difference, with SolI NTS - NA projecting neurons being more numerous than SolI NTS - BötC. Very few retrograde labelled neurons were present in the sub area prostrema and SolC, similar to that seen for BötC microinjections.
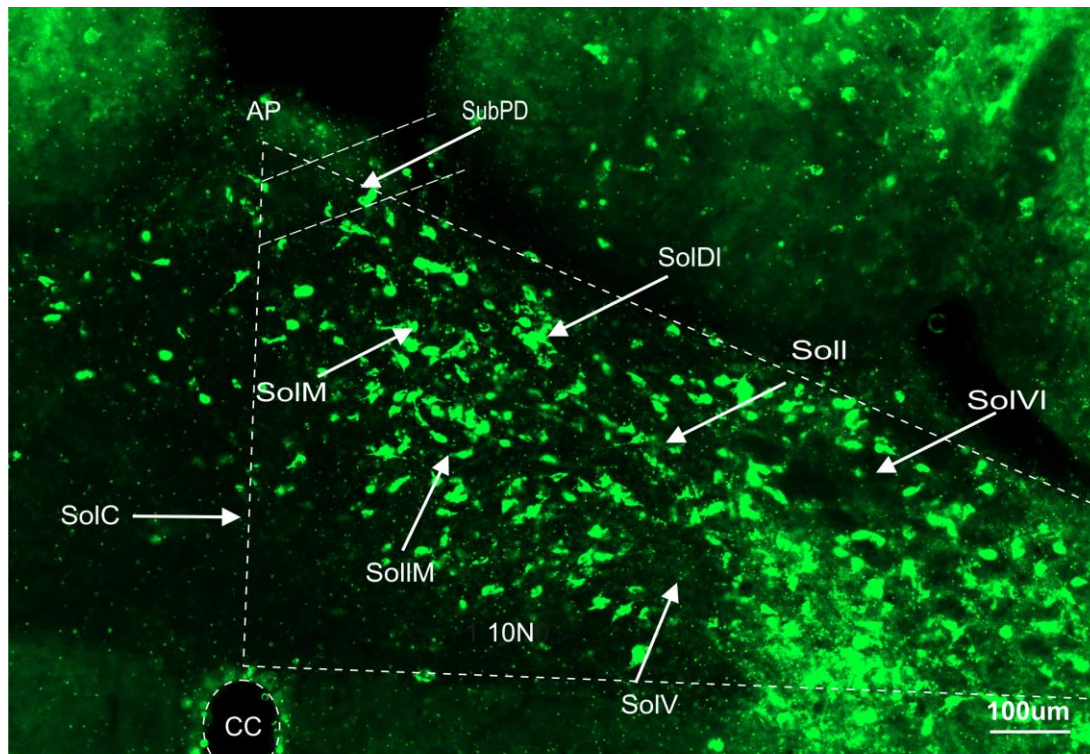
Figure 3.8. Distribution of neurons retrogradely labelled from the nucleus ambiguus (NA) within the different subcompartments of the nucleus tractus solitarii (NTS). Figure illustrates the NTS ipsilateral to the NA microinjection. The dorsal regions of the NTS are the dorsolateral (SolDl), interstitial (Soll) and venrolateral (SolV) regions. The other sub- compartments include the ventral NTS (SolV) and medial (SolM), intermediate (SollM), commissural NTS (SolC) AP (area prostrema) and Sub AP (sub area prostrema). The CC (central canal) is also indicated.

3.3 Distribution, numbers and location of double labelled neurons in the NTS

The double labelled neurons (identifying those NTS neurons with projections to both the BötC and NA) were identified in the most caudal part of the NTS at the level of the obex and only ipsilateral to the microinjections (Fig. 3.9). The different interaural levels where double labelled neurons were identified are illustrated in the Fig. 3.10.
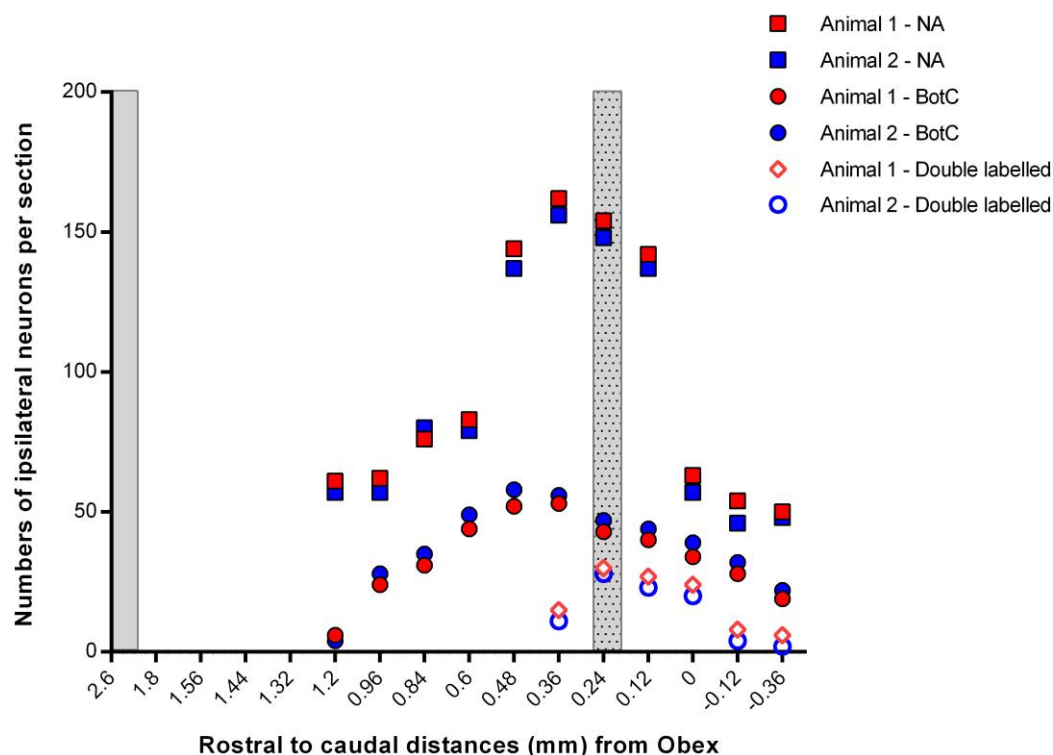
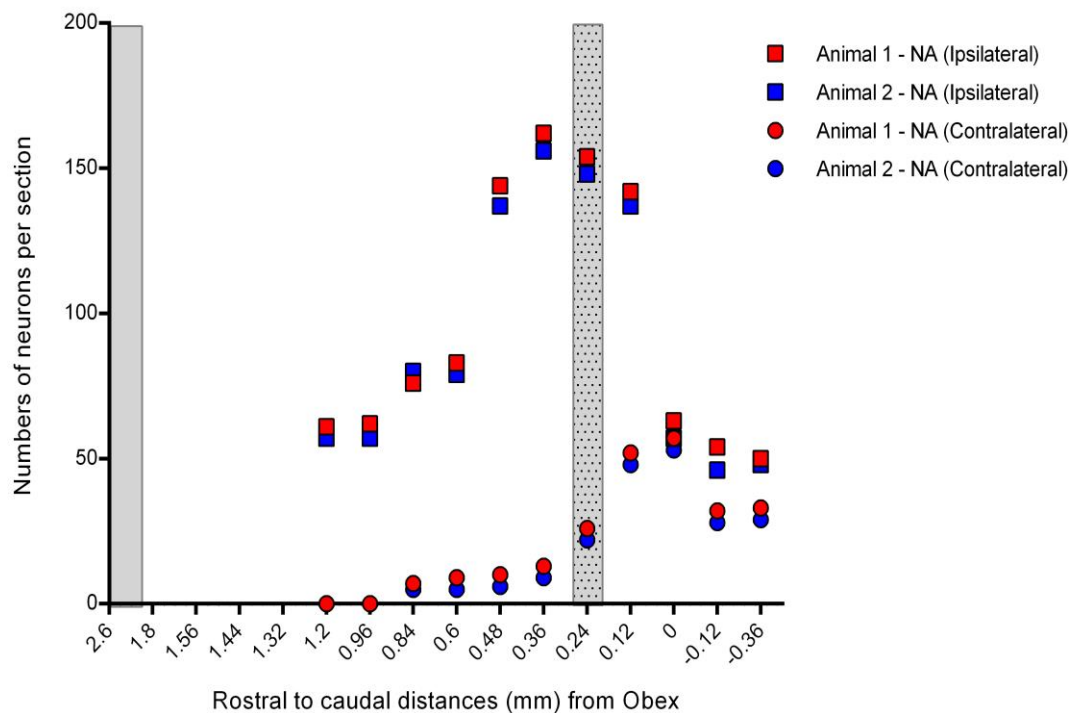**Figure 3.9**. **Rostral to caudal distribution of nucleus tractus solitarii (NTS) neurons with dual projections to the nucleus ambiguus (NA) and BötC.** Neurons were mapped from the BötC injection site (2.6mm rostral) to -0.36mm caudal to the obex point at zero. The number of single (either NA or BötC projecting) or double labelled neurons counted per section at each level is shown for Animals 1 and 2. Only neurons ipsilateral to the injection sites are shown. The grey column at 2.6mm represents the level of BötC injection site and the hashed grey column at 0.24mm represents the NA injection site.

The peak number of double labelled neurons were found from 0.24mm rostral to obex to obex. In the rostral NTS, double labelled neurons were scattered throughout the whole NTS, being present in the ipsilateral NTS in medial, dorsal and lateral sub-divisions (Fig. 3.10A). More caudally the double label neurons appeared to cluster dorsally (SolDl and SolI) while no double labelled neurons were found in the medial NTS (SolM) (Fig. 3.10B). Around the level of the obex, double label neurons were present in the SolDl and ventrolateral part of the NTS (SolVl), with no double labelled neurons was found in the medial part of the NTS (Figure 3.10C). At -0.36mm caudal to the obex, the number of double labelled neurons reduced. Overall, the NTS at the level of obex particularly within the dorsolateral sub-divisions (SolI, SolVl) appeared to possess the most neurons with dual projection to the BötC and the caudal NA.
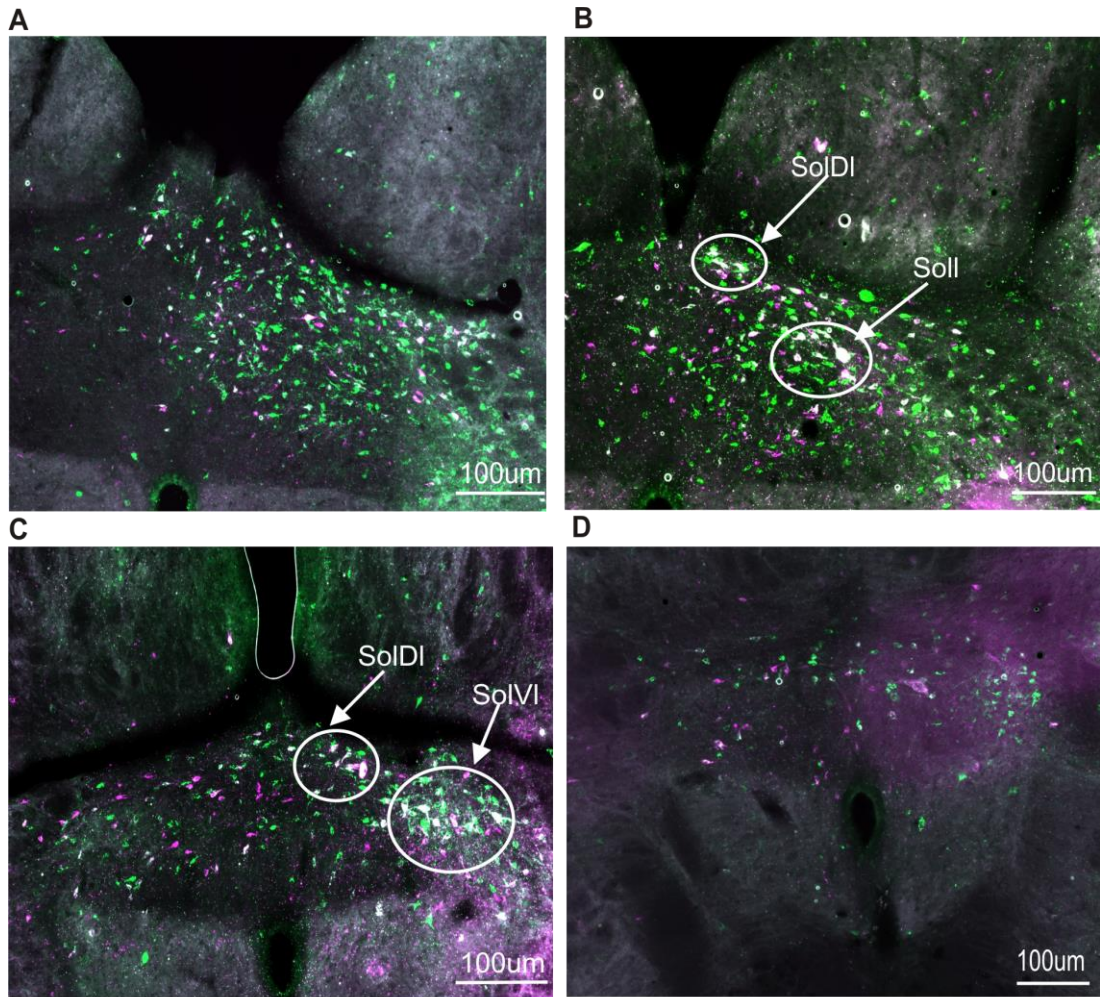
Figure 3.10. Rostral to caudal differences in the location of of neurons in the nucleus tractus solitarii (NTS) with dual projections to the nucleus ambiguus (NA) and BötC. Panel **(A)** at 0.36mm rostral to obex labelled neurons were scattered throughout the NTS. **(B)** At 0.12mm rostral to the obex, double labelled neurons were located predominantly in the dorsal NTS (SolDl, SolI). **(C)** At the level of the obex, double label neurons were located more towards the lateral NTS (SolVl). **(D)** Labelling at -0.36mm caudal to the obex both on ipsilateral and contralateral side. SolDl (Dorsolateral NTS), SolI (Interstitial NTS), SolVl (Ventrolateral NTS).

Chapter 4: Discussion

Superior laryngeal nerve stimulation is known to produce burst activity in laryngeal motoneurons that is accompanied by a brief cessation in central breathing (Barillot et al., 1984a). This relationship was studied by Sun et al (Sun et al., 2011a), who proposed a bifurcating pathway of burst relaying neurons in the NTS with dual projections to the BötC and caudal NA, being the anatomical substrate by which a temporal association between apnoea and vocal cord adduction could occur.

The present study was designed to provide anatomical evidence for the presence of these neurons, using multiple retrograde tracing techniques. The results identified such a dual projecting neurons, providing support for the hypothesis that dual projecting neurons exist in the NTS with simultaneous projections to the BötC and the caudal NA. Notably, the double-labelled or dual projecting neurons were found in the interstitial compartment of the NTS, which also contains the highest density terminal projections from the SLN.

Further studies however, are required to determine how the SLN terminals interact with the dual projecting neurons in the NTS. Nevertheless, this study provides the required anatomical proof of neurons with dual projection to downstream central nuclei for the coordinated motor output for apnoea and vocal cord adduction. These two important physiological events serve to protect the airways from aspiration during swallowing. The delineation of the sensory pathway involved therefore, is the first step towards understanding the neurogenic mechanism underlying the production of the airway protective mechanism and also how dysfunction in basic neurogenic mechanism leads to life threatening situations.

4. 1 Methodological considerations

The problems encountered by using different tracers, immunohistochemistry for tracer detection, microinjection, facial mapping and surgical site in this study are discussed below.

4.1.1 Multiple tract tracing and choice of cholera toxin B

The multiple tracts tracing technique was chosen to identify dual projecting neurons in the NTS, based on the ease by which it allows the discovery of neural connections

to be achieved (Vercelli et al., 2000; Morecraft et al., 2002; Wouterlood et al., 2014) as compared to electrophysiological techniques such as antidromic response recording and spike triggered averaging (STA), which are technically very difficult (Lipski et al., 1978; Lipski, 1981; Lipski et al., 1995).

The tract tracing technique has evolved over time with a long list of the tracers used to trace the projection of the neurons (Nauta and Gygax, 1954; Cowan et al., 1972; LaVail and LaVail, 1974; Lanciego and Wouterlood, 2011). They range from chemical tracers (Vercelli et al., 2000; Lanciego and Wouterlood, 2011) to biological tracers (viruses) (Yoshihara, 2002; Marshel et al., 2010; Ugolini, 2010; Wouterlood et al., 2014). In addition to tracing the neural pathway the viral tracers allow possibility of studying neuronal behaviour by using optogenetic tools (Zhang et al., 2006; Gradinaru et al., 2010; Yizhar et al., 2011).

The caveat however, in multiple tracts tracing is the choice of tracer for the specific experimental need (Vercelli et al., 2000). To see terminal projections, anterograde tracers can be selected, while to see the neurons themselves retrograde tracers are used, with anterograde tracers traveling from the cell body to axonal terminals, and retrograde tracers moving from the terminals towards the cell body (Wouterlood et al., 2014). In this study we wished to see neurons in the NTS with simultaneous projections to BötC and the caudal NA, thereby requiring two retrograde tracers for microinjections into the BötC and caudal NA. To choose the appropriate tracers consideration needs to made of differences in quality of uptake and transport, survival time, tendency to spread within the tissue and their capacity to produce necrosis at the injection site (Lanciego et al., 2000; Van Haeften and Wouterlood, 2000; Conte et al., 2009a).

Horse radish peroxidase (HRP) alone was long been used as a retrograde tracer (Wan et al., 1982). However, cholera toxin B (CTB) is highly effective both in the peripheral and central nervous system and is a well-known tracer which moves in both directions (anterograde and retrograde) (Angelucci et al., 1996; Vercelli et al., 2000). Until recently, CTB has mostly been used as retrograde tracer in conjugated (CTB-HRP) (Trojanowski et al., 1981) and non-conjugated forms (CTB) (Luppi et al., 1990). It can be detected both by histochemical and immunofluorescence detection method (Luppi et al., 1990). With the development of fluorescent conjugates, CTB tracers can

be used to determine multiple neuronal connections simultaneously, being directly visible under a fluorescence microscope (Conte et al., 2009b). CTB conjugated to Alexa-Fluor 488 and 555 have been shown to be brighter and more stable than conventional fluorescent tracers such as Diamidino yellow, Fast blue, Propidium iodide and Fluorogold (Vercelli et al., 2000; Conte et al., 2009b). Using different conjugates of the same tracer in multiple tract tracing provides a way to avoid the problems such as non-specific labelling (Lanciego et al., 1998; Pace, 2009). These conjugates can be injected either by pressure injection or by iontophoresis and have been reported to produce very bright labelling with high resolution even with small injection site of < 100□m (Luppi et al., 1990; Conte et al., 2009b). The smaller size of injections gives a realistic account of the neuronal projection by avoiding labelling of unwanted fibres of the passage.

Unfortunately in this study, we could not use multiple fluorescent conjugates of CTB tracer as CTB-488 did not work at all in our experiments, which was an unexpected outcome considering there are some very good reviews available for CTB-488 (Conte et al., 2009b; a). As a result we trialled different tracers in combination with CTB-555. Fluorogold has been described as the first choice of retrograde tracers in many different studies due its ability to stay within the neuron cell body and its robust labelling (Schmued and Fallon, 1986; Schmued et al., 1990). At the company recommended concentration of 4% (w/v) we found that Fluorogold produced necrosis at the injection site. A further dilution of Fluorogold to 2% did not cause cell necrosis but did not provide effective retrograde neuronal labelling The Fluorogold injections also had a larger spread at the injection site compared to the other tracers such as CTB-555.

We also trialled Dextran, which we have previously used to success as a retrograde tracer upon its application on a nerve. The different forms of the Dextran vary according to molecular weight and their efficiency of travelling in anterograde and retrograde direction. The 3KDa Dextran which we used has been categorised as suitable for retrograde tracing (Reiner et al., 2000; Lanciego and Wouterlood, 2011). Dextran fluoresces at the same wavelength as CTB-555, so we used dextran in combination with unconjugated CTB. The unconjugated CTB increased the time required for the experimental protocol as its visualization required an

immunohistochemical step, however, it produced excellent neuronal labelling without background labelling. Dextran however, spread to a large region around the injection site with no evidence of retrograde labelling, indicating that it is suitable only for nerve application, not for the brain microinjection.

Lastly we tested the combination of CTB-555 and unconjugated CTB. Both tracers worked well when used singly, however when used together, we needed to overcome the primary antibody (goat anti-CTB) binding to the conjugated CTB-555. The cross labelling was most obvious at the injection site, suggesting a concentration interaction between the conjugated tracer and primary antibody for unconjugated CTB. To overcome this problem we titrated the primary antibody to determine if there was an optimal concentration that produced no crossover binding. At a concentration of 1:50,000 there was no cross-labelling observed between both tracers which produced effective labelling of neurons at this concentration. The optimised concentration was later used for subsequent experiments. We also determined the optimal time required for each tracer to allow effective retrograde labelling. This occurs at different rates with each tracer and our studies indicated that a period of 4-5 days was required for retrograde labelling of the neuron in the NTS from BötC injection site with CTB-555 and a period of 2-3 days was sufficient for retrograde labelling of neurons in the NTS after injection of unconjugated CTB to the caudal NA. A time frame of 4-5 days was therefore required for our protocol.

4.1.2 Pressure microinjection

The pressure microinjection technique used in this study resulted in bigger injection sites in most of the experiments which resulted in the spread of tracer to nearby area. As the VRC and NA both run as intimate columns of cells in the ventrolateral medulla, along with the cardiorespiratory compartment which is ventral to the VRC. The various divisions within each column receive sensory input from the NTS and likely to produce their own retrograde labelling (Ross et al., 1985; Dobbins and Feldman, 1994; Alheid et al., 2011). Off target tracer uptake therefore is a consideration for these types of studies, and more so for pressure microinjection compared to the iontophoresis. Iontophoresis injections are controlled by electric current, as compared to pressure injection, which, as the name suggests, uses pressure to inject the tracer. Although iontophoresis has some clear advantages over pressure injection in terms of

providing a smaller injection site and the least damage to the fibres of the passage, the effective delivery of the drugs by iontophoresis depends on a slow current and longer time periods. The longer time required for iontophoresis lengthens the anaesthesia period, which is not ideal for animals undergoing recovery surgery and prolongs the recovery period. As two microinjections were required in this study iontophoresis was therefore not considered a suitable option (Kratskin et al., 1997).

4.1.3 Facial mapping and surgical site

The two injection sites (BötC and NA) are roughly 1.3-1.5mm apart in brain. In order to avoid two surgical exposures at different sites, we combined the exposures to one surgical area - caudal to the lambda suture line. The coordinates for the caudal pole of BötC injection sites were determined by thoroughly mapping the facial nucleus, which required multiple needle tracks at various sites around the facial nucleus. The approach was refined during the first series of acute non-recovery experiments to limit the risk of haemorrhage interfering recovery of the animal. For the recovery experiments the facial mapping was therefore started near the caudal pole of the facial nucleus to reduce the risk of bleeding and facilitate recovery.

Our chosen surgical site for penetration into the caudal NA may have contributed to the low rate of success for NA injection sites. Normally the microinjections into the caudal NA are easy to target via an open brain surface. With such an approach, the neck muscles are removed and injections are made using the obex as a point of reference, resulting in a more precise location of brain sites for microinjections (Bautista et al., 2010). However, since we required recovery for the animals, such a dissection was not possible. Consequently, we only had 2 animals with successful BötC and NA microinjections and this approach to the microinjections will need to be reconsidered for future experiments.

4.2 NTS projection to the BötC

All the NTS neurons with projections to the BötC were located in the caudal NTS region. The caudal NTS provides viscerosensory control of the body as it receives sensory input from the visceral organs through the glossopharyngeal and vagus nerves (Kalia and Sullivan, 1982; Spyer, 1982; Housley et al., 1987; Herbert et al., 1990; Mifflin and Felder, 1990; Finley and Katz, 1992; Ciriello et al., 1994; Ruggiero et al., 1996).

4.2.1. Structural and functional anatomy of the NTS

The NTS as a whole provides a complex interface between the peripheral sensory input and central brain areas for a variety of neural controls (Barraco, 1993; Bradley, 2010). There is no definitive boundary between the caudal and rostral parts of the NTS because histologically the NTS appears as a long contiguous rostral to caudal column. Some define the regions, dependent upon the type of termination of the peripheral sensory nerves and their functional differences, as rostral and caudal portions (Bradley, 2010), while other divide the NTS is into rostral, intermediate and caudal regions (Torrealba and Müller, 1999; Llewellyn-Smith and Verberne, 2011; Corson et al., 2012). At the caudal level, the NTS spans the midline and forms the commissural sub-nucleus above the central canal. Moving from caudal to rostral in the brainstem, rostral to the area postrema, the NTS splits into left and right halves that straddle the midline and at the more rostral level adjoin the ventrolateral edge of the fourth ventricle. After this point the NTS moves in the rostral direction as two well separated columns away from the midline up to the dorsal cochlear nucleus (Paxinos and Franklin, 2004).

Rostral NTS receives gustatory and orosensory primary afferent inputs (King et al.; Grabauskas and Bradley, 1996; Bradley, 2010; Oliveira-Maia et al., 2011). The caudal two-thirds, that consists of the intermediate and caudal NTS, starts from the point where area prostrema just opens to the forth ventricle to caudal to the pyramidal decussation and together is categorised as the caudal sub-division of the NTS (Bradley, 2010). The NTS adjacent to area prostrema (intermediate NTS) receive gastrointestinal sensory inputs and cardiovascular afferents synapse primarily in the medial NTS, whereas respiratory tract and pulmonary sensory fibres synapse in the lateral and ventrolateral parts of intermediate NTS. The caudal NTS receives innervation from the vagus nerve and is involved in processing of viscerosensory information (Herbert et al., 1990; Mifflin and Felder, 1990; Finley and Katz, 1992; Ciriello et al., 1994; Ruggiero et al., 1996). In this part of the nucleus the cardiovascular, gastrointestinal, respiratory tract and pulmonary afferents synapse in broad mediolateral patterns making it a much more complex site for controlling many vital functions of the body (Andresen and Mendelowitz, 1996).

In addition to a rostral-caudal division of the NTS, it has also been subdivided into various compartments based on the cytoarchitecture of the cell within the NTS: medial

(SolM), intermediate (SolIM), ventral (SolV), ventrolateral (SolVl), dorsolateral (SolDl), interstitial (SolI) NTS and commissural nucleus of solitary tract (SolC) (Kalia and Sullivan, 1982; Alheid et al., 2011). Again the division of the NTS into different sub-nuclei is not categorical and varies between the species due to variation in cytoarchitecture (Allen, 1923; Meessen and Olszewski, 1949; Torvik, 1956).

The distribution pattern of NTS neurons that we identified as projecting to BötC was in accordance with a study done by Nunez Abades et al (Núñez-Abades et al., 1993) (Núñez-Abades et al., 1993) who reported a similar pattern of projections from the NTS neurons to the BötC. However, our results are in contrast with another study conducted by (Alheid et al., 2011). They reported very few neuronal projections to the BötC from neurons within the NTS rostral to the obex, with only the NTS region caudal to the obex being found to contain neurons projecting to the BötC. These contrasting results might be due to different techniques being used to inject the tracers. We used a pressure microinjection technique like Nunez-Abades et al (Núñez-Abades et al., 1993) in contrast to the work of (Alheid et al., 2011) who use iontophoresis for microinjections.

The diffusion of tracer into the compact formation of the NA (AmbC), which receive lots of sensory input from NTS neurons for motor control of oesophageal muscles during swallowing and peristalsis (Bao et al., 1995; Gai et al., 1995; Hayakawa et al., 1997; Broussard et al., 1998) is a possibility, however our histological analysis for the BötC injection sites did not show spread to the AmbC. Another possibility for the discrepancy between our studies with work of (Alheid et al., 2011) could be the spread of microinjection to the ventrally located rostral ventral medulla (RVLM) region. The neurons within this region also receive sensory input from the NTS and in particular sensory input for baroreception via the intermediate sub-nucleus of the NTS (Kalia and Mesulam, 1980b; Kalia, 1981a; Agarwal and Calaresu, 1990). However, most of these projections from the NTS to RVLM are indirect via the caudal ventrolateral medulla (CVLM), with NTS neurons receiving the sensory input from the baroreceptor afferents (Ciriello, 1983), and second order NTS neurons projecting to the CVLM that in turn projects to the RVLM (Granata et al., 1986; Terui et al., 1990; Li et al., 1991; Masuda et al., 1991).

4.2.2 NTS sub-compartment projections to BötC

In addition to determining the rostral-caudal projection pattern of the NTS projections to the BötC, we also examined the different sub-compartments of the NTS that contained retrograde labelled neurons, focusing on that level of the NTS that had the greatest number of retrograde labelled neurons. Overall, though the neurons were scattered throughout the NTS, most of the neurons were found towards the medial (SolM & SollM) and dorsal aspect (SolDl) of the NTS with few neurons labelled in the ventral NTS and central part of the NTS. The NTS sub-compartments SolC and SolM have been reported as sites for termination of a variety of afferent projections including for example, the carotid body which provides peripheral chemosensory inputs (Finley and Katz, 1992; Ciriello et al., 1994). In addition, peripheral sensory input from the pulmonary rapidly adapting stretch receptors (RAR) (Kubin and Davies, 1988; Ezure et al., 1991; Otake et al., 2001) and broncho-pulmonary C-fibre afferents (Kubin et al., 1991; Paton, 1998; Moreira et al., 2007) also end in SolC and SolM.

The sensory inputs from all these afferent projections have the capacity to alter respiratory frequency. However, the transfer of the sensory input from the NTS to rCPGs via direct connections from SolC and SolM (Kubin et al., 2006) or indirectly via pons (Song and Poon, 2004; Song et al., 2011), rVRG (Alheid et al., 2002; Monnier et al., 2003; Moreira et al., 2007) and RTN (Takakura et al., 2006; Moreira et al., 2007; Takakura et al., 2007) have been reported to ultimately influence pre-BötC neurons through BötC. In addition, in other retrograde tracing studies including microinjection into the BötC, the retrograde labelled neurons were found in various subdivisions such as commissural (SolC) (Otake et al., 1992; Núñez-Abades et al., 1993) intermediate (Soll) and ventrolateral SolVl of the NTS (Núñez-Abades et al., 1993) suggesting a direct interaction between NTS and rCPG (BötC, pre-BötC, and RTN/pFRG) exist.

4.2.3. Physiological significance of connection between BötC and NTS

The NTS provides a critical interface between peripheral sensory information and the central nervous system for a variety of neural control responses. The sensory information via different sensory nerves comes into various subdivisions of the NTS. The sensory information in the NTS, either via second order neurons or through a

series of neurons, is converged to the appropriate nuclei in the brain for various motor control and reflex responses (Bradley, 2010). As described above, afferent inputs in the caudal NTS bring about changes in breathing pattern and frequency and overall respiratory system work in coordination with the vascular system to achieve a healthy homeostatic status.

The caudal NTS is a site with maximum overlap of afferents from different viscerosensory parts of the body and offers a challenging task for an anatomist to work out how these systems work in synchronisation while maintaining their own functional identity (Mendelowitz et al., 1992; Andersen and Kunze, 1994; Lawrence and Jarrott, 1996; Kline, 2010). The sensory inputs that bring about the alteration in respiratory frequency suggest access to the rCPG that influence the pattern of breathing. The breathing adjustments in response to peripheral sensory input via the NTS are important to understand the variety of different pathways and also to understand the complex reconfiguration of rCPGs in response to sensory inputs and the role of compartments in VRC which are involved in receiving this information (one of the least touched area in respiratory studies). The role of pons, RTN/pFRG as a receiver of sensory input from NTS has been debated in many different studies however, other than these region BötC could be another VRC compartment involved in receiving direct input from the NTS.

When considering the role of the BötC in VRC, first of all, it forms an integral part of rCPG in such a way that the activities of the neurons within BötC are important for the expiratory phase of the respiratory cycle during normal rhythmic breathing. Coronal transection just below this nucleus results in loss of expiratory output (Smith et al., 2007; Abdala et al., 2009) which is an integral phase of the respiratory cycle and critical for normal respiratory rhythmogenesis. In addition, BötC neurons play an important role in respiratory rhythmogenesis through mutual inhibitory connections which exist not only among the neurons within BötC but also with the neurons in the preBötC (Bongianni et al., 2010) and across the medulla (Berger, 1977; Merrill et al., 1983).

The inspiratory neurons of the BötC inhibit the firing of expiratory neurons of both BötC and cVRG. Both inspiratory and expiratory inhibitory neurons within BötC express glycine and Y-amino-butyric acid (GABA) neurotransmitters for their neurotransmission (Haji et al., 1992; Shao and Feldman, 1997; Schreihofer et al.,

36

1999; Ezure et al., 2003). The expiratory neurons in BötC have been reported to inhibit the activity inspiratory neurons in the DRG (Merrill et al., 1983), VRG (Ezure and Manabe, 1988; Fedorko et al., 1989), phrenic motor neurons (Merrill and Fedorko, 1984; Ellenberger and Feldman, 1988; Tian et al., 1998) and laryngeal motoneurons (Peever et al., 2002; Ono et al., 2006; Shiba et al., 2007).

The inhibitory input from BötC neurons plays an important role in transitioning from inspiratory phase to expiratory phase through a process called inspiratory switch off. The neural substrates that constitute to the inspiratory off switch are thought to lie within the BötC and pre–Bot regions (Haji et al., 2002; Okazaki et al., 2002; Segers et al., 2008; Mörschel and Dutschmann, 2009). The inspiratory switch off can result from the activation of the Hering-Breuer reflex and also by the direct stimulation of the dorsolateral pons. The sensory information from peripheral and central areas converge on medullary respiratory neurons to switch off inspiration by inhibiting the activity of neurons in the pre-Bot (Okazaki et al., 2002) via the BötC, which contains a substantial amount of post inspiratory neurons. A bilateral microinjection of the inhibitor peptide somatostatin in the BötC resulted in loss of post-inspiratory (PI) activity which changed the three phase respiratory (inspiration, post-inspiration, expiration) rhythm to a two phase (inspiration, expiration) respiratory rhythm (apneusis) (Burke et al., 2010).

There is evidence that the inspiratory off switch involves sequential activation of BötC late inspiratory (late-I) and expiratory decrementing (E-DEC) neurons. The excitation of late-I neurons in BötC excitation is thought to switch off inspiration because of the timing. They start firing during the post inspiratory phase and their peak of firing coincides with the cessation of firing in inspiratory augmenting (I-AUG) neurons in the rVRG (phrenic premotor neurons) (Richter, 1982; Oku and Dick, 1992; Pierrefiche et al., 1995; Haji et al., 2002). Late-I neurons have been found to possess inhibitory markers and project to phrenic premotor neurons (Oku and Dick, 1992; Haji et al., 2002). Depending upon the different physiological needs, the rCPGs adjust the breathing rhythm in a particular pattern, which is then converged to rVRG and cVRG for variety of motor output.

To understand how the BötC interact with the neurons in the preBötC is explained in the simplistic model of respiratory rhythmogenesis. According to this model, the pacemaker neurons within PreBötC produce inspiratory rhythm. Recurrent excitations

in pre-inspiratory neurons of the PreBöt excite the bulbospinal neurons in the rVRG that provide the majority of the excitatory premotor input to phrenic motoneurons. The phrenic motoneurons drive the inspiratory muscles of the diaphragm, which in turn contract to increase the volume of thoracic cavity during inspiration. The neurons in the rVRG also send excitatory drive to laryngeal motoneurons in the NA, which controls the movement of the vocal cords during inspiration. The excitatory inputs from the rVRG to ILMs dilate the vocal cords. The collective movement of inspiratory muscles and opened airway trigger the passive flow of air into the lungs during inspiration. The termination of the inspiration is initiated and maintained by the inhibitory action of the BötC neurons which inhibit the activity of inspiratory neurons in the preBötC, DRG, and also laryngeal motoneurons, while receiving the sensory information from pulmonary stretch receptors via vagus and pontine respiratory group (PRG) for inspiratory switch off and bring the smooth transitioning of inspiration to early expiration or post-inspiration. During active expiration, an active expiratory oscillator in the vicinity of the RTN is recruited and drives the expiratory neurons in the cVRG that provide excitatory premotor input to motoneurons in the spinal cord to drive active muscles of expiration. The expiratory oscillator interacts with the inspiratory oscillator through mutual interactive connections. The end of expiration triggers the start of inspiration and so the process continues (Smith et al., 2007; Smith et al., 2009; Feldman et al., 2013; Richter and Smith, 2014; Feldman and Kam, 2015).

In view of all these different roles of BötC neurons in maintaining respiratory rhythm, including controlling the activities of neurons within the brainstem while keeping simultaneous inhibitory connections to pacemaker interneurons in the preBötC, it is reasonable to think that the BötC can interact with a variety of sensory information that ends up in the NTS. Sensory information from the upper airways via the SLN nerve also terminates at the NTS for a number of upper airway behaviours such as coughing, sneezing and swallowing. Many BötC neurons have been found to change their pattern of firing during these non-respiratory behaviours, implicating their interaction with the sensory input that terminates in NTS for these behaviours (Oku et al., 1994; Baekey et al., 2004; Shiba et al., 2007). Similarly during SLN induced apnoea (Bongianni et al., 2000), blocking of the pathway from the NTS to the BötC attenuates the apnoeic response (Sun et al., 2011b) suggesting the existence of direct

connection between NTS and BötC, a concept for which the present study provides the anatomical proof.

4.3 NTS projections to the caudal NA

Our microinjection into the caudal NA resulted in extensive retrograde labelling of neurons in the NTS. The caudal NA is also known as the loose part of the NA (AmbL). The NA is a small column of heterogeneous cells embedded in the ventrolateral reticular formation of the brainstem starting from the caudal end of the facial nucleus to the spinal-medullary junction. This long column of cells runs parallel and dorsal to the VRC compartments of the brainstem. Rostral to caudal, the nucleus is divided into four distinct subdivisions incorporating the compact formation (AmbC), the semi-compact formations (Ambsc and AmbL) and the external formation (Ambe) (Bieger and Hopkins, 1987).

The AmbC contains densely packed oesophageal motoneurons, which provide motor control of the muscles in the oesophagus. The Ambsc contains pharyngeal motoneurons, which provide motor control of the pharyngeal muscles. In addition it also contains ILMs that send their axons to the corocothyroid (CT) muscles of the larynx through the SLN. The AmbL contains majority of the ILMs and ELMs that provide control of laryngeal muscles and their axons run in RLN. The Ambe contains airways related vagal pre-ganglionic neurons (AVPNs) and cardiac vagal pre-ganglionic neurons (CVPNs). The AVPNs supply the lower airways and CVPNs supply the heart (Bieger and Hopkins, 1987). The ILMs and ELMs within the AmbL provide control of vocal cord movement during inspiration and expiration (Ono et al., 2006; Shiba et al., 2007; Bautista et al., 2012; Zhao et al., 2015). ILMs provides the motor control of laryngeal dilator muscles CT and posterior coricoarytenoid (PCA) whereas, the ELMs supply the motor control of laryngeal constrictor muscles: the lateral coricoarteniod (LCA), thyroarytenoid (TA) and intraarytenoid (IA) which close the vocal cords (Ludlow, 2005).

The microinjection into the caudal NA resulted in extensive retrograde labelling of the neurons in the ipsilateral side of the NTS with a few scattered neurons found on the contralateral side. The result of the present study are in accordance with a study performed by (Cunningham and Sawchenko, 2000). They studied the interaction of the NTS region with the NA, also by using the same neuroanatomical tract tracing.

They injected an anterograde tracer into the NTS and found efferent projections to the various sub-divisions of the NA. Retrograde tracer injections targeted to the AmbL resulted in retrograde labelled neurons in the ipsilateral NTS mainly in the ventrolateral, intermediate and interstitial sub-division of the NTS. Secondary less dense population of neurons were also found in the medial and the commissural part of the NTS (Cunningham and Sawchenko, 2000). Interestingly, although the retrograde tracer injections were targeted to AmbL, they found labelling all across the NTS. Similarly, in another study examining catecholamine inputs to ELMs in rats, microinjections targeted to the caudal NA resulted in labelled neurons in the ipsilateral NTS at the obex level (Zhao et al., 2015). Similar to the work of (Cunningham and Sawchenko, 2000), in this study all the NTS subdivisions were found to have projections to the AmbL with neurons found in medial, intermediate, dorsolateral, interstitial, ventral, and ventrolateral regions. In addition, labelled neurons were also present in the solitary tract. The equal input from the various subdivisions of the NTS to AmbL is not surprising considering the role of neurons in the AmbL (ILMs & ELMs) that provide control of the vocal cords.

Vocal cord movements are required for a variety of different behaviours such as phonation, crying, and singing, respiration and glottis closure (laryngeal adductor response or LAR), swallowing and coughing. Therefore they receive a lot of sensory information from higher brain areas and from the NTS, which is one of the most important somatosensory nuclei to provide sensory input for the control of vocal cords during upper airways protective behaviours (Jürgens, 2002). In another study involving transsynaptic tracers injection into the thyroarytenoid muscle, retrograde labelled neurons were found in all the NA subdivisions and respective NTS compartments (Van Daele and Cassell, 2009). As the virus spread, retrograde labelled neurons were found subsequently in the BötC and higher brain areas confirming the role of brain areas involved in the control of vocal cords. The sensory input that is relayed to AmbL for the control of different upper airway behaviour such as swallowing, coughing and laryngeal adductor response (LAR) is given below.

4.3.1 Swallowing related sensory input to caudal NA

Because the laryngeal motoneurons (LMs) CT, ILM and ELMs receive swallow related input from the second order neurons in the NTS (Hayakawa et al., 2000), our

microinjection targeted at the AmbL might also include pathway neurons involved in swallowing. Also, as described above in section 4.3 (NA sub-divisions), although there is topographic separation between the distribution of motoneurons as they shows some overlap in all the NA compartments (Bieger and Hopkins, 1987). It is therefore highly likely that the retrograde labelled neurons in the NTS found in this study also included the neurons involved in providing laryngeal control during swallowing.

Swallowing is the coordinated motor activity of muscles in the oral, pharyngeal and laryngeal regions that starts in response to the presence of food or liquid in the oral cavity. This sequential contraction of the muscles in pharynx, oesophagus and laryngeal wall is highly coordinated and controlled by motoneurons in the various division of the NA (Odutola, 1976; Altschuler et al., 1994; Cunningham and Sawchenko, 2000). As shown by (Hayakawa et al., 2000) the injection of retrograde tracer into the RLN resulted in neuronal labelling in all the NA subdivisions i.e., loose, semi and compact formations, indicating that the various compartments of the NA interact with each other during swallowing.

Each phase of swallowing receives sensory input via relevant afferents that ends in different NTS sub-divisions. Most of the sensory input from the oesophageal region comes to the central sub-division of the NTS and project to the compact formation of the NA (Cunningham et al., 1991; Broussard et al., 1994; Bao et al., 1995; Gai et al., 1995; Hayakawa et al., 1997; Broussard et al., 1998). Similarly, the glossopharyngeal afferent fibres project mainly to medial, intermediate and interstitial sub-nuclei of the NTS and project to the NA for motor-control of tongue and pharynx (Ootani et al., 1995; Brining and Smith, 1996).

4.3.2. Cough related sensory input to caudal NA

Laryngeal motoneurons also play an important role in the coughing reflex. During a cough, vocal folds are tightly closed which in turn increases the pulmonary pressure and then the airway is cleared by forceful expiration (Widdicombe, 1980). As cough is a protective response to noxious irritant stimuli in the airways, and is thought to be mediated via pulmonary rapidly adapting stretch receptors, also known as irritant receptors, the afferents of which run in the vagus nerve. The vagus nerve terminates at various NTS subdivision. In cough, according to many studies, the sensory information through RAR (Canning et al., 2004; Chou et al., 2008) is relayed via the

dorsolateral medial and commissural subdivisions of the caudal NTS (Canning, 2009; Canning and Mori, 2010; McGovern et al., 2012) to the ventral respiratory column (Rybak et al., 2008) and NA for motor control (Jordan, 2001; Ludlow, 2005). The greater numbers of retrograde labelled neurons in the NTS likely to include some of the pathway neurons of cough reflex.

4.3.3 Laryngeal adductor response related sensory input to caudal NA

Another important reflex that is mediated through the NTS to the laryngeal motoneurons is the laryngeal adductor response (LAR). The LAR is referred to as simple closure of the vocal cords in response to very light (0.5Hz) single stimulation of the SLN (Sasaki and Suzuki, 1976; Ambalavanar et al., 2004). It only involves the closure of the vocal fold without the further added movement involved in cough and swallowing responses (Ludlow et al., 1992), which occur in response to more intense SLN stimulation. In mammals, stimulation of the SLN at 2-10 Hz produced sneezing and coughing (Bolser, 1991; Gestreau et al., 1997; Satoh et al., 1998), 10-50 Hz produced respiratory slowing (Lawson, 1981; Bongianni et al., 1988; Bongianni et al., 2000) and 20-30 Hz produced fictive swallowing (Dick et al., 1993). In addition, the LAR is thought to play a very important role in laryngospasm (Ikari and Sasaki, 1980).

The sensory input from the SLN nerve ends at the NTS from where it is transferred to the laryngeal motoneurons in the NA (Goding et al., 1987). As shown in another study, LAR related FOS activity in response to SLN stimulation was produced in the interstitial sub-nucleus of the NTS, the lateral tegmental field of the reticular formation and the NA, confirming the transfer of sensory input to laryngeal motoneurons. As also reported by (Hayakawa et al., 2000) they also found a close association between the NTS and laryngeal motoneurons in the NA. They injected an anterograde tracer in the NTS and found that the terminal endings of the neurons were in close association with the laryngeal motoneurons in the NA that had been labelled using CTB as retrograde tracer applied to the CT and posterior PCA muscle. The retrograde labelled neurons found in this study might also include some of the neurons of LAR pathway.

As described above, the laryngeal motoneurons receive a variety of sensory input for different SLN induced upper-airway behaviours via the NTS. (Miller and Loizzi, 1974). It is interesting to note that the different upper airway behaviours share the same sensory afferents, the SLN nerve, however, depending upon the intensity, rate

and timing of stimuli, the motor outputs differs. It is possible that different neurons in the NTS are specifically recruited for a particular behaviour such as the one has been described well for swallowing (Jean, 1984) and equally possible that the NTS circuitry is highly plastic, deciding the type of motor output by integrating sensory information with input from local networks, higher brain regions and circulating neurotransmitters to form a coherent reflex output (Bonham et al., 2006) in the form of different upper-airways behaviours. Given the diverse role of the motoneurons in the AmbL, also the fact that tracers injection will likely be including all of the pathway neurons commonly share between laryngeal motoneurons, it is highly difficult to segregate the neuronal circuitry specifically recruited to a particular airway reflex and therefore the sensory pathway for apnoea.

4.5. Double labelled neuron in the interstitial NTS

The caudal most part of the NTS (~350um rostral to ~350um caudal to the obex) towards the spinal-medullary junction contained the highest number of double labelled neurons, which were predominantly in the interstitial and ventrolateral NTS. A population of double-labelled neurons were found in the interstitial (SolI) part of the NTS. According to many studies, the SolI is heavily innervated by afferents from the SLN nerve terminals (Hanamori and Smith, 1986; Lucier et al., 1986; Furusawa et al., 1996; Pascual-Font et al., 2011). In addition to SolI, some SLN terminals projections have been reported in other sub-divisions (SolDl, SolVL, SolC) of the NTS (Bellingham and Lipski, 1992). Preliminary studies in our lab (Sun et al unpublished) also suggest SLN terminal distribution in the SolI NTS but much rostral to the obex defined in the rat.

In this study, we defined the regions of the NTS with relevance to the obex, the definition of which varies between species. For example according to Paxinos and Franklin (Paxinos and Franklin, 2004) the caudal most tip of the area prostrema (Interaural (-5.40 mm) (also referred to as calamus scriptorius) is referred to as obex in animals with midline area prostrema such as in rats and mice, whereas in animals where area prostrema is bilateral, the obex refers to a point where central canal opens to 4th ventricle (Intermural (-4.56 mm) as in the rabbit (Gromysz and Karczewski, 1981; Ellenberger et al., 1990; Bowler et al., 2013) and in cat (Kalia and Mesulam, 1980b; a) for example. Due to these differences in defining the regions of NTS, the

definition of various divisions of the NTS also vary across different species, which is a source of confusion with regard to which area of NTS is being described as a point of reference and makes comparison of anatomical studies between different species very difficult (Alheid et al., 2011).

Interestingly, in our preliminary studies examining SLN terminal projections (Sun et al unpublished) results do not support the hypothesis that there is an overlap between the SLN terminals and NTS neurons with dual projections to BötC and caudal NA. The transfer of sensory information from the SLN terminals to dual projecting neurons may therefore involve interneurons and suggests the presence of a complex circuitry to relay sensory information to produce different upper airways behaviours including apnoea. Several extracellular studies have found non-respiratory neurons in the region of the NTS which respond at a short latency to SLN and vagus stimulation (Porter, 1963; Biscoe and Sampson, 1970; Sessle, 1973) and could act as a source of SLN induced burst activity, however, it is not known if the double-labelled neurons that we have identified are part of those non-respiratory neurons. Nevertheless, if the second order SLN neurons (which receive direct sensory input from the SLN nerve terminals) and the burst relaying neurons are from different groups, the double-labelled neurons we identified in the SolI would be the ideal candidate for relaying non-respiratory burst-activity to BötC and the caudal NA.

4.5.1 Double-labelled neurons in the Ventrolateral NTS

A group of double-labelled neurons were also found in the ventrolateral subdivision (SolVl) of the NTS. SolVL, (also abbreviated as vlNTS) is highly diverse with regard to the variety of neurons present in this region of the NTS. Most importantly, SolVl contains neurons that form the dorsal respiratory group (DRG) (Berger, 1977; Lipski et al., 1979; Graham and Duffin, 1982; Averill et al., 1984; Graham and Duffin, 1985). It has been established that bulbospinal inspiratory neurons within the DRG send excitatory drive to the phrenic motoneurons (Fedorko et al., 1983) and intercostal motoneurons (Duffin and Lipski, 1987) in cats, however in rats confirmation about the connection between the DRG neurons and phrenic motoneurons is lacking (de Castro et al., 1994; Tian and Duffin, 1998; Saito et al., 2002b). The neurons within the DRG region send their collaterals to the neurons in the VRG (Otake et al., 1989).

Although the neurons in the DRG are thought to play a role in inspiration, inspiratory activity can continue without the DRG inspiratory neurons. An electrical lesion of DRG neurons did not abolish the three phase respiratory rhythm but produced a transient apnoea (McCrimmon et al., 1987; Hilaire et al., 1990) confirming that the neurons in DRG are not crucial for respiratory rhythm generation. The kernel for inspiratory activity is present within the preBötC due to the pacemaker activity of the neurons that generate inspiratory rhythm (Feldman et al., 2013; Richter and Smith, 2014; Feldman and Kam, 2015). The exact role of the DRG as an imperative element of CPGs is still equivocal (McCrimmon et al., 1987; Hilaire et al., 1990; Wasserman et al., 2000). However some studies suggest they have a role in inspiratory switch off. For example, a bilateral microinjection of the ionotropic glutamate receptor antagonist kynurenic acid and the Na^+ channel blocker tetrodotoxin into the region of the vlNTS produced a prolongation of inspiratory duration and an apneustic (two-phase respiration) pattern of breathing (Wasserman et al., 2000).

Several DRG neurons have also been found to receive monosynaptic and oligosynaptic excitatory input during SLN stimulation (Berger, 1977). Some of the inspiratory modulated neurons in the DRG produce burst like activity during SLN stimulation and have been reported to present locally (interneurons) within DRG without having connection with phrenic motoneurons in the spinal cord (Gestreau et al., 1996; Saito et al., 2002b). The SolVl also contains pump cells (P-cells) and inspiratory beta (Iβ) cells (Berger, 1977; Cohen and Feldman, 1984; Donoghue et al., 1985; Kubin et al., 2006). The P-cells and Iβ cells receive monosynaptic input from slowly adapting stretch receptors (SARs) in the lungs via the vagus nerve and are considered important relay neurons in the Hering–Breuer reflex (Berger, 1977; Davies et al., 1987; Kubin and Davies, 1988; Bonham and McCrimmon, 1990; Miyazaki et al., 1998). As detailed in the Introduction, the Hering–Breuer reflex is considered to be the main instigator of inspiratory switch off, the second being in the pons in the absence of vagus input in vagotomised animals (Dutschmann and Herbert, 2006b; Dutschmann and Dick, 2012). During normal rhythmic breathing (Hayashi et al., 1996; Ezure et al., 2002) the smooth transitioning from inspiration to expiration during normal breathing is thought to be mediated though these pump cells which relay sensory input, received from pulmonary stretch receptors, to the pons and bring about

termination of inspiration (Clark and von Euler, 1972; Cohen and Feldman, 1977; Bonham and McCrimmon, 1990).

Apart from the above-mentioned types of neurons, functionally, the neurons in the SolVl have been reported to interact with the neurons in the BötC compartment of the VRC. The expiratory activity detected from the neurons in the SolVl was found to be due to BötC neurons that project to the DRG and from expiratory laryngeal motoneurons (Berger, 1977). Many BötC neurons had been found to have inhibitory connections with the inspiratory modulated neurons in the DRG and inhibit their activity at the start of expiration. In addition, the neurons in SolVL had also been found to have connections with motoneurons (Norgren, 1978; Merrill et al., 1983). It is to be noted that the interaction between DRG and BötC was from the BötC neurons that project to DRG. There is no report to date about the neurons in SolVl that project to the BötC compartment. The double-labelled neurons found in this study had their cell body in the NTS with projections to the BötC suggesting the influencing role of NTS neuron over neurons in BötC

Considering that the SolVl contains burst producing neurons in response to SLN stimulation (Gestreau et al., 1996; Saito et al., 2002b) and that this region has connections with the BötC (Berger, 1977; Merrill et al., 1983) and ELMs (Norgren, 1978; Merrill et al., 1983), the dual projecting neurons we identified in the SolVl could be the neurons to mediate short latency visceral and somatic reflexes as reported earlier(Kalia and Mesulam, 1980b; a). However, this ideal model of having burst relaying neurons in SolVl is subject to the question of how they are connected with SLN terminals. Although some afferent projections form the larynx, extrathoracic trachea and intrathoracic trachea (including lungs and heart) (Kalia, 1981b; Merrill et al., 1983) have been reported in SolVl, it receives terminal endings mainly from the vagus nerve (Kalia and Sullivan, 1982) and thought to be involved mainly in the Hering–Breuer reflex via P-cells. Due to the existence of a variety of sensory inputs from different peripheral organs in this region and the variety of neurons in SolVL it is difficult to conclude the relationship of the dual BötC/NA projecting neurons with sensory input they receive. Further, if SLN induced apnoea is mediated via this pathway, what is the role of the interstitial NTS where most of the SLN terminals exist? Also, the presence of different cells in the SolVl adds further to confusion about the nature of these dual BötC/NA projecting neurons.

4.6 Future directions

Like many earlier studies, this study provided affirmation that the NTS provides a complex interface between peripheral sensory input and the central nervous system for a variety of neural functions. The caudal NTS is a site of maximum overlap between the sensory afferents (Kalia and Mesulam, 1980a; Contreras et al., 1982; Hanamori and Smith, 1986; Lucier et al., 1986; Pascual-Font et al., 2011) and the same NTS compartment has been reported to have terminals from the different nerves (Kalia, 1981b). For example in this study, the SolVl and SolI, which contained the double-labelled neurons, have been reported to contain some if not highest density terminal projection from the vagus and SLN nerves (Kalia, 1981b; Bellingham and Lipski, 1992). This fact makes it hard to establish the connection of these dual-projecting neurons with the type of sensory input they receive and their functional significance.

In addition, what are the functional properties of the dual projecting neurons we identified? How do they respond to stimulation of the nerves that end in the same NTS region? For example, Iβ and P-cells have also been found to be monosynaptically activated by SLN stimulation and play role in laryngeal afferent pathways (Berger, 1977; Donnelly et al., 1989a; b). Further, we do not know if the double-labelled cells are inspiratory neurons of the DRG, or Iβ or P-cells, which have already been reported to exist in the ventrolateral NTS, or if they are part of a new non-respiratory burst relaying circuit that might be present within or among the different NTS compartments. Although previously studies have been done to show sensory inputs to and efferent outputs from the individual NTS compartments and the neural substrate is well established for some of the upper airway behaviour such as swallowing (Jean, 1984). The sensory pathways involved in the apnoeic response to SLN stimulation are not yet clear. In the present study, we have provided, for the first time, anatomical evidence to support the hypothesis that the NTS contains neurons that project simultaneously to the BötC and the caudal NA, and may function to control the temporal association between apnoea and vocal cords adduction. However, it remains to be further studied if these NTS neurons are modulated with a non-respiratory burst activity during the SLN stimulation.

In order to show their neuronal activity, single unit recordings would be required from these dual BötC/ NA-projecting neurons. In order to identify the NTS neurons single

unit recordings could be made extracellularly from the locations we have identified in the NTS. Three criterions would need to be used for neuronal identification: 1) orthodromic response from the SLN stimulation, 2) antidromic response from ipsilateral stimulation of the caudal NA and/or BötC using bi-polar stimulating electrode, and 3) burst activity occurring simultaneously with the RLN burst activity during the SLN stimulation. Further characteristics of the identified neurons would be required in order to define their burst activities including their neuronal activity in relation to respiration and the lung ventilation before the SLN stimulation. During SLN stimulation (1-20 Hz), their burst activityneed to be carefully analysed, including the duration, mean firing frequencies and minute activities.

In previous work from our laboratory, we have found during recording from the ELM that a much higher occurrence rate of orthodromic response was evoked during high but not low frequency SLN stimulation (REF or unpublished). We would want to know if the same feature can be found in dual projecting NTS neurons. Since the orthodromic response is not likely affected by the stimulation frequency itself, but by the weakened central respiration caused by the increased stimulation frequency, such a study may help to better understand mutual influences between respiration and airway protective reflexes. Further electrophysiological studies after the individual identification of the NTS neurons could include intracellular recording to demonstrate more details of synaptic activities, such as depolarization or hyperpolarization of their membrane potential during certain respiratory phase, intracellular labelling or juxtacellular labelling to show their anatomical features.

Summary figure
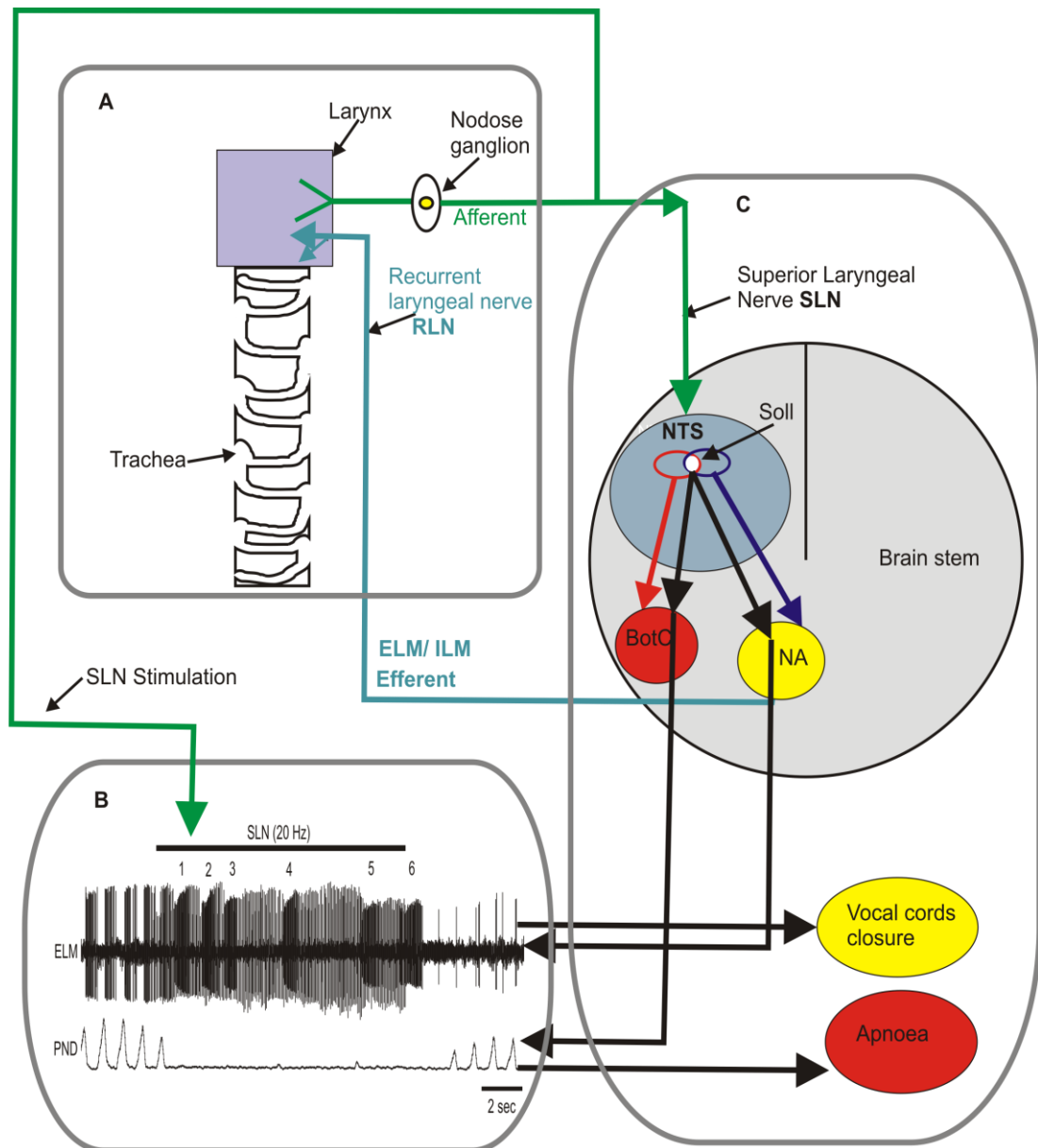
Figure 5.1 Overall summary of the project. **A)** Laryngeal sensory pathway (afferent and efferent). The laryngeal sensory information reaches central nervous system via SLN nerve which terminates at NTS. **B)** The responses recorded from ELM and phrenic nerve during SLN stimulation. The temporal association between ELM burst activity and phrenic nerve apnoea (PND) was predicted to be controlled by dual projecting neurons in the NTS, allowing for vocal cord closure and apnoea **C)** In the NTS, neurons were identified with single projections to the BotC (solid red line), to the NA (solid blue line) and a small population of neurons in the interstitial NTS (Soll) with dual projects to BotC and NA were also identified (thick black line).

Conclusion

The present study provides the first anatomical proof of the existence of dual BötC /NA projecting neurons in the caudal NTS and defines their location as being in the interstitial and ventrolateral NTS (Fig 5.1). Given the fact that SLN terminals exclusively project to the SolI with some less dense projections to the other compartments including SolVL, it is highly likely that the neurons receive inputs from the SLN and that the close temporal association of apnoea and vocal cords adduction during SLN stimulation is due to the activity of these neurons. Further studies, however, are needed to confirm this sensory pathway and to establish the functional properties and connections of the dual projecting neurons.

References

Abbott, S.B., Stornetta, R.L., Fortuna, M.G., Depuy, S.D., West, G.H., Harris, T.E., and Guyenet, P.G. (2009). Photostimulation of retrotrapezoid nucleus phox2b-expressing neurons in vivo produces long-lasting activation of breathing in rats. *J. Neurosci.* 29**,** 5806-5819.

Abdala, A.P., Rybak, I.A., Smith, J.C., and Paton, J.F. (2009). Abdominal expiratory activity in the rat brainstem–spinal cord in situ: patterns, origins and implications for respiratory rhythm generation. *J. Physiol.* 587**,** 3539-3559.

Abu-Shaweesh, J.M., Dreshaj, I.A., Haxhiu, M.A., and Martin, R.J. (2001). Central GABAergic mechanisms are involved in apnea induced by SLN stimulation in piglets. *J. Appl. Physiol. (1985)* 90**,** 1570-1576.

Agarwal, S., and Calaresu, F. (1990). Reciprocal connections between nucleus tractus solitarii and rostral ventrolateral medulla. *Brain Res.* 523**,** 305-308.

Alheid, G., Gray, P., Jiang, M., Feldman, J., and Mccrimmon, D. (2002). Parvalbumin in respiratory neurons of the ventrolateral medulla of the adult rat. *J. Neurocytol.* 31**,** 693-717.

Alheid, G.F., Jiao, W., and Mccrimmon, D.R. (2011). Caudal nuclei of the rat nucleus of the solitary tract differentially innervate respiratory compartments within the ventrolateral medulla. *Neuroscience* 190**,** 207-227.

Allen, W.F. (1923). Origin and distribution of the tractus solitarius in the guinea pig. *J. Comp. Neurol.* 35**,** 171-204.

Altschuler, S.M., Bao, X., and Miselis, R.R. (1994). Dendritic architecture of hypoglossal motoneurons projecting to extrinsic tongue musculature in the rat. *J. Comp. Neurol.* 342**,** 538-550.

Ambalavanar, R., Tanaka, Y., Selbie, W.S., and Ludlow, C.L. (2004). Neuronal activation in the medulla oblongata during selective elicitation of the laryngeal adductor response. *J. Neurophysiol.* 92**,** 2920-2932.

Andersen, M.C., and Kunze, D.L. (1994). Nucleus tractus solitarius-gateway to neural circulatory control. *Annu. Rev. Physiol.* 56**,** 93-116.

Andresen, M.C., and Mendelowitz, D. (1996). Sensory afferent neurotransmission in caudal nucleus tractus solitarius—common denominators. *Chem. Senses* 21**,** 387-395.

Angelucci, A., Clascá, F., and Sur, M. (1996). Anterograde axonal tracing with the subunit B of cholera toxin: a highly sensitive immunohistochemical protocol for revealing fine axonal morphology in adult and neonatal brains. *J. Neurosci. Methods* 65**,** 101-112.

Averill, D.B., Cameron, W.E., and Berger, A.J. (1984). Monosynaptic excitation of dorsal medullary respiratory neurons by slowly adapting pulmonary stretch receptors. *J. Neurophysiol.* 52**,** 771-785.

Baekey, D.M., Morris, K.F., Gestreau, C., Li, Z., Lindsey, B.G., and Shannon, R. (2001). Medullary respiratory neurones and control of laryngeal motoneurones during fictive eupnoea and cough in the cat. *J. Physiol.* 534**,** 565-581.

Baekey, D.M., Morris, K.F., Nuding, S.C., Segers, L.S., Lindsey, B.G., and Shannon, R. (2004). Ventrolateral medullary respiratory network participation in the expiration reflex in the cat. *J. Appl. Physiol.* 96**,** 2057-2072.

Bao, X., Wiedner, E.B., and Altschuler, S.M. (1995). Transsynaptic localization of pharyngeal premotor neurons in rat. *Brain Res.* 696**,** 246-249.

Barillot, J., Bianchi, A., and Gogan, P. (1984a). Laryngeal respiratory motoneurones: morphology and electrophysiological evidence of separate sites for excitatory and inhibitory synaptic inputs. *Neurosci. Lett.* 47**,** 107-112.

Barillot, J.C., Bianchi, A.L., and Gogan, P. (1984b). Laryngeal respiratory motoneurones: morphology and electrophysiological evidence of separate sites for excitatory and inhibitory synaptic inputs. *Neurosci. Lett.* 47**,** 107-112.

Barraco, I.R.A. (1993). *Nucleus of the solitary tract.* CRC Press.

Bautista, T.G., Sun, Q.J., and Pilowsky, P.M. (2012). Expiratory-modulated laryngeal motoneurons exhibit a hyperpolarization preceding depolarization during superior laryngeal nerve stimulation in the in vivo adult rat. *Brain Res.* 1445**,** 52-61.

Bautista, T.G., Sun, Q.J., Zhao, W.J., and Pilowsky, P.M. (2010). Cholinergic inputs to laryngeal motoneurons functionally identified in vivo in rat: a combined electrophysiological and microscopic study. *J. Comp. Neurol.* 518**,** 4903-4916.

Bellingham, M., Lipski, J., and Voss, M. (1989). Synaptic inhibition of phrenic motoneurons evoked by stimulation of the superior laryngeal nerve. *Brain Res. Protoc.* 486**,** 391-395.

Bellingham, M.C., and Lipski, J. (1992). Morphology and electrophysiology of superior laryngeal nerve afferents and postsynaptic neurons in the medulla oblongata of the cat. *Neuroscience* 48**,** 205-216.

Berger, A.J. (1977). Dorsal respiratory group neurons in the medulla of cat: spinal projections, responses to lung inflation and superior laryngeal nerve stimulation. *Brain Res.* 135**,** 231-254.

Berkowitz, R.G., Sun, Q.-J., and Pilowsky, P.M. (2005). Congenital bilateral vocal cord paralysis and the role of glycine. *Ann. Otol. Rhinol. Laryngol.* 114**,** 494-498.

Bieger, D., and Hopkins, D.A. (1987). Viscerotopic representation of the upper alimentary tract in the medulla oblongata in the rat: the nucleus ambiguus. *J. Comp. Neurol.* 262**,** 546-562.

Biscoe, T., and Sampson, S. (1970). Responses of cells in the brain stem of the cat to stimulation of the sinus, glossopharyngeal, aortic and superior laryngeal nerves. *J. Physiol.* 209**,** 359-373.

Bolser, D.C. (1991). Fictive cough in the cat. *J. Appl. Physiol.* 71**,** 2325-2331.

Bongianni, F., Corda, M., Fontana, G., and Pantaleo, T. (1988). Influences of superior laryngeal afferent stimulation on expiratory activity in cats. *J. Appl. Physiol.* 65**,** 385-392.

Bongianni, F., Mutolo, D., Carfì, M., Fontana, G.A., and Pantaleo, T. (2000). Respiratory neuronal activity during apnea and poststimulatory effects of laryngeal origin in the cat. *J. Appl. Physiol.* 89**,** 917-925.

Bongianni, F., Mutolo, D., Cinelli, E., and Pantaleo, T. (2010). Respiratory responses induced by blockades of GABA and glycine receptors within the Bötzinger complex and the pre-Bötzinger complex of the rabbit. *Brain Res.* 1344**,** 134-147.

Bonham, A., and Mccrimmon, D. (1990). Neurones in a discrete region of the nucleus tractus solitarius are required for the Breuer-Hering reflex in rat. *J. Physiol.* 427**,** 261-280.

Bonham, A.C., Chen, C.-Y., Sekizawa, S.-I., and Joad, J.P. (2006). Plasticity in the nucleus tractus solitarius and its influence on lung and airway reflexes. *J. Appl. Physiol.* 101**,** 322-327.

Bosma, J.F. (1957). Deglutition: Pharpgeal Stage'.

Bowler, K., Worsley, M., Broad, L., Sher, E., Benschop, R., Johnson, K., Yates, J., Robinson, P., and Boissonade, F. (2013). Evidence for anti-inflammatory and putative analgesic effects of a monoclonal antibody to calcitonin gene-related peptide. *Neuroscience* 228**,** 271-282.

Bradley, R.M. (2010). *The role of the nucleus of the solitary tract in gustatory processing.* CRC Press.

Brining, S.K., and Smith, D.V. (1996). Distribution and synaptology of glossopharyngeal afferent nerve terminals in the nucleus of the solitary tract of the hamster. *J. Comp. Neurol.* 365**,** 556-574.

Broussard, D., Wiedner, E., Li, X., and Altschuler, S. (1994). NMDAR1 mRNA expression in the brainstem circuit controlling esophageal peristalsis. *Mol. Brain Res.* 27**,** 329-332.

Broussard, D.L., Bao, X., and Altschuler, S.M. (1998). Somatostatin immunoreactivity in esophageal premotor neurons of the rat. *Neurosci. Lett.* 250**,** 201-204.

Burke, P., Abbott, S., Mcmullan, S., Goodchild, A., and Pilowsky, P. (2010). Somatostatin selectively ablates post-inspiratory activity after injection into the Bötzinger complex. *Neuroscience* 167**,** 528-539.

Canning, B.J. (2009). Central regulation of the cough reflex: therapeutic implications. *Pulm. Pharmacol. Ther.* 22**,** 75-81.

Canning, B.J., Mazzone, S.B., Meeker, S.N., Mori, N., Reynolds, S.M., and Undem, B.J. (2004). Identification of the tracheal and laryngeal afferent neurones mediating cough in anaesthetized guinea-pigs. *J. Physiol.* 557**,** 543-558.

Canning, B.J., and Mori, N. (2010). An essential component to brainstem cough gating identified in anesthetized guinea pigs. *FASEB J.* 24**,** 3916-3926.

Chou, Y.-L., Scarupa, M.D., Mori, N., and Canning, B.J. (2008). Differential effects of airway afferent nerve subtypes on cough and respiration in anesthetized guinea pigs. *Am. J. Physiol. Regul. Integr. Comp. Physiol.* 295**,** R1572-R1584.

Ciriello, J. (1983). Brainstem projections of aortic baroreceptor afferent fibers in the rat. *Neurosci. Lett.* 36**,** 37-42.

Ciriello, J., Hochstenbach, S.L., and Roder, S. (1994). Central projections of baroreceptor and chemoreceptor afferent fibers in the rat. *Nucleus of the solitary tract*, 35-50.

Clark, F., and Von Euler, C.V. (1972). On the regulation of depth and rate of breathing. *J. Physiol.* 222, 267-295.

Cohen, M.I., and Feldman, J.L. (Year). "Models of respiratory phase-switching", in: *Fed. Proc.*), 2367.

Cohen, M.I., and Feldman, J.L. (1984). Discharge properties of dorsal medullary inspiratory neurons: relation to pulmonary afferent and phrenic efferent discharge. *J. Neurophysiol.* 51, 753-776.

Conte, W.L., Kamishina, H., and Reep, R.L. (2009a). The efficacy of the fluorescent conjugates of cholera toxin subunit B for multiple retrograde tract tracing in the central nervous system. *Brain. Struct. Funct.* 213, 367-373.

Conte, W.L., Kamishina, H., and Reep, R.L. (2009b). Multiple neuroanatomical tract-tracing using fluorescent Alexa Fluor conjugates of cholera toxin subunit B in rats. *Nat. Protoc.* 4, 1157-1166.

Contreras, R.J., Beckstead, R.M., and Norgren, R. (1982). The central projections of the trigeminal, facial, glossopharyngeal and vagus nerves: an autoradiographic study in the rat. *J. Auton. Nerv. Syst.* 6, 303-322.

Corson, J., Aldridge, A., Wilmoth, K., and Erisir, A. (2012). A survey of oral cavity afferents to the rat nucleus tractus solitarii. *J. Comp. Neurol.* 520, 495-527.

Cowan, W.M., Gottlieb, D., Hendrickson, A.E., Price, J., and Woolsey, T. (1972). The autoradiographic demonstration of axonal connections in the central nervous system. *Brain Res.* 37, 21-51.

Cunningham, E., Simmons, D., Swanson, L., and Sawchenko, P. (1991). Enkephalin immunoreactivity and messenger RNA in a discrete projection from the nucleus of the solitary tract to the nucleus ambiguus in the rat. *J. Comp. Neurol.* 307, 1-16.

Cunningham, E.T., and Sawchenko, P.E. (2000). Dorsal medullary pathways subserving oromotor reflexes in the rat: implications for the central neural control of swallowing. *J. Comp. Neurol.* 417, 448-466.

Curran, A.K., Xia, L., Leiter, J., and Bartlett, D. (2005a). Elevated body temperature enhances the laryngeal chemoreflex in decerebrate piglets. *J. Appl. Physiol.* 98, 780-786.

Curran, A.K., Xia, L., Leiter, J.C., and Bartlett, D., Jr. (2005b). Elevated body temperature enhances the laryngeal chemoreflex in decerebrate piglets. *J. Appl. Physiol. (1985)* 98**,** 780-786.

Czyzyk-Krzeska, M.F., and Lawson, E. (1991). Synaptic events in ventral respiratory neurones during apnoea induced by laryngeal nerve stimulation in neonatal pig. *J. Physiol.* 436**,** 131-147.

Davies, R., Kubin, L., and Pack, A. (1987). Pulmonary stretch receptor relay neurones of the cat: location and contralateral medullary projections. *J. Physiol.* 383**,** 571-585.

De Castro, D., Lipski, J., and Kanjhan, R. (1994). Electrophysiological study of dorsal respiratory neurons in the medulla oblongata of the rat. *Brain Res.* 639**,** 49-56.

Dick, T.E., Oku, Y., Romaniuk, J.R., and Cherniack, N.S. (1993). Interaction between central pattern generators for breathing and swallowing in the cat. *J. Physiol.* 465**,** 715-730.

Dobbins, E.G., and Feldman, J.L. (1994). Brainstem network controlling descending drive to phrenic motoneurons in rat. *J. Comp. Neurol.* 347**,** 64-86.

Donnelly, D.F., Sica, A.L., Cohen, M.I., and Zhang, H. (1989a). Dorsal medullary inspiratory neurons: effects of superior laryngeal afferent stimulation. *Brain Res.* 491**,** 243-252.

Donnelly, D.F., Sica, A.L., Cohen, M.I., and Zhang, H. (1989b). Effects of contralateral superior laryngeal nerve stimulation on dorsal medullary inspiratory neurons. *Brain Res.* 505**,** 149-152.

Donoghue, S., Felder, R., Gilbey, M., Jordan, D., and Spyer, K. (1985). Post-synaptic activity evoked in the nucleus tractus solitarius by carotid sinus and aortic nerve afferents in the cat. *J. Physiol.* 360**,** 261-273.

Doty, R.W. (1951). Influence of stimulus pattern on reflex deglutition. *Am. J. Physiol.* 166**,** 142-158.

Downing, S.E., and Lee, J.C. (1975). Laryngeal chemosensitivity: a possible mechanism for sudden infant death. *Pediatrics* 55**,** 640-649.

Duffin, J. (2004). Functional organization of respiratory neurones: a brief review of current questions and speculations. *Exp. Physiol.* 89**,** 517-529.

Duffin, J., Ezure, K., and Lipski, J. (1995). Breathing rhythm generation: focus on the rostral ventrolateral medulla. *Physiology* 10**,** 133-140.

Duffin, J., and Lipski, J. (1987). Monosynaptic excitation of thoracic motoneurones by inspiratory neurones of the nucleus tractus solitarius in the cat. *J. Physiol.* 390, 415-431.

Dutschmann, M., and Dick, T.E. (2012). *Pontine mechanisms of respiratory control.*

Dutschmann, M., and Herbert, H. (2006a). The Kolliker-Fuse nucleus gates the postinspiratory phase of the respiratory cycle to control inspiratory off-switch and upper airway resistance in rat. *Eur. J. Neurosci.* 24, 1071-1084.

Dutschmann, M., and Herbert, H. (2006b). The Kölliker-Fuse nucleus gates the postinspiratory phase of the respiratory cycle to control inspiratory off-switch and upper airway resistance in rat. *Eur. J. Neurosci.* 24, 1071-1084.

Ellenberger, H.H., and Feldman, J.L. (1988). Monosynaptic transmission of respiratory drive to phrenic motoneurons from brainstem bulbospinal neurons in rats. *J. Comp. Neurol.* 269, 47-57.

Ellenberger, H.H., Vera, P.L., Haselton, J.R., Haselton, C.L., and Schneiderman, N. (1990). Brainstem projections to the phrenic nucleus: an anterograde and retrograde HRP study in the rabbit. *Brain Res. Bull.* 24, 163-174.

Ezure, K. (1990). Synaptic connections between medullary respiratory neurons and considerations on the genesis of respiratory rhythm. *Prog. Neurobiol.* 35, 429-450.

Ezure, K. (2004). Respiration-related afferents to parabrachial pontine regions. *Respir. Physiol. Neurobiol.* 143, 167-175.

Ezure, K., and Manabe, M. (1988). Decrementing expiratory neurons of the Bötzinger complex. *Exp. Brain. Res.* 72, 159-166.

Ezure, K., Oku, Y., and Tanaka, I. (1993). Location and axonal projection of one type of swallowing interneurons in cat medulla. *Brain Res.* 632, 216-224.

Ezure, K., Otake, K., Lipski, J., and She, R.B.W. (1991). Efferent projections of pulmonary rapidly adapting receptor relay neurons in the cat. *Brain Res.* 564, 268-278.

Ezure, K., Tanaka, I., and Kondo, M. (2003). Glycine is used as a transmitter by decrementing expiratory neurons of the ventrolateral medulla in the rat. *J. Neurosci.* 23, 8941-8948.

Ezure, K., Tanaka, I., Saito, Y., and Otake, K. (2002). Axonal projections of pulmonary slowly adapting receptor relay neurons in the rat. *J. Comp. Neurol.* 446, 81-94.

Fedorko, L., Duffin, J., and England, S. (1989). Inhibition of inspiratory neurons of the nucleus retroambigualis by expiratory neurons of the Botzinger complex in the cat. *Exp. Neurol.* 106**,** 74-77.

Fedorko, L., Merrill, E., and Lipski, J. (1983). Two descending medullary inspiratory pathways to phrenic motoneurones. *Neurosci. Lett.* 43**,** 285-291.

Feldman, J.L., Del Negro, C.A., and Gray, P.A. (2013). Understanding the rhythm of breathing: so near yet so far. *Annu. Rev. Physiol.* 75**,** 423.

Feldman, J.L., and Kam, K. (2015). Facing the challenge of mammalian neural microcircuits: Taking a few breaths may help. *J. Physiol.* 593**,** 3-23.

Feldman, J.L., Loewy, A.D., and Speck, D.F. (1985). Projections from the ventral respiratory group to phrenic and intercostal motoneurons in cat: an autoradiographic study. *J. Neurosci.* 5**,** 1993-2000.

Feldman, J.L., Mitchell, G.S., and Nattie, E.E. (2003). Breathing: rhythmicity, plasticity, chemosensitivity. *Annu. Rev. Neurosci.* 26**,** 239.

Feroah, T.R., Forster, H., Fuentes, C.G., Lang, I.M., Beste, D., Martino, P., Pan, L., and Rice, T. (2002). Effects of spontaneous swallows on breathing in awake goats. *J. Appl. Physiol.* 92**,** 1923-1935.

Finley, J.C., and Katz, D.M. (1992). The central organization of carotid body afferent projections to the brainstem of the rat. *Brain Res.* 572**,** 108-116.

Furusawa, K., Yasuda, K., Okuda, D., Tanaka, M., and Yamaoka, M. (1996). Central distribution and peripheral functional properties of afferent and efferent components of the superior laryngeal nerve: morphological and electrophysiological studies in the rat. *J. Comp. Neurol.* 375**,** 147-156.

Gai, W.P., Messenger, J., Yu, Y.H., Gieroba, Z., and Blessing, W. (1995). Nitric oxide-synthesising neurons in the central subnucleus of the nucleus tractus solitarius provide a major innervation of the rostral nucleus ambiguus in the rabbit. *J. Comp. Neurol.* 357**,** 348-361.

Gestreau, C., Bianchi, A.L., and Grélot, L. (1997). Differential brainstem Fos-like immunoreactivity after laryngeal-induced coughing and its reduction by codeine. *J. Neurosci.* 17**,** 9340-9352.

Gestreau, C., Milano, S., Bianchi, A.L., and Grélot, L. (1996). Activity of dorsal respiratory group inspiratory neurons during laryngeal-induced fictive coughing and swallowing in decerebrate cats. *Exp. Brain. Res.* 108**,** 247-256.

Goding, G.S., Richardson, M.A., and Trachy, R.E. (1987). Laryngeal chemoreflex: anatomic and physiologic study by use of the superior laryngeal nerve in the piglet. *Otolaryngol. Head Neck Surg.* 97**,** 28-38.

Grabauskas, G., and Bradley, R.M. (1996). Synaptic interactions due to convergent input from gustatory afferent fibers in the rostral nucleus of the solitary tract. *J. Neurophysiol.* 76**,** 2919-2927.

Gradinaru, V., Zhang, F., Ramakrishnan, C., Mattis, J., Prakash, R., Diester, I., Goshen, I., Thompson, K.R., and Deisseroth, K. (2010). Molecular and cellular approaches for diversifying and extending optogenetics. *Cell* 141**,** 154-165.

Graham, K., and Duffin, J. (1982). Cross-correlation of medullary dorsomedial inspiratory neurons in the cat. *Exp. Neurol.* 75**,** 627-643.

Graham, K., and Duffin, J. (1985). Short-latency interactions among dorsomedial medullary inspiratory neurons in the cat. *Exp. Neurol.* 88**,** 726-741.

Granata, A.R., Numao, Y., Kumada, M., and Reis, D.J. (1986). A1 noradrenergic neurons tonically inhibit sympathoexcitatory neurons of C1 area in rat brainstem. *Brain Res.* 377**,** 127-146.

Gromysz, H., and Karczewski, W. (1981). Respiratory activity generated by a split brainstem preparation of the rabbit. *Acta Neurobiol. Exp.* 41**,** 237-242.

Guyenet, P.G., Bayliss, D.A., Stornetta, R.L., Fortuna, M.G., Abbott, S.B., and Depuy, S.D. (2009). Retrotrapezoid nucleus, respiratory chemosensitivity and breathing automaticity. *Respir. Physiol. Neurobiol.* 168**,** 59-68.

Haji, A., Okazaki, M., Yamazaki, H., and Takeda, R. (2002). Physiological properties of late inspiratory neurons and their possible involvement in inspiratory off-switching in cats. *J. Neurophysiol.* 87**,** 1057-1067.

Haji, A., Takeda, R., and Remmers, J.E. (1992). Evidence that glycine and GABA mediate postsynaptic inhibition of bulbar respiratory neurons in the cat. *J. Appl. Physiol.* 73**,** 2333-2342.

Hanamori, T., and Smith, D.V. (1986). Central projections of the hamster superior laryngeal nerve. *Brain Res. Bull.* 16**,** 271-279.

Hayakawa, T., Takanaga, A., Maeda, S., Ito, H., and Seki, M. (2000). Monosynaptic inputs from the nucleus tractus solitarii to the laryngeal motoneurons in the nucleus ambiguus of the rat. *Anat. Embryol. (Berl)* 202**,** 411-420.

Hayakawa, T., Zheng, J.Q., and Yajima, Y. (1997). Direct synaptic projections to esophageal motoneurons in the nucleus ambiguus from the nucleus of the solitary tract of the rat. *J. Comp. Neurol.* 381**,** 18-30.

Hayashi, F., Coles, S.K., and Mccrimmon, D.R. (1996). Respiratory neurons mediating the Breuer–Hering reflex prolongation of expiration in rat. *J. Neurosci.* 16**,** 6526-6536.

Heman-Ackah, Y.D., Pernell, K.J., and Goding, G.S., Jr. (2009). The laryngeal chemoreflex: an evaluation of the normoxic response. *Laryngoscope* 119**,** 370-379.

Heman-Ackah, Y.D., Pernell, K.J., and Goding, G.S. (2009). The laryngeal chemoreflex: An evaluation of the normoxic response. *Laryngoscope* 119**,** 370-379.

Herbert, H., Moga, M.M., and Saper, C.B. (1990). Connections of the parabrachial nucleus with the nucleus of the solitary tract and the medullary reticular formation in the rat. *J. Comp. Neurol.* 293**,** 540-580.

Hilaire, G., Monteau, R., Gauthier, P., Rega, P., and Morin, D. (1990). Functional significance of the dorsal respiratory group in adult and newborn rats: in vivo and in vitro studies. *Neurosci. Lett.* 111**,** 133-138.

Housley, G., Martin-Body, R., Dawson, N., and Sinclair, J. (1987). Brain stem projections of the glossopharyngeal nerve and its carotid sinus branch in the rat. *Neuroscience* 22**,** 237-250.

Ikari, T., and Sasaki, C.T. (1980). Glottic closure reflex: control mechanisms. *Ann. Otol. Rhinol. Laryngol.* 89**,** 220-224.

Jean, A. (1984). Brainstem organization of the swallowing network. *Brain Behav. Evol.* 25**,** 109-116.

Jean, A. (2001). Brain stem control of swallowing: neuronal network and cellular mechanisms. *Physiol. Rev.* 81**,** 929-969.

Jiang, C., and Lipski, J. (1990). Extensive monosynaptic inhibition of ventral respiratory group neurons by augmenting neurons in the Bötzinger complex in the cat. *Exp. Brain. Res.* 81**,** 639-648.

Johnson, P., Dawes, G., and Robinson, J. (1972). Maintenance of breathing in newborn lamb. *Arch. Dis. Child.* 47**,** 151.

Jordan, D. (2001). Central nervous pathways and control of the airways. *Respir Physiol.* 125**,** 67-81.

Jürgens, U. (2002). Neural pathways underlying vocal control. *Neurosci. Biobehav. Rev.* 26**,** 235-258.

Kalia, M. (1981a). "Localization of aortic and carotid baroreceptor and chemoreceptor primary afferents in the brain stem," in *Central nervous system mechanisms in hypertension*. Raven New York), 9-24.

Kalia, M., and Mesulam, M. (1980a). Brain stem projections of sensory and motor components of the vagus complex in the cat: I. The cervical vagus and nodose ganglion. *J. Comp. Neurol.* 193**,** 435-465.

Kalia, M., and Mesulam, M. (1980b). Brain stem projections of sensory and motor components of the vagus complex in the cat: II. Laryngeal, tracheobronchial, pulmonary, cardiac, and gastrointestinal branches. *J. Comp. Neurol.* 193**,** 467-508.

Kalia, M., and Sullivan, J.M. (1982). Brainstem projections of sensory and motor components of the vagus nerve in the rat. *J. Comp. Neurol.* 211**,** 248-264.

Kalia, M.P. (1981b). Anatomical organization of central respiratory neurons. *Annu. Rev. Physiol.* 43**,** 105-120.

Kessler, J., and Jean, A. (1985). Identification of the medullary swallowing regions in the rat. *Exp. Brain. Res.* 57**,** 256-263.

King, H., Kohsin, B., and Salisbury, M. NCBI Bookshelf.

Kline, D.D. (2010). Chronic intermittent hypoxia affects integration of sensory input by neurons in the nucleus tractus solitarii. *Respir. Physiol. Neurobiol.* 174**,** 29-36.

Kratskin, I.L., Yu, X., and Doty, R.L. (1997). An easily constructed pipette for pressure microinjections into the brain. *Brain Res. Bull.* 44**,** 199-203.

Kubin, L., Alheid, G.F., Zuperku, E.J., and Mccrimmon, D.R. (2006). Central pathways of pulmonary and lower airway vagal afferents. *J. Appl. Physiol.* 101**,** 618-627.

Kubin, L., and Davies, R.O. (1988). Sites of termination and relay of pulmonary rapidly adapting receptors as studied by spike-triggered averaging. *Brain Res.* 443**,** 215-221.

Kubin, L., Kimura, H., and Davies, R. (1991). The medullary projections of afferent bronchopulmonary C fibres in the cat as shown by antidromic mapping. *J. Physiol.* 435**,** 207-228.

Lanciego, J.L., and Wouterlood, F.G. (2011). A half century of experimental neuroanatomical tracing. *J. Chem. Neuroanat.* 42**,** 157-183.

Lanciego, J.L., Wouterlood, F.G., Erro, E., Arribas, J., Gonzalo, N., Urra, X., Cervantes, S., and Gimenez-Amaya, J.M. (2000). Complex brain circuits studied via simultaneous and permanent detection of three transported neuroanatomical tracers in the same histological section. *J. Neurosci. Methods* 103**,** 127-135.

Lanciego, J.L., Wouterlood, F.G., Erro, E., and Gimenez-Amaya, J.M. (1998). Multiple axonal tracing: simultaneous detection of three tracers in the same section. *Histochem. Cell Biol.* 110**,** 509-515.

Lavail, J.H., and Lavail, M.M. (1974). The retrograde intraaxonal transport of horseradish peroxidase in the chick visual system: a light and electron microscopic study. *J. Comp. Neurol.* 157**,** 303-357.

Lawrence, A.J., and Jarrott, B. (1996). Neurochemical modulation of cardiovascular control in the nucleus tractus solitarius. *Prog Neurobiol.* 48**,** 21-53.

Lawson, E.E. (1981). Prolonged central respiratory inhibition following reflex-induced apnea. *J. Appl. Physiol.* 50**,** 874-879.

Li, Y., Gieroba, Z., Mcallen, R., and Blessing, W. (1991). Neurons in rabbit caudal ventrolateral medulla inhibit bulbospinal barosensitive neurons in rostral medulla. *Am. J. Physiol. Regul. Integr. Comp. Physiol.* 261**,** R44-R51.

Lipski, J. (1981). Antidromic activation of neurones as an analytic tool in the study of the central nervous system. *J. Neurosci. Methods* 4**,** 1-32.

Lipski, J., Kanjhan, R., Kruszewska, B., and Rong, W.F. (1995). Criteria for intracellular identification of pre-sympathetic neurons in the rostral ventrolateral medulla in the rat. *Clin. Exp. Hypertens.* 17**,** 51-65.

Lipski, J., Kedra, J., and Kubin, L. (1978). A method for averaging response latency patterns of antidromically excited neurons. *Acta Neurobiol. Exp. (Wars)* 38**,** 79-84.

Lipski, J., Trzebski, A., and Kubin, L. (1979). Excitability changes of dorsal inspiratory neurons during lung inflations as studied by measurement of antidromic invasion latencies. *Brain Res.* 161**,** 25-38.

Llewellyn-Smith, I.J., and Verberne, A.J. (2011). *Central regulation of autonomic functions.* Oxford University Press.

Lucier, G.E., Egizii, R., and Dostrovsky, J.O. (1986). Projections of the internal branch of the superior laryngeal nerve of the cat. *Brain Res. Bull.* 16**,** 713-721.

Ludlow, C.L. (2005). Central nervous system control of the laryngeal muscles in humans. *Respir. Physiol. Neurobiol.* 147**,** 205-222.

Ludlow, C.L., Van Pelt, F., and Koda, J. (1992). Characteristics of late responses to superior laryngeal nerve stimulation in humans. *Ann. Otol. Rhinol. Laryngol.* 101**,** 127-134.

Luppi, P.H., Fort, P., and Jouvet, M. (1990). Iontophoretic application of unconjugated cholera toxin B subunit (CTb) combined with immunohistochemistry of neurochemical substances: a method for transmitter identification of retrogradely labeled neurons. *Brain Res.* 534**,** 209-224.

Marchenko, V., and Sapru, H. (2000). Different patterns of respiratory and cardiovascular responses elicited by chemical stimulation of dorsal medulla in the rat. *Brain Res.* 857**,** 99-109.

Marshel, J.H., Mori, T., Nielsen, K.J., and Callaway, E.M. (2010). Targeting single neuronal networks for gene expression and cell labeling in vivo. *Neuron* 67**,** 562-574.

Masuda, N., Terui, N., Koshiya, N., and Kumada, M. (1991). Neurons in the caudal ventrolateral medulla mediate the arterial baroreceptor reflex by inhibiting barosensitive reticulospinal neurons in the rostral ventrolateral medulla in rabbits. *J. Auton. Nerv. Syst.* 34**,** 103-117.

Mccrimmon, D., Speck, D., and Feldman, J. (1987). Role of the ventrolateral region of the nucleus of the tractus solitarius in processing respiratory afferent input from vagus and superior laryngeal nerves. *Exp. Brain. Res.* 67**,** 449-459.

Mccrimmon, D.R., Monnier, A., Hayashi, F., and Zuperku, E.J. (2000). Pattern formation and rhythm generation in the ventral respiratory group. *Clin. Exp. Pharmacol. Physiol.* 27**,** 126-131.

Mcgovern, A., Davis-Poynter, N., Farrell, M., and Mazzone, S. (2012). Transneuronal tracing of airways-related sensory circuitry using herpes simplex virus 1, strain H129. *Neuroscience* 207**,** 148-166.

Mcmullan, S. (2013). "Identification of spinally projecting neurons in the rostral ventrolateral medulla in vivo," in *Stimulation and Inhibition of Neurons.* Springer), 123-140.

Meessen, H., and Olszewski, J. (1949). A Cytoarchitectonic Atlas of the Rhombencephalon of the Rabbit. *Cytoarchitektonischer Atlas des Rautenhirns des Kaninchens.*

Mendelowitz, D., Yang, M., Andresen, M.C., and Kunze, D.L. (1992). Localization and retention in vitro of fluorescently labeled aortic baroreceptor terminals on neurons from the nucleus tractus solitarius. *Brain Res.* 581**,** 339-343.

Merrill, E., and Fedorko, L. (1984). Monosynaptic inhibition of phrenic motoneurons: a long descending projection from Botzinger neurons. *J. Neurosci.* 4**,** 2350-2353.

Merrill, E., and Lipski, J. (1987). Inputs to intercostal motoneurons from ventrolateral medullary respiratory neurons in the cat. *J. Neurophysiol.* 57**,** 1837-1853.

Merrill, E., Lipski, J., Kubin, L., and Fedorko, L. (1983). Origin of the expiratory inhibition of nucleus tractus solitarius inspiratory neurones. *Brain Res.* 263**,** 43-50.

Mifflin, S.W., and Felder, R.B. (1990). Synaptic mechanisms regulating cardiovascular afferent inputs to solitary tract nucleus. *Am. J. Physiol. Heart Circ. Physiol.* 259**,** H653-H661.

Miller, A.J., and Loizzi, R.F. (1974). Anatomical and functional differentiation of superior laryngeal nerve fibers affecting swallowing and respiration. *Exp. Neurol.* 42**,** 369-387.

Miyazaki, M., Arata, A., Tanaka, I., and Ezure, K. (1998). Activity of rat pump neurons is modulated with central respiratory rhythm. *Neurosci. Lett.* 249**,** 61-64.

Monnier, A., Alheid, G., and Mccrimmon, D. (2003). Defining ventral medullary respiratory compartments with a glutamate receptor agonist in the rat. *J. Physiol.* 548**,** 859-874.

Morecraft, R.J., Herrick, J.L., Stilwell-Morecraft, K.S., Louie, J.L., Schroeder, C.M., Ottenbacher, J.G., and Schoolfield, M.W. (2002). Localization of arm representation in the corona radiata and internal capsule in the non-human primate. *Brain* 125**,** 176-198.

Moreira, T.S., Takakura, A.C., Colombari, E., and Guyenet, P.G. (2007). Activation of 5-hydroxytryptamine type 3 receptor-expressing C-fiber vagal afferents inhibits retrotrapezoid nucleus chemoreceptors in rats. *J. Neurophysiol.* 98**,** 3627-3637.

Mörschel, M., and Dutschmann, M. (2009). Pontine respiratory activity involved in inspiratory/expiratory phase transition. *Philos. Trans. R. Soc. Lond. B. Biol. Sci.* 364**,** 2517-2526.

Nauta, W.J., and Gygax, P.A. (1954). Silver impregnation of degenerating axons in the central nervous system: a modified technic. *Stain Technol.* 29**,** 91-93.

Norgren, R. (1978). Projections from the nucleus of the solitary tract in the rat. *Neuroscience* 3**,** 207-218.

Núñez-Abades, P.A., Morillo, A.M., and Pásaro, R. (1993). Brainstem connections of the rat ventral respiratory subgroups: afferent projections. *J. Auton. Nerv. Syst.* 42**,** 99-118.

Odutola, A.B. (1976). Cell grouping and Golgi architecture of the hypoglossal nucleus of the rat. *Exp. Neurol.* 52**,** 356-371.

Okazaki, M., Takeda, R., Yamazaki, H., and Haji, A. (2002). Synaptic mechanisms of inspiratory off-switching evoked by pontine pneumotaxic stimulation in cats. *Neurosci. Res.* 44**,** 101-110.

Oku, Y., and Dick, T.E. (1992). Phase resetting of the respiratory cycle before and after unilateral pontine lesion in cat. *J. Appl. Physiol.* 72**,** 721-730.

Oku, Y., Tanaka, I., and Ezure, K. (1994). Activity of bulbar respiratory neurons during fictive coughing and swallowing in the decerebrate cat. *J. Physiol.* 480**,** 309-324.

Oliveira-Maia, A.J., Roberts, C.D., Simon, S.A., and Nicolelis, M.A. (2011). "Gustatory and reward brain circuits in the control of food intake," in *Adv. Tech. Stand. Neurosurg.*: Springer), 31-59.

Ono, K., Shiba, K., Nakazawa, K., and Shimoyama, I. (2006). Synaptic origin of the respiratory-modulated activity of laryngeal motoneurons. *Neuroscience* 140**,** 1079-1088.

Ootani, S., Umezaki, T., Shin, T., and Murata, Y. (1995). Convergence of afferents from the SLN and GPN in cat medullary swallowing neurons. *Brain Res. Bull.* 37**,** 397-404.

Otake, K., Ezure, K., Lipski, J., and Wongshe, R.B. (1992). Projections from the commissural subnucleus of the nucleus of the solitary tract: an anterograde tracing study in the cat. *J. Comp. Neurol.* 324**,** 365-378.

Otake, K., Nakamura, Y., Tanaka, I., and Ezure, K. (2001). Morphology of pulmonary rapidly adapting receptor relay neurons in the rat. *J. Comp. Neurol.* 430**,** 458-470.

Otake, K., Sasaki, H., Ezure, K., and Manabe, M. (1989). Axonal trajectory and terminal distribution of inspiratory neurons of the dorsal respiratory group in the cat's medulla. *J. Comp. Neurol.* 286**,** 218-230.

Pace, G.E. (2009). "Optimization of immunohistochemical reactions," in *Immunohistochemical staining methods*. Dako), 109-114.

Page, M., Jeffery, H., Post, E., and Wood, A. (1996). Simulated Pharyngeal Reflux Can Lead to Life-Threatening Apnea. if Swallowing and Arousal Are Depressed. *J Sud. Inf. Death Syn. Inf. Mort.* 1**,** 281-294.

Pagliardini, S., Janczewski, W.A., Tan, W., Dickson, C.T., Deisseroth, K., and Feldman, J.L. (2011). Active expiration induced by excitation of ventral medulla in adult anesthetized rats. *J. Neurosci.* 31**,** 2895-2905.

Pantaleo, T., and Corda, M. (1985). Expiration-related neurons in the region of the retrofacial nucleus: vagal and laryngeal inhibitory influences. *Brain Res.* 359**,** 343-346.

Pascual-Font, A., Hernández-Morato, I., Mchanwell, S., Vázquez, T., Maranillo, E., Sañudo, J., and Valderrama-Canales, F.J. (2011). The central projections of the laryngeal nerves in the rat. *J. Anat.* 219**,** 217-228.

Paton, J.F. (1998). Pattern of cardiorespiratory afferent convergence to solitary tract neurons driven by pulmonary vagal C-fiber stimulation in the mouse. *J. Neurophysiol.* 79**,** 2365-2373.

Paxinos, G., and Franklin, K.B. (2004). *The mouse brain in stereotaxic coordinates.* Gulf Professional Publishing.

Paxinos, G., Watson, C., Carrive, P., Kirkcaldie, M., and Ashwell, K. (2009). Chemoarchitectonic atlas of the rat brain.

Peever, J., Shen, L., and Duffin, J. (2002). Respiratory pre-motor control of hypoglossal motoneurons in the rat. *Neuroscience* 110**,** 711-722.

Pickens, D.L., Schefft, G.L., Storch, G.A., and Thach, B.T. (1989). Characterization of prolonged apneic episodes associated with respiratory syncytial virus infection. *Pediatr. Pulmonol.* 6**,** 195-201.

Pierrefiche, O., Champagnat, J., and Richter, D.W. (1995). Calcium-dependent conductances control neurones involved in termination of inspiration in cats. *Neurosci. Lett.* 184**,** 101-104.

Pilowsky, P.M., Jiang, C., and Lipski, J. (1990). An intracellular study of respiratory neurons in the rostral ventrolateral medulla of the rat and their relationship to catecholamine-containing neurons. *J. Comp. Neurol.* 301**,** 604-617.

Porter, R. (1963). Unit responses evoked in the medulla oblongata by vagus nerve stimulation. *J. Physiol.* 168**,** 717-735.

Reiner, A., Veenman, C.L., Medina, L., Jiao, Y., Del Mar, N., and Honig, M.G. (2000). Pathway tracing using biotinylated dextran amines. *J. Neurosci. Methods* 103**,** 23-37.

Richter, D. (1982). Generation and maintenance of the respiratory rhythm. *J. Exp. Biol.* 100**,** 93-107.

Richter, D.W., and Smith, J.C. (2014). Respiratory rhythm generation in vivo. *Physiology* 29**,** 58-71.

Ross, C.A., Ruggiero, D.A., and Reis, D.J. (1985). Projections from the nucleus tractus solitarii to the rostral ventrolateral medulla. *J. Comp. Neurol.* 242**,** 511-534.

Ruggiero, D., Mtui, E., Otake, K., and Anwar, M. (1996). Central and primary visceral afferents to nucleus tractus solitarii may generate nitric oxide as a membrane-permeant neuronal messenger. *J. Comp. Neurol.* 364**,** 51-67.

Rybak, I.A., O'connor, R., Ross, A., Shevtsova, N., Nuding, S.C., Segers, L.S., Shannon, R., Dick, T.E., Dunin-Barkowski, W.L., and Orem, J.M. (2008). Reconfiguration of the pontomedullary respiratory network: a computational modeling study with coordinated in vivo experiments. *J. Neurophysiol.*

Saito, Y., Ezure, K., and Tanaka, I. (2002a). Swallowing-related activities of respiratory and non-respiratory neurons in the nucleus of solitary tract in the rat. *J. Physiol.* 540**,** 1047-1060.

Saito, Y., Ezure, K., and Tanaka, I. (2002b). Swallowing-related activities of respiratory and non-respiratory neurons in the nucleus of solitary tract in the rat. *J. Physiol.* 540**,** 1047-1060.

Sant'ambrogio, G., and Mathew, O. (1986). Laryngeal receptors and their reflex responses. *Clin. Chest. Med.* 7**,** 211-222.

Sasaki, C.T., and Suzuki, M. (1976). Laryngeal reflexes in cat, dog, and man. *Arch. Otolaryngol.* 102**,** 400-402.

Satoh, I., Shiba, K., Kobayashi, N., Nakajima, Y., and Konno, A. (1998). Upper airway motor outputs during sneezing and coughing in decerebrate cats. *Neurosci. Res.* 32**,** 131-135.

Schmued, L., Kyriakidis, K., and Heimer, L. (1990). In vivo anterograde and retrograde axonal trnasport of the fluoresecent rhodamine-dextran-amine, Fluor-Ruby, within the CNS. *Brain Res.* 526**,** 127-134.

Schmued, L.C., and Fallon, J.H. (1986). Fluoro-Gold: a new fluorescent retrograde axonal tracer with numerous unique properties. *Brain Res.* 377**,** 147-154.

Schreihofer, A.M., Stornetta, R.L., and Guyenet, P.G. (1999). Evidence for glycinergic respiratory neurons: Bötzinger neurons express mRNA for glycinergic transporter 2. *J. Comp. Neurol.* 407**,** 583-597.

Segers, L.S., Nuding, S.C., Dick, T.E., Shannon, R., Baekey, D.M., Solomon, I.C., Morris, K.F., and Lindsey, B.G. (2008). Functional connectivity in the pontomedullary respiratory network. *J. Neurophysiol.* 100**,** 1749-1769.

Sessle, B.J. (1973). Excitatory and inhibitory inputs to single neurones in the solitary tract nucleus and adjacent reticular formation. *Brain Res.* 53**,** 319-331.

Shao, X.M., and Feldman, J.L. (1997). Respiratory rhythm generation and synaptic inhibition of expiratory neurons in pre-Bötzinger complex: differential roles of glycinergic and GABAergic neural transmission. *J. Neurophysiol.* 77**,** 1853-1860.

Shiba, K., Nakazawa, K., Ono, K., and Umezaki, T. (2007). Multifunctional laryngeal premotor neurons: their activities during breathing, coughing, sneezing, and swallowing. *J. Neurosci.* 27**,** 5156-5162.

Shiba, K., Satoh, I., Kobayashi, N., and Hayashi, F. (1999). Multifunctional laryngeal motoneurons: an intracellular study in the cat. *J. Neurosci.* 19**,** 2717-2727.

Simera, M., Poliacek, I., Dobrolubov, B., Veternik, M., Plevkova, J., and Jakus, J. (2015). Interactions of mechanically induced coughing and sneezing in cat. *Respir. Physiol. Neurobiol.* 205**,** 21-27.

Smith, J.C., Abdala, A., Koizumi, H., Rybak, I.A., and Paton, J.F. (2007). Spatial and functional architecture of the mammalian brain stem respiratory network: a hierarchy of three oscillatory mechanisms. *J. Neurophysiol.* 98**,** 3370-3387.

Smith, J.C., Abdala, A.P., Rybak, I.A., and Paton, J.F. (2009). Structural and functional architecture of respiratory networks in the mammalian brainstem. *Philos. Trans. R. Soc. Lond. B. Biol. Sci.* 364**,** 2577-2587.

Smith, J.C., Morrison, D.E., Ellenberger, H.H., Otto, M.R., and Feldman, J.L. (1989). Brainstem projections to the major respiratory neuron populations in the medulla of the cat. *J. Comp. Neurol.* 281**,** 69-96.

Song, G., and Poon, C.-S. (2004). Functional and structural models of pontine modulation of mechanoreceptor and chemoreceptor reflexes. *Respir. Physiol. Neurobiol.* 143**,** 281-292.

Song, G., Xu, H., Wang, H., Macdonald, S.M., and Poon, C.-S. (2011). Hypoxia-excited neurons in NTS send axonal projections to Kölliker-Fuse/parabrachial complex in dorsolateral pons. *Neuroscience* 175**,** 145-153.

Spyer, K. (1982). Central nervous integration of cardiovascular control. *J. Exp. Biol.* 100**,** 109-128.

St-Hilaire, M., Nsegbe, E., Gagnon-Gervais, K., Samson, N., Moreau-Bussiere, F., Fortier, P.-H., and Praud, J.-P. (2005). Laryngeal chemoreflexes induced by acid, water, and saline in nonsedated newborn lambs during quiet sleep. *J. Appl. Physiol.* 98**,** 2197-2203.

Sugiyama, Y., Shiba, K., Mukudai, S., Umezaki, T., and Hisa, Y. (2014). Activity of respiratory neurons in the rostral medulla during vocalization, swallowing, and coughing in guinea pigs. *Neurosci. Res.* 80**,** 17-31.

Sugiyama, Y., Shiba, K., Nakazawa, K., Suzuki, T., Umezaki, T., Ezure, K., Abo, N., Yoshihara, T., and Hisa, Y. (2011). Axonal projections of medullary swallowing neurons in guinea pigs. *J. Comp. Neurol.* 519**,** 2193-2211.

Sun, Q.-J., Berkowitz, R.G., and Pilowsky, P.M. (2008). GABA A mediated inhibition and post-inspiratory pattern of laryngeal constrictor motoneurons in rat. *Respir. Physiol. Neurobiol.* 162**,** 41-47.

Sun, Q.J., Bautista, T.G., Berkowitz, R.G., Zhao, W.J., and Pilowsky, P.M. (2011a). The temporal relationship between non-respiratory burst activity of expiratory laryngeal motoneurons and phrenic apnoea during stimulation of the superior laryngeal nerve in rat. *J. Physiol.* 589**,** 1819-1830.

Sun, Q.J., Bautista, T.G., Berkowitz, R.G., Zhao, W.J., and Pilowsky, P.M. (2011b). The temporal relationship between non-respiratory burst activity of expiratory

laryngeal motoneurons and phrenic apnoea during stimulation of the superior laryngeal nerve in rat. *J. Physiol.* 589**,** 1819-1830.

Sun, Q.J., Berkowitz, R.G., Goodchild, A.K., and Pilowsky, P.M. (2002). Serotonin inputs to inspiratory laryngeal motoneurons in the rat. *J. Comp. Neurol.* 451**,** 91-98.

Takakura, A.C., Barna, B.F., Cruz, J.C., Colombari, E., and Moreira, T.S. (2014). Phox2b-expressing retrotrapezoid neurons and the integration of central and peripheral chemosensory control of breathing in conscious rats. *Exp. Physiol.* 99**,** 571-585.

Takakura, A.C., Moreira, T.S., West, G.H., Gwilt, J.M., Colombari, E., Stornetta, R.L., and Guyenet, P.G. (2007). GABAergic pump cells of solitary tract nucleus innervate retrotrapezoid nucleus chemoreceptors. *J. Neurophysiol.* 98**,** 374-381.

Takakura, A.C.T., Moreira, T.S., Colombari, E., West, G.H., Stornetta, R.L., and Guyenet, P.G. (2006). Peripheral chemoreceptor inputs to retrotrapezoid nucleus (RTN) CO2-sensitive neurons in rats. *J. Physiol.* 572**,** 503-523.

Terui, N., Masuda, N., Saeki, Y., and Kumada, M. (1990). Activity of barosensitive neurons in the caudal ventrolateral medulla that send axonal projections to the rostral ventrolateral medulla in rabbits. *Neurosci. Lett.* 118**,** 211-214.

Thach, B.T. (2001). Maturation and transformation of reflexes that protect the laryngeal airway from liquid aspiration from fetal to adult life. *Am. J. Med.* 111 Suppl 8A**,** 69s-77s.

Thach, B.T. (2008). Some aspects of clinical relevance in the maturation of respiratory control in infants. *J. Appl. Physiol.* 104**,** 1828-1834.

Tian, G.-F., and Duffin, J. (1998). The role of dorsal respiratory group neurons studied with cross-correlation in the decerebrate rat. *Exp. Brain. Res.* 121**,** 29-34.

Tian, G.-F., Peever, J.H., and Duffin, J. (1998). Bötzinger-complex expiratory neurons monosynaptically inhibit phrenic motoneurons in the decerebrate rat. *Exp. Brain. Res.* 122**,** 149-156.

Torrealba, F., and Müller, C. (1999). Ultrastructure of glutamate and GABA immunoreactive axon terminals of the rat nucleus tractus solitarius, with a note on infralimbic cortex afferents. *Brain Res.* 820**,** 20-30.

Torvik, A. (1956). Afferent connections to the sensory trigeminal nuclei, the nucleus of the solitary tract and adjacent structures. An experimental study in the rat. *J. Comp. Neurol.* 106**,** 51-141.

Trojanowski, J.Q., Gonatas, J.O., and Gonatas, N.K. (1981). Conjugates of horseradish peroxidase (HRP) with cholera toxin and wheat germ agglutinin are superior to free HRP as orthogradely transported markers. *Brain Res.* 223**,** 381-385.

Ugolini, G. (2010). Advances in viral transneuronal tracing. *J. Neurosci. Methods* 194**,** 2-20.

Van Daele, D.J., and Cassell, M.D. (2009). Multiple forebrain systems converge on motor neurons innervating the thyroarytenoid muscle. *Neuroscience* 162**,** 501-524.

Van Der Velde, L., Curran, A.K., Filiano, J.J., Darnall, R.A., Bartlett, D., Jr., and Leiter, J.C. (2003). Prolongation of the laryngeal chemoreflex after inhibition of the rostral ventral medulla in piglets: a role in SIDS? *J. Appl. Physiol. (1985)* 94**,** 1883-1895.

Van Haeften, T., and Wouterlood, F.G. (2000). Neuroanatomical tracing at high resolution. *J. Neurosci. Methods* 103**,** 107-116.

Vercelli, A., Repici, M., Garbossa, D., and Grimaldi, A. (2000). Recent techniques for tracing pathways in the central nervous system of developing and adult mammals. *Brain Res. Bull.* 51**,** 11-28.

Wan, X.C., Trojanowski, J.Q., and Gonatas, J.O. (1982). Cholera toxin and wheat germ agglutinin conjugates as neuroanatomical probes: their uptake and clearance, transganglionic and retrograde transport and sensitivity. *Brain Res.* 243**,** 215-224.

Wasserman, A.M., Sahibzada, N., Hernandez, Y.M., and Gillis, R.A. (2000). Specific subnuclei of the nucleus tractus solitarius play a role in determining the duration of inspiration in the rat. *Brain Res.* 880**,** 118-130.

Wetmore, R.F. (1993). Effects of acid on the larynx of the maturing rabbit and their possible significance to the sudden infant death syndrome. *The Laryngoscope* 103**,** 1242-1254.

Widdicombe, J. (1980). Mechanism of cough and its regulation. *Eur. J Respir. Dis. Suppl.* 110**,** 11.

Wouterlood, F.G., Bloem, B., Mansvelder, H.D., Luchicchi, A., and Deisseroth, K. (2014). A fourth generation of neuroanatomical tracing techniques: Exploiting the offspring of genetic engineering. *J. Neurosci. Methods* 235c**,** 331-348.

Xia, L., Bartlett, D., and Leiter, J. (2008). An adenosine A 2A antagonist injected in the NTS reverses thermal prolongation of the LCR in decerebrate piglets. *Respir. Physiol. Neurobiol.* 164**,** 358-365.

Xia, L., Damon, T., Niblock, M.M., Bartlett, D., Jr., and Leiter, J.C. (2007). Unilateral microdialysis of gabazine in the dorsal medulla reverses thermal prolongation of the laryngeal chemoreflex in decerebrate piglets. *J. Appl. Physiol. (1985)* 103**,** 1864-1872.

Xia, L., Leiter, J.C., and Bartlett, D., Jr. (2013). Laryngeal reflex apnea in neonates: effects of CO2 and the complex influence of hypoxia. *Respir. Physiol. Neurobiol.* 186**,** 109-113.

Yizhar, O., Fenno, L.E., Davidson, T.J., Mogri, M., and Deisseroth, K. (2011). Optogenetics in neural systems. *Neuron* 71**,** 9-34.

Yoshida, Y., Tanaka, Y., Hirano, M., and Nakashima, T. (2000). Sensory innervation of the pharynx and larynx. *Am. J. Med.* 108 Suppl 4a**,** 51s-61s.

Yoshihara, Y. (2002). Visualizing selective neural pathways with WGA transgene: combination of neuroanatomy with gene technology. *Neurosci. Res.* 44**,** 133-140.

Zhang, F., Wang, L.P., Boyden, E.S., and Deisseroth, K. (2006). Channelrhodopsin-2 and optical control of excitable cells. *Nat. Methods* 3**,** 785-792.

Zhao, W.J., Sun, Q.J., Guo, R.C., and Pilowsky, P.M. (2015). Catecholamine inputs to expiratory laryngeal motoneurons in rats. *J. Comp. Neurol.* 523**,** 381-390.

Appendix

A Short communication for Oxford conference on breathing, proceedings 2014

A novel neuronal population in the nucleus tractus solitarius that projects simultaneously to the Bötzinger complex and caudal nucleus ambiguus

Summan R. Toor[1], Jacqueline K. Phillips[1], Paul. M. Pilowsky[2], Qi-Jian Sun[1]

[1]Faculty of Medicine and Health Sciences, Macquarie University, NSW 2109, Australia.
[2]Heart Research Institute and University of Sydney, NSW 2042, Australia

Abstract

The neuronal mechanism that stops central breathing (apnoea) during laryngeal stimulation is poorly understood. In a recent study, the apnoeic response was found to be closely associated with a non-respiratory burst activity (Sun et al., 2011) relayed possibly to the Bötzinger complex (BötC) and caudal nucleus ambiguus (NA) simultaneously from the neurons in the nucleus tractus solitarius (NTS). The present study is aimed to provide anatomical proof of dual projecting neurons exist in the NTS to support this hypothesis. Experiments were performed on adult male anaesthetised Sprague Dawley rats. Four to 5 days after microinjection of the fluorescent retrograde tracer CTB-555 into the BötC and unconjugated CTB into the caudal NA, rats were perfused transcardially with 4% paraformaldehyde. After immunohistochemistry for unconjugated CTB, the sections were visualized for the presence of retrograde labelled neurons in the NTS. A small number of double-labelled neurons with dual projections to BötC and NA were found in caudal NTS mainly in the interstitial and dorsolateral subdivisions. The study provides anatomical evidence for dual projecting neurons that may be responsible for the apnoeic response and vocal cords adduction.

Introduction

The stimulation of laryngeal afferents produces a strong central nervous system mediated inhibitory reflex to stop breathing (apnoea) and is called laryngeal chemoreflex (LCR) apnoea (Curran et al., 2005; Heman-Ackah et al., 2009). It works closely with vocal cords closure to prevent aspiration (Yoshida et al., 2000; Thach, 2008). Dysfunction of this reflex is thought to underlie life threatening conditions such as Sudden Infant Death Syndrome (Xia et al., 2013). GABAergic neurons in the nucleus tractus solitarius (NTS) are known to be involved in LCR apnoea (Xia et al., 2008), however, the basic neurogenic mechanism is not known and in particular, there is a lack of anatomical studies describing the neurons that mediate this reflex. The sensory pathway for LCR apnoea involves sensory neurons in nodose ganglion sending their afferents to central nervous system via superior laryngeal nerve (SLN) which terminates in the NTS (Furusawa et al., 1996). We would predict that there are neurons in the NTS that should be able to direct the laryngeal sensory input to respiratory pattern generators in order to induce the temporary shutdown of breathing, however such neurons have not been documented. In a recent study, we demonstrated that the burst activity recorded from the expiratory laryngeal motoneurons in the caudal nucleus ambiguus (NA) during SLN stimulation plays an important role in producing apnoea (Sun et al., 2011). Furthermore, blocking of generated burst activity in Bötzinger complex (BötC) neurons during SLN stimulation attenuated the apnoeic response (Sun et al., 2011). Based on these findings, we predicted a bifurcating sensory pathway consisting of burst producing neurons in the NTS with a simultaneous projection to the caudal NA for closing the vocal cords and to the BötC to drive apnoea (Sun et al., 2011). The present study therefore aimed to identify NTS dual projecting neurons with simultaneous projection to BötC and caudal NA, and therefore the

anatomical proof for a neuronal pathway capable of coordinating apnoea with vocal cords adduction.

Methods

Surgery and microinjections

The study was approved by the Animal Ethics Committee of Macquarie University, Australia. Experiments were performed on male Sprague Dawley rats (380-550 g n=2). Animals were anaesthetized with an intraperitoneal (i.p.) injection of ketamine (0.75 mg/kg)/medetomidine (0.5 mg/kg), followed by subcutaneous (s.c.) injection of carprofen (5 mg/kg) for pain relief and antibiotic cephazoline (20-40 mg/kg, s.c.) for preventing infection. For craniotomy, a hole was drilled extending 1.25 mm lateral from the midline and from 0-4.5 mm caudal from lambda suture line (zero being the lambda suture line and 4.5 near to cerebrospinal junction). A 20-40 nl pressure microinjection of retrograde tracer (CTB-555, 0.5% w/v) was made into the BötC (2.6-2.8 mm caudal, 1.6-1.7 mm lateral and 8.8-9.2 mm deep) localised by mapping the facial nucleus (Pilowsky et al., 1990). A second microinjection of unconjugated CTB (1% w/v) was made into the caudal NA at 4.0-4.5 mm caudal, 1.5-1.6 mm lateral and 8.6-8.9 mm deep (Paxinos et al., 2009) on the ipsilateral side. Atipamazole (1.5mg/kg, i.p.) were given for recovery of the animal.

Perfusion/fixation/ immunohistochemistry

Following recovery of 3-5 days, the animals were perfused transcardially using 4% paraformaldehyde following deep anaesthesia with sodium pentobarbital (72 mg/kg, i.p. 20% v/v). The brain stem was removed, postfixed overnight, cut into 50 μm thick sections using vibrotome (Leica Biosystems, VT1200 S), collected in tris phosphate-buffered saline (TPBS, 10 mmol/L Tris, 0.9% NaCl, 10 mmol/L phosphate buffer, pH 7.4) in four consecutive series such that sections in each were separated by 200μm. One series of sections was used for direct visualisation of CTB-555. The other series were incubated in goat anti CTB primary antibody (1:50,000) for 72 hours and then visualised with a secondary fluorescent antibody (donkey anti goat conjugated to fluorescein isothiocyanate (FITC) 1:500). Sections were mounted and visualized using a ZENPRO epifluorescence microscope (Zeiss), with standard band pass fluorescent filters for FITC and tetramethylrhodamine (CTB-555).

Image analysis

Digital micrographs of the injection sites and retrograde labelled neurons in the NTS (spanning across interaural regions -3.00 to -5.64mm) were obtained using a 5X and 10X objective lenses respectively, using tiled menu (ZEN 2012, GmbH 2011). The retrograde single and double-labelled neurons were counted at each interaural level identified as positive distance rostral and negative distance caudal (mm) to the obex. The location of double-labelled neurons within the various NTS sub-divisions was also determined. Graphs were constructed using GraphPad Prism Version 6 software (Graphpad software Inc. La Jolla, USA)

Results

BötC and NA projecting NTS neurons

Microinjection of retrograde tracers into the BötC and caudal NA was confirmed histologically using the known landmark described for BötC and caudal NA (Fig. 1A, B). The injections successfully resulted in retrograde labelling of neurons in the NTS (Fig. 1C, D). The majority of retrograde neurons were found ipsilateral to the site of injection however there were some labelled neurons on the contralateral side. The rostral to caudal distribution

of retrograde labelled neurons in the NTS from 1.2 mm rostral to -3.6 mm caudal to obex point was compared between the two injection sites (Fig. 2C). The numbers of retrograde labelled neurons in the NTS from the NA injection appeared to be greater compared to the number of retrograde labelled neurons from the BötC injection. The peak number of NA retrograde neurons was found at 0.48 mm rostral to obex while for BötC retrograde neurons it was 0.36 mm rostral to the Obex.

Double-labelled neurons

Double-labelled neurons (identifying those NTS neurons with projections to both the BötC and NA) were identified in the most caudal part of the NTS at the level of the obex and were only identified ipsilateral to the microinjection sites (Fig. 2C). The peak number of double labelled neurons was from 0.24 mm rostral to obex to the obex (Fig. 2C) and then declined caudal to the obex. Examples of double labelled neurons are illustrated in Fig. 2A and B at different interaural levels. In the rostral NTS (0.36 mm) double-labelled neurons were scattered throughout the whole NTS. More caudally the double-label neurons appeared to cluster in dorsal aspect of the NTS such as in dorsolateral NTS (SolDl) and intersititial NTS (Soll).

Discussion

The present study has provided preliminary anatomical evidence for the existence of dual projecting neurons in the NTS with simultaneous projections to the BötC and the caudal NA (Sun et al., 2011). Notably, double-labelled neurons were found in the caudal NTS, consistent with the complex architecture of this region containing maximum overlap among afferents from various viscerosensory parts of body (Lawrence and Jarrott, 1996; Kline, 2010). More importantly, the double-labelled neurons were found the interstitial compartment of the NTS (Soll), which has been described as a region containing the highest density terminal projections from the SLN (Furusawa et al., 1996). Although Soll contains terminal projection from the SLN nerve, the question remains unclear as which level of the caudal NTS, with reference to obex, contains the maximum SLN terminal projection, keeping in mind that the obex is differently described across different species of animals such as cat (Kalia and Mesulam, 1980), rabbit (Ellenberger and Feldman, 1990) and rat (Alheid et al., 2011). Further studies are required to determine how the SLN terminals coordinate, either by direct or indirect connections, with the dual projecting neurons in the NTS. Nevertheless, this study provides strong anatomical proof of neurons with dual projection to downstream central nuclei for the coordinated motor output for apnoea and vocal cord adduction. These two important physiological events serve to protect the airways from aspiration during swallowing. The delineation of the sensory pathway involved therefore, is the first step towards understanding the neurogenic mechanism underlying the production of the airway protective reflex and also how dysfunction in such a basic neurogenic mechanism may lead to life threatening situations.

References

1. Alheid, G.F., Jiao, W., and Mccrimmon, D.R. (2011). Caudal nuclei of the rat nucleus of the solitary tract differentially innervate respiratory compartments within the ventrolateral medulla. *Neuroscience* 190**,** 207-227.
2. Curran, A.K., Xia, L., Leiter, J., and Bartlett, D. (2005). Elevated body temperature enhances the laryngeal chemoreflex in decerebrate piglets. *J. Appl. Physiol.* 98**,** 780-786.
3. Ellenberger, H., and Feldman, J. (1990). Subnuclear organization of the lateral tegmental field of the rat. I: Nucleus ambiguus and ventral respiratory group. *J. Comp. Neurol.* 294**,** 202-211.

4. Furusawa, K., Yasuda, K., Okuda, D., Tanaka, M., and Yamaoka, M. (1996). Central distribution and peripheral functional properties of afferent and efferent components of the superior laryngeal nerve: morphological and electrophysiological studies in the rat. *J. Comp. Neurol.* 375**,** 147-156.
5. Heman-Ackah, Y.D., Pernell, K.J., and Goding, G.S., Jr. (2009). The laryngeal chemoreflex: an evaluation of the normoxic response. *Laryngoscope* 119**,** 370-379.
6. Kalia, M., and Mesulam, M. (1980). Brain stem projections of sensory and motor components of the vagus complex in the cat: I. The cervical vagus and nodose ganglion. *J. Comp. Neurol.* 193**,** 435-465.
7. Kline, D.D. (2010). Chronic intermittent hypoxia affects integration of sensory input by neurons in the nucleus tractus solitarii. *Respir. Physiol. Neurobiol.* 174**,** 29-36.
8. Lawrence, A.J., and Jarrott, B. (1996). Neurochemical modulation of cardiovascular control in the nucleus tractus solitarius. *Prog Neurobiol.* 48**,** 21-53.
9. Paxinos, G., Watson, C., Carrive, P., Kirkcaldie, M., and Ashwell, K. (2009). Chemoarchitectonic atlas of the rat brain.
10. Pilowsky, P.M., Jiang, C., and Lipski, J. (1990). An intracellular study of respiratory neurons in the rostral ventrolateral medulla of the rat and their relationship to catecholamine-containing neurons. *J. Comp. Neurol.* 301**,** 604-617.
11. Sun, Q.J., Bautista, T.G., Berkowitz, R.G., Zhao, W.J., and Pilowsky, P.M. (2011). The temporal relationship between non-respiratory burst activity of expiratory laryngeal motoneurons and phrenic apnoea during stimulation of the superior laryngeal nerve in rat. *J. Physiol.* 589**,** 1819-1830.
12. Thach, B.T. (2008). Some aspects of clinical relevance in the maturation of respiratory control in infants. *J. Appl. Physiol.* 104**,** 1828-1834.
13. Xia, L., Bartlett, D., and Leiter, J. (2008). An adenosine A 2A antagonist injected in the NTS reverses thermal prolongation of the LCR in decerebrate piglets. *Respir. Physiol. Neurobiol.* 164**,** 358-365.
14. Xia, L., Leiter, J.C., and Bartlett, D., Jr. (2013). Laryngeal reflex apnea in neonates: effects of CO2 and the complex influence of hypoxia. *Respir. Physiol. Neurobiol.* 186**,** 109-113.
15. Yoshida, Y., Tanaka, Y., Hirano, M., and Nakashima, T. (2000). Sensory innervation of the pharynx and larynx. *Am. J. Med.* 108 Suppl 4a**,** 51s-61s

Figure legends

Figure 1. Retrograde labelled neurons in the NTS after microinjection into the BötC and caudal NA. **A)** BötC injection site. The BötC injection site was caudal to facial nucleus and ventral to the compact formation of the NA (AmbC). The NTS (outlined) shows no retrograde labelled neurons at the level of the injection site **B)** Caudal NA (AmbL) injection site. The NTS region (outlined) does contain retrograde labelled neurons at the same level as the injection site. **C)** Higher magnification image of retrograde labelled neurons in the NTS after injection into the BötC **D)** Higher magnification image of retrograde labelled neurons in the NTS after injection into the caudal NA.

Figure 2. Distribution of dual projecting neurons in the NTS. **A)** The double-labelled neuron were found scattered across various NTS sub compartments at the level of 0.36 mm rostral to obex. **B)** At 0.12 mm rostral to obex, double-labelled neuron were clustered within the dorsolateral (SolDl) and interstitial (SolI) subdivision of the NTS. **C)** Rostral to caudal distribution of single and double labelled neurons in the nucleus tractus solitarii (NTS) ipsilateral to the injection sites. Neurons were mapped from the BötC injection site (2.6 mm rostral) to -0.36 mm caudal to the obex (zero). The number of single (either NA or BötC projecting) or double labelled neurons counted per section at each level is shown for animal 1 and 2 (Animal #1= White colour, Animal #2 = Grey colour, Squares = NA, Circles = BötC, Blue diamonds = Double labelled neurons animal 1, Red diamonds = Double labelled neurons animal 2).
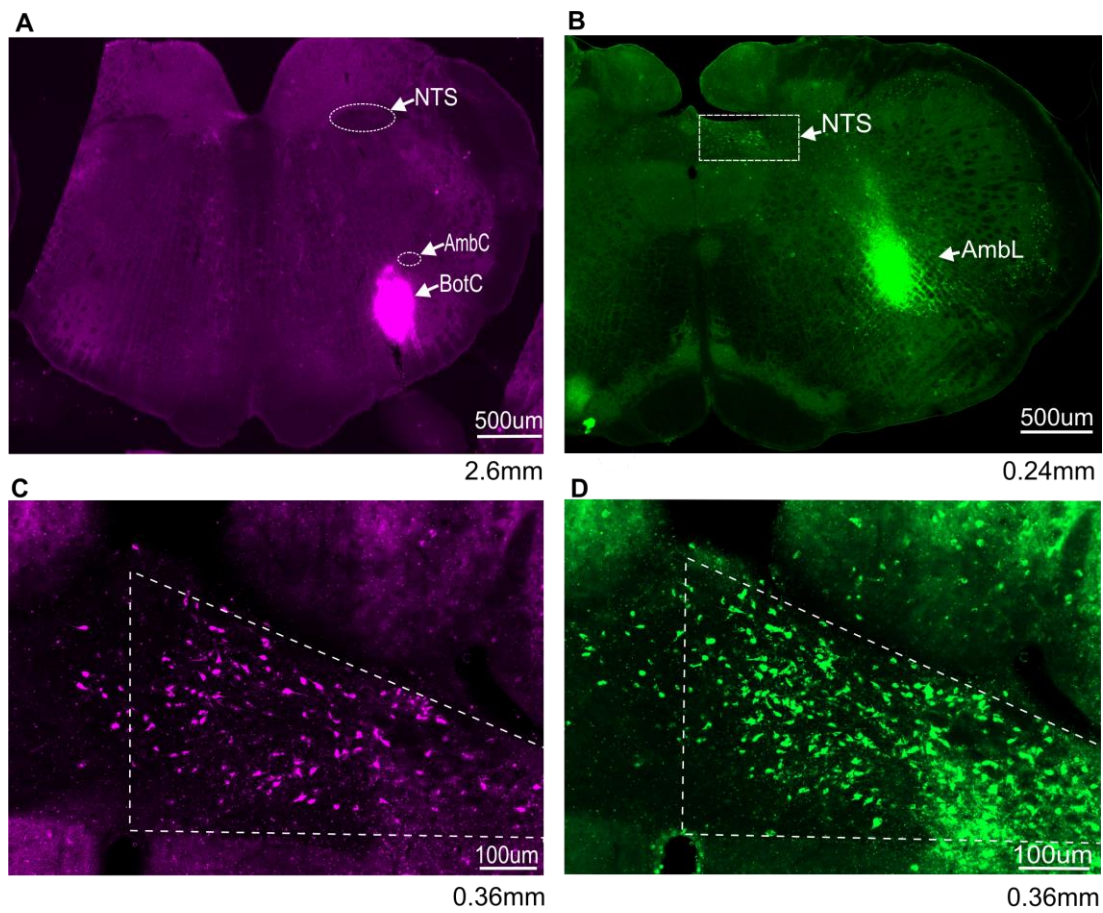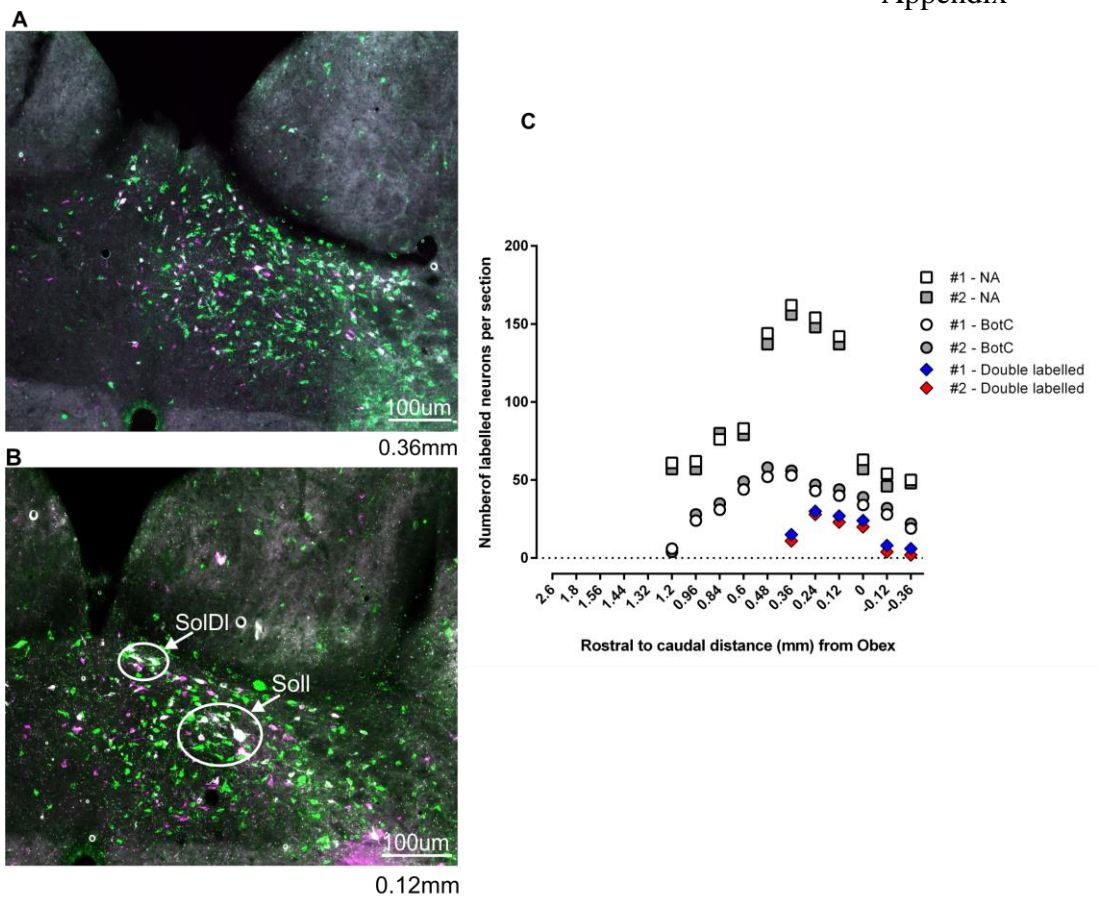
A NTS, AmbC, BotC — 500um — 2.6mm

B NTS, AmbL — 500um — 0.24mm

C 100um — 0.36mm

D 100um — 0.36mm

Figure 1

Figure 2